Ultimate Bearing Capacity of Strip Footing On Granular Soil Under Eccentrically Inclined Load- A Numerical Approach

A Thesis submitted in partial fulfillment of the requirements

for the award of the Degree of

Master of Technology

in

Civil Engineering

REGOTI MAHENDAR
Roll No. 213CE1047

DEPARTMENT OF CIVIL ENGINEERING

NATIONAL INSTITUTE OF TECHNOLOGY ROURKELA

ROURKELA-769008

MAY 2015

Ultimate Bearing Capacity of Strip Footing On Granular Soil Under Eccentrically Inclined Load- A Numerical Approach

A Thesis submitted in partial fulfillment of the requirements

for the award of the Degree of

Master of Technology

in

Civil Engineering

By

REGOTI MAHENDAR
Roll No. 213CE1047

Under the guidance of

Dr. RABI NARAYAN BEHERA

DEPARTMENT OF CIVIL ENGINEERING

NATIONAL INSTITUTE OF TECHNOLOGY ROURKELA

ROURKELA-769008

MAY 2015

Department of Civil Engineering
NIT Rourkela
Rourkela – 769008
Odisha, India
www.nitrkl.ac.in

CERTIFICATE

This is to certify that the thesis entitled "**Ultimate Bearing Capacity of Strip Footing on Granular Soil under Eccentrically Inclined Load- A Numerical Approach**" submitted by **Mr. Regoti Mahendar** (Roll No. 213CE1047) in partial fulfillment of the requirements for the award of Master of Technology Degree in Civil Engineering with specialization in Geotechnical Engineering at National Institute of Technology Rourkela is an authentic work carried out by him under my supervision and guidance.

To the best of my knowledge, the matter embodied in the thesis has not been submitted to any other University / Institute for the award of any Degree or Diploma.

Date:
Place:

Dr. Rabi Narayan Behera
Assistant Professor
Department of Civil Engineering
NIT Rourkela
Rourkela – 769008

Acknowledgement

First of all I would like to express my heartfelt gratitude to my project supervisor **Dr. Rabi Narayan Behera**, Department of Civil Engineering for his able guidance, encouragement, support and suggestions during the project work.

I would like to thank **Prof. S.K. Sahu**, Head of Civil Engineering Department, National Institute of Technology Rourkela, for his valuable suggestions during other review meeting and necessary facilities for the research work. I am also thankful to all the faculty members of the Civil Engineering Department, who have directly or indirectly helped me during the project work.

I would like to thank **Prof. N. Roy** and other faculty members of Geotechnical Engineering specialization for providing me solid background and their kind suggestions during the entire course of my project work.

Finally, I would like to thank my parents and family members for their unwavering support and invariable source of motivation.

Regoti Mahendar

Roll No: 213ce1047

M. Tech (Geotechnical engineering)

Department of Civil Engineering

NIT Rourkela

Odisha-769008

ABSTRACT

Since the publication of Terzaghi's theory on the ultimate bearing capacity of shallow foundations in 1943, results of numerous studies—theoretical, experimental and numerical—by various investigators have been published. Most of the studies relate to the case of a vertical load applied centrally to the foundation. Meyerhof (1953) developed empirical procedures for estimating the ultimate bearing capacity of foundations subjected to eccentric and inclined loads. Recently, Patra et al. (2012a, 2012b) developed two empirical equations to determine the ultimate bearing capacity of eccentrically inclined loaded strip footing. Based on the review of the existing literature on the bearing capacity of shallow foundations, it appears that limited attention has been paid to estimate the ultimate bearing capacity when the foundation is subjected to both eccentric and inclined load and the objective of present study stems from this paucity.

In order to arrive at the objective and to quantify certain parameters, extensive numerical models have been made to determine the ultimate bearing capacity of shallow strip foundation resting over sand bed and subjected to eccentric and inclined loads. The models are made with three relative density of sand i.e. dense sand and medium dense sand. The load inclination has been varied from 0° to 20° whereas the eccentricity varies from 0 to 0.15B (B = width of footing). Depth of the footing is varied from 0 to B with an increment of 0.5B. In most cases of analysis of such problems; the line of load application is towards the center line of the footing. However, in this thesis, it is investigated for the two possible ways of line of load application i.e. (i) towards and (ii) away from the center line of the footing.

Based on the analysis of numerical models result, the results of medium dense and dense sand are compared with the reduction factor developed by Patra et al. (2012a, 2012b) for each mode

of load application. This reduction factor will compute the ultimate bearing capacity of footing subjected to eccentric and inclined load by knowing the ultimate bearing capacity of footings under centric vertical load at the same depth of footing. Finally, the numerical model results are compared with the existing theories and the comparison seems to be good.

Table of Contents

Certificate……...i

Acknowledgement…… ii

Abstract…….....iii

Contents…….iv

List of Tables…….…..viii

List of Figures…….x

1. INTRODUCTION…….....1

2. LITERATURE REVIEW…….....4

2.1 Introduction……4

2.2 Bearing Capacity of Shallow Foundations on granular soil……..4

2.2.1 Central Vertical Loading ……5

2.2.2 Eccentric Vertical Condition…….10

2.2.3 Central Inclined Condition ……...11

2.2.4 Eccentric Inclined Condition……14

2.3 Scope of the present study...……16

3. METHODOLOGY AND MODELLING……..17

3.1 Introduction ……17

3.2 Methodology……17

3.2.1 Modelling……..18

4. ULTIMATE BEARING CAPACITY OF ECCENTRICALLY INCLINED LOADED STRIP FOOTING WHEN THE LINE OF LOAD APPLICATION THE CENTER LINE OF THE FOOTING……..…20

4.1 Introduction……..….20

4.2 Numerical Module ……..….21

4.3 Numerical model Results ……...……..…21

4.3.1 Central Vertical Loading Conditions ……...21

4.3.2 Eccentric Vertical Loading Conditions…….27

4.3.3 Centric Inclined Loading Condition ……34

4.3.4 Eccentric Inclined Loading Conditions ……...……43

4.4 Comparison……..50

4.4.1 Comparison with Patra et al. [2012] ……50

4.4.2 Comparison with Meyerhof [1963] …….53

4.4.3 Comparison with Saran and Agarwal [1991] ……..55

4.4.4 Comparison with Loukidis et al. [2008]……...57

4.4.5 Comparison with Viladkar et al. [2013]……...……58

5. ULTIMATE BEARING CAPACITY OF ECCENTRICALLY INCLINED LOADED STRIP FOOTING ON GRANULAR SOIL WHEN THE LINE OF LOAD APPLICATION IS AWAY FROM THE CENTER LINE OF THE FOOTING……..…….61

5.1 Introduction……..61

5.2 Numerical Module. …….62

5.3 Numerical Model Results……....62

5.4 Comparison……..70

5.4.1 Comparison with Patra et al. [2008]…….70

5.4.2 Comparison with Loukidis et al. [2008]……...…73

6. CONCLUSIONS AND SCOPE FOR FUTURE RESEARCH WORK ……76

6.1 Conclusions……..76

6.2 Future research work ……...…77

References…….78

List of Tables

Table 2.1: Summary of Bearing Capacity factors (Behera R N 2013)……6

Table 2.2: Summary of Shape and Depth factors……8

Table 3.1: Soil properties……...18

Table 3.2: Footing properties……18

Table 4.1: Sequence of numerical models for Dense and Medium dense sand in partially compensated condition...……...……21

Table 4.2: Numerical model parameters for Centric Vertical Loading condition….…….....….22

Table 4.3: Calculated values of ultimate bearing capacities *qu* by Terzaghi (1943), Meyerhof (1951) and Hansen (1970) for centric vertical condition……..….25

Table 4.4: Calculated values of ultimate bearing capacities *qu* by Vesic (1973), Patra et al. (2012) for centric vertical condition along with Present results……26

Table 4.5: Numerical Model parameters for Eccentric Vertical Loading condition ……27

Table 4.6: Calculated values of ultimate bearing capacities *qu* by Meyerhof (1951), Prakash and Saran (1971) and Purkayastha and Char (1977) for centric vertical condition……..31

Table 4.7: Calculated values of ultimate bearing capacities *qu* by Loukidis et al. (2008), Patra et al. (2012a) for centric vertical condition along with Present results…….……....32

Table 4.8: Calculated values of R_k by Purkayastha and Char (1977) for eccentric vertical condition along with Present results……..…33

Table 4.9: Numerical Model parameters for Centric Inclined Loading condition……35

Table 4.10: Calculated values of ultimate bearing capacities (*qu*) by using formulae of existing theories for centric inclined condition along with Present numerical model values……38

Table 4.11: Calculated values of ultimate bearing capacities (*qu*) by using formulae of existing

theories for centric inclined condition along with Present numerical values……...39

Table 4.12: Calculated values of Muhs and Weiss (1973) ratio for centric inclined condition along with Present numerical model values…….…….41

Table 4.13: Numerical model parameters for Eccentric Inclined Loading condition….....43

Table 4.14: Numerical model results for eccentric inclined condition……..……47

Table 4.15: Comparison of RF corresponding to Patra et al. (2012a) with present results……...50

Table 4.16: Reduction Factor Comparison of Meyerhof (1963) with Present results……...53

Table 4.17: Comparison of Reduction Factors corresponding to Saran and Agarwal (1991) along with Present results……55

Table 4.18: Comparison of Reduction Factors corresponding to Loukidis et al. (2008) for $Df/B = 0$ with present results…….57

Table 4.19: Comparison of RF corresponding to Viladkar et al. (2013) with Patra et al. (2012)…….58

Table 5.1: Sequence of Numerical models for Dense and Medium dense sand in *Reinforced* condition……....62

Table 5.2: Ratio of ultimate bearing capacity *qu* in both conditions i.e. partially compensated and reinforced case with ultimate bearing capacity *qu* in central vertical condition and ratio of q_u- reinforced to q_u- partially compensated……...68

Table 5.3: Comparison of RF corresponding to Patra et al. (2012b) with present results…….....71

Table 5.4: Comparison of RF corresponding to Loukidis et al. (2008) with present result for $Df/B = 0$…….74

List of Figures

Figure 2.1: Vertical central load per unit length on the strip foundation (Q_u)……..….6

Figure 2.2: Eccentrically loaded footing……....10

Figure 2.3: Ultimate load Q on a foundation for centric inclined load……..11

Figure 2.4: Eccentrically inclined load on a strip foundation: line of load application (a) towards the center line and (b) away from the center line of the footing……14

Figure 3.1: Geometric model for central vertical loading case……..19

Figure 4.1: Eccentrically inclined load on strip foundation: line of load application towards the center line of the footing……20

Figure 4.2: Interpretation of Ultimate bearing capacity q_u by Break Point method (Mosallanezhad et al. 2008)……...22

Figure 4.3: Variation of load-settlement curve with embedment ratio (D_f/B) at e/B=0 and α=0° in Medium dense sand……...23

Figure 4.4: Variation of load-settlement curve with Relative Density (D_r) of sand at D_f/B=0, e/B=0 and α=0°……23

Figure 4.5: Variation of q_u with D_f/B for $\alpha = 0°$ and $e/B = 0$ using formulae of existing theories along with present numerical model values for (a) dense and (b) medium dense sand……....25

Figure 4.6: Failure surface observed in medium dense sand in surface condition at $D_f/B = 0$, $\alpha = 0°$ and $e/B = 0$……..26

Figure 4.7: Developed numerical model for eccentric vertical loading condition……...…….28

Figure 4.8: Variation of load-settlement curve with eccentricity in dense sand in surface

condition for α=0°……28

Figure 4.9: Effect of embedment on eccentricity in medium sand for α=0°, *e/B*=0.05……..…..29

Figure 4.10: Variation of load settlement curve with relative density for α=0°, *e/B*=0.15 and D_f/B=1……..……..29

Figure 4.11: Comparison of ultimate bearing capacities of Present results with existing theories for (a) medium and (b) dense sand…….……..31

Figure 4.12: Comparison of Present numerical model results with Purkayastha and Char (1977)…….33

Figure 4.13: Failure surface observed in dense sand at D_f/B = 0.5, α = 0° and *e/B* = 0.15……..34

Figure 4.14: Developed numerical model for centric inclined loading condition…….35

Figure 4.15: Variation of load settlement curve with load inclination (α) in medium sand for D_f/B=0 and *e/B*=0……..36

Figure 4.16: Variation of load-settlement curve with load inclination (α) in dense sand for D_f/B=0 and *e/B*=0……..36

Figure 4.17: Variation of load-settlement curve with embedment ratio (D_f/B) in medium dense sand for α = 5°, *e/B*=0……...37

Figure 4.18: Variation of load-settlement curve with relative density of sand at α=20°, *e/B* = 0 and D_f/B=0…….37

Figure 4.19: Comparison of ultimate bearing capacities of Present results with existing theories for (a) medium and (b) dense sand…….……..40

Figure 4.20: Comparison of Present Numerical model results with Muhs and Weiss (1973)…...41

Figure 4.21: Failure surface observed in dense sand at D_f/B = 1, α = 15° and *e/B* = 0……42

Figure 4.22: Developed numerical model for eccentric inclined loading condition when the line of load application is towards the center line……..44

Figure 4.23: Variation of load-settlement curve with load inclination (α) at D_f/B=0.5 and e/B=0.05 in dense sand……..45

Figure 4.24: Variation of load-settlement curve with e/B at D_f/B=0 and α=10° in medium dense sand……....45

Figure 4.25: Variation of load-settlement curve with embedment ratio (D_f/B) at e/B =0.15 and α=20° in dense sand……46

Figure 4.26: Variation of load-settlement curve with Relative Density (D_r) at e/B =0.1, α=10°and D_f/B=0.5……46

Figure 4.27: Failure surface observed in dense sand at D_f/B = 0.5, α = 10° and e/B = 0.1…….49

Figure 4.28: Comparison of Present results with Patra et al. (2012a) for dense and medium dense Sand……52

Figure 4.29: Comparison of Present results with Meyerhof (1963)……..55

Figure 4.30: Comparison: Present results with Saran and Agarwal (1991)……...56

Figure 4.31: Comparison of Present results with Loukidis et al. (2008)……...58

Figure 4.32: Comparison of Reduction factor corresponding to Viladkar et al. (2013) with Patra et al. (2012)……....60

Figure 5.1: Eccentrically inclined load on a strip foundation: (a) *Partially compensated* case, (b) *Reinforced* case……..61

Figure 5.2: Developed numerical model for eccentric inclined loading condition when the line of load application is away from the center line……63

Figure 5.3: Variation of load-settlement curve with α at D_f/B=1, e/B =0.05 in dense sand…...63

Figure 5.4: Variation of load-settlement curve with *e/B* at D_f/B=1, α=10° in medium dense sand……64

Figure 5.5: Variation of load-settlement curve with D_f/B *at* α=5 °, *e/B* =0.15 in dense sand…..64

Figure 5.6: Variation of load-settlement curve with relative density (D_r) *at* D_f/B=1, α=20°, *e/B* =0.15……65

Figure 5.7: Variation of load-settlement curve with load inclination (*α*) for towards and away cases *at* D_f/B=0.5, α=20°, *e/B* =0.05 for dense sand……..…….65

Figure 5.8: Failure surface observed in medium dense sand at D_f/B = 0.5, α = 15° and *e*/*B* = 0.1…….66

Figure 5.9: Plot of (q_u– reinforced)/(q_u– partially compensated) for cases of eccentrically inclined loading in dense sand……...67

Figure 5.10: Comparison of Present results with Patra et al. (2012b) for dense and medium dense Sand……73

Figure 5.11: Comparison of Loukidis et al. (2008) with present results……..….75

Figure 5.12: Comparison of (q_u– reinforced)/(q_u– partially compensated) for Present results with Loukidis et al. (2008)…….75

1. INTRODUCTION

Every civil engineering structure, whether it is a building, bridge, highway pavement or railway track, will in general have a superstructure and a foundation. The function of the foundation is to receive the loads from the superstructure and transmit safely them to the soil or rock below as the case may be. The design of shallow foundation (i.e. the plan dimensions of the foundation) is accomplished by satisfying two requirements: (1) bearing capacity and (2) settlement. Bearing capacity refers to the ultimate, i.e., the maximum load the soil can bear or sustain under given circumstances.

Engineers need to be able to calculate the capacity of foundations subject to; at least, central vertical loads. This need has led to the development of the theories of bearing capacity, notably Terzaghi's method. Bearing capacity predictions based on Terzaghi's (1943) superposition method are partly theoretical and partly empirical in which the contribution of different loading and soil strength parameters (cohesion, friction angle, surface surcharge and self-weight) expressed in the form of non-dimensional bearing capacity factors N_c, N_q, and N_γ are summed. Several analytical solutions have been proposed for computing these factors. The literature contains many theoretical derivations, as well as experimental results from model tests and prototype footings.

All the bearing capacity estimation methods may be classified into the following four categories: (1) the limit equilibrium method; (2) the method of characteristics; (3) the upper-bound plastic limit analysis and (4) the numerical methods based on either the finite-element method or finite-difference method. The problems can be solved by two different approaches: experimentally, by conducting model and full-scale tests; or, by using numerical methods such as finite element analyses. Full-scale tests are the ideal method for obtaining data, however, practical difficulties

and economic considerations either eliminate or considerably restrict the possibility of full-scale testing. As an alternative model tests may be employed, but they have disadvantages. The results of these model tests are usually affected by the boundary conditions of the test box, the size of the footing, the sample disturbance, the test setup and procedure. It is advantageous to use the techniques of numerical methods to simulate the conditions of model tests to verify the theoretical models. Due to the fortunate developments in numerical methods and computer programming, it is advantageous to use these techniques to simulate the conditions of model tests to verify the theoretical models. The theoretical study can then be extended to cover a wide range of field cases which engineers omitted using full-scale testing.

Most of the studies for bearing capacity calculation are based on the foundation under vertical and central load. However in some cases due to bending moments and horizontal thrusts transferred from the superstructure, shallow foundations of structures like retaining walls, abutments, waterfront structures, oil/gas platforms in offshore area, industrial machines, and portal framed buildings are very often subjected to eccentric and inclined loads. This may be due to (a) moments with or without axial forces (b) the oblique loading (c) their location near the property line (d) wind force and (e) earth pressure and water pressure. They can be analyzed as eccentrically inclined loaded strip footings, with eccentricity of e and load inclination of α to the vertical. Due to load eccentricity and inclination, the overall stability of foundation decreases along with differential settlement and tilting of the foundation which reduces the bearing capacity.

The estimation of bearing capacity of foundations under eccentric and inclined loads is of considerable importance in geotechnical engineering. In order to study further in this area, extensive literature review is made to narrow down the objective of the present investigation.

Detailed investigation and analyses are presented in the subsequent chapters for estimating ultimate bearing capacity of shallow strip footing subjected to eccentrically inclined load resting over a dry sand bed.

2. LITERATURE REVIEW

2.1 Introduction

Foundation is a part of the structure which transfers the loads to the soil or rock below it. And it is classified into two types namely, (1) shallow foundation and (2) deep foundation by depending on depth of embedment. These foundations like earth retaining walls, oil/gas platforms etc. may be subjected to eccentric and inclined loads. This may be due to (i) inclined loading (ii) wind force (iii) moments due to axial forces (iv) earth pressure and water pressure. Pressure under the footing may not be uniform due to the eccentric or inclined loading, this causes the footing tilts and pressure changes below it. The tilt of footing is proportional to the eccentricity and inclination. That means with increase in inclination bearing capacity reduces continuously and undergoes differential settlements.

2.2 Bearing Capacity of Foundation on granular soil

Stability of a structure mainly depends upon stability of supporting soil. For that the foundation must be stable against shear failure of the supporting soil and must not settle beyond a tolerable limit to avoid damage to the structure. For a given foundation to perform its optimum capacity, one must be ensured that it does not exceed its safe bearing capacity. The ultimate bearing capacity (q_u) is defined as shear failure occurs in the supporting soil immediately below the foundation.

Since the publications of Terzaghi's theory on the bearing capacity of shallow foundations in 1943, numerous studies (both experimental and theoretical) have been made by various investigators. Most of these studies are related to footings subjected to vertical and central loads.

Meyerhof (1953) developed empirical procedures for estimating the ultimate bearing capacity of foundations subjected to eccentric vertical loads. Researchers like Prakash and Saran (1971) and Purkayastha and Char (1977) also studied the behavior of eccentrically loaded footings. Similarly, the effect of inclined load on the foundation has been investigated by few investigators (Meyerhof 1953; Muhs and Weiss 1973; Hanna and Meyerhof 1981; Sastry and Meyerhof 1987). However a few works have been done by Meyerhof 1963, Saran and Agarwal (1991), Loukidis et al. (2008), Patra et al. (2012a, 2012b), Viladkar et al. (2013) and Krabbenhoft et al. (2014) towards the bearing capacity of footings subjected to combined action of eccentric and inclined load which is the subject of the thesis. An extensive review of literature based on bearing capacity of shallow foundations under different loading conditions is presented below.

2.2.1 Central Vertical Loading

Terzaghi (1943) proposed that the ultimate bearing capacity of a strip foundation subjected to a vertical central load over a homogenous soil can be expressed as

$$q_u = cN_c + qN_q + 0.5\gamma BN_\gamma \tag{2.1}$$

For granular soil the above equation is expressed by:

$$q_u = qN_q + 0.5\gamma BN_\gamma \tag{2.2}$$

Similarly, generalized equation for centrally vertical loaded foundation was proposed by Meyerhof (1951) and it is expressed as

$$q_u = cN_c s_c\, d_c + qN_q s_q d_q + 0.5\gamma BN_\gamma s_\gamma d_\gamma \tag{2.3}$$

For granular soil the above equation is reduced to the form as:

$$q_u = qN_q s_q d_q + 0.5\gamma BN_\gamma s_\gamma d_\gamma \tag{2.4}$$

Where q_u= ultimate bearing capacity; q= surcharge pressure at footing level (γD_f); γ = unit weight of soil; D_f = depth of foundation; N_c, N_q, N_γ= bearing capacity factors; s_c, s_q, s_γ= shape factors; d_c, d_q, d_γ = depth factors;

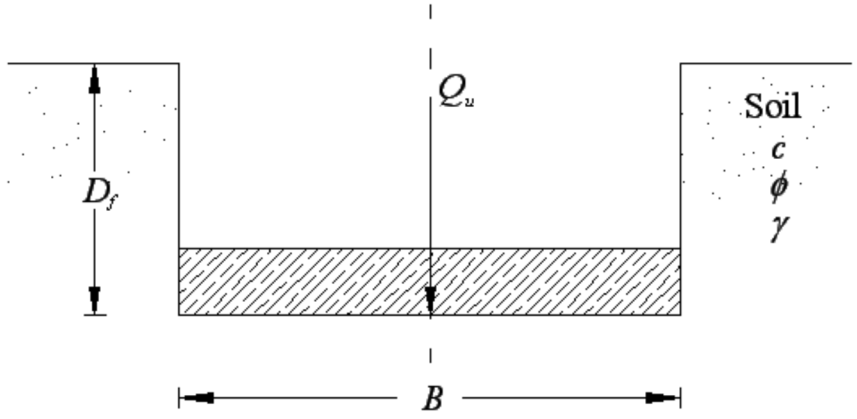

Figure 2.1: Vertical central load per unit length on the strip foundation (Q_u)

In Table 2.1 and Table 2.2 bearing capacity factors and depth and shape factors are presented.

Using these equations, ultimate bearing capacity of footings can be estimated.

Table 2.1: Summary of Bearing Capacity factors (Behera R N 2013)

Bearing Capacity Factors	**Equation**	**Investigator**
N_c	$N_c = (N_q - 1)\cot\phi$	Prandtl (1921), Reissner (1924), Terzaghi (1943), Meyerhof (1963)
N_c	$N_c = \frac{228 + 4.3\phi}{40 - \phi}$	Krizek (1965)
N_q	$N_q = \tan^2\left(45 + \frac{\phi}{2}\right) e^{\pi \tan\phi}$	Prandtl (1921), Reissner (1924), Meyerhof (1963)

Bearing Capacity Factors	Equation	Investigator
N_q	$N_q = \frac{e^{2\left(\frac{3\pi}{4}-\frac{\phi}{2}\right)\tan\phi}}{2\cos\left(45+\frac{\phi}{2}\right)^2}$	Terzaghi (1943)
N_q	$N_q = \frac{40+5\phi}{40-\phi}$	Krizek (1965)
N_γ	$N_\gamma \approx 1.8\left(N_q-1\right)\cot\phi\left(\tan\phi\right)^2$	Terzaghi (1943)
N_γ	$N_\gamma = 1.5\left(N_q-1\right)\tan\phi$	Lundgren and Mortensen (1953) and Hansen (1970)
N_γ	$N_\gamma = 1.8\left(N_q-1\right)\tan\phi$	Biarez et al. (1961)
N_γ	$N_\gamma = 0.01e^{0.25\phi}$	Feda (1961)
N_γ	$N_\gamma = \left(N_q-1\right)\tan\left(1.4\phi\right)$	Meyerhof (1963)
N_γ	$N_\gamma = \frac{6\phi}{40-\phi}$	Krizek (1965)
N_γ	$N_\gamma = 1.5\,N_c\left(\tan\phi\right)^2$	Hansen (1970)
N_γ	$N_\gamma = 2\left(N_q+1\right)\tan\phi$	Vesic (1973)
N_γ	$N_\gamma = 1.1\left(N_q-1\right)\tan\left(1.3\phi\right)$	Spangler and Handy (1982)
N_γ	$N_\gamma = e^{\left(-1.646+0.173\phi\right)}$	Ingra and Baecher (1983)
N_γ	$N_\gamma = e^{\left(0.66+5.1\tan\phi\right)}\tan\phi$	Michalowski (1997)
N_γ	$N_\gamma \approx 0.1045e^{9.6\phi}$ ϕ is in radians	Poulos et al. (2001)
N_γ	$N_\gamma = e^{\frac{1}{6}\left(\pi+3\pi^2\tan\varphi\right)}\left(\tan\phi\right)^{\frac{2\pi}{5}}$	Hjiaj et al. (2005)
N_γ	$N_\gamma = \left(N_q-1\right)\tan\left(1.32\phi\right)$	Salgado (2008)

Table 0.2: Summary of Shape and Depth factors

Factors	Equation	Investigator
Shape	For $\phi = 0^0$: $s_c = 1 + 0.2\left(\frac{B}{L}\right)$ $s_q = s_\gamma = 1$ For $\phi \geq 10^0$: $s_c = 1 + 0.2\left(\frac{B}{L}\right)\tan\left(45 + \frac{\phi}{2}\right)^2$ $s_q = s_\gamma = 1 + 0.1\left(\frac{B}{L}\right)\tan\left(45 + \frac{\phi}{2}\right)^2$	Meyerhof (1963)
	$s_c = 1 + \left(\frac{N_q}{N_c}\right)\left(\frac{B}{L}\right)$ [Use N_c and N_q given by Meyerhof (1963)] $s_q = 1 + \left(\frac{B}{L}\right)\tan\phi$ $s_\gamma = 1 - 0.4\left(\frac{B}{L}\right)$	DeBeer (1970), Vesic (1975)
	$s_c = 1 + \left(1.8(\tan\phi)^2 + 0.1\right)\left(\frac{B}{L}\right)^{0.5}$ $s_q = 1 + 1.9(\tan\phi)^2\left(\frac{B}{L}\right)^{0.5}$ $s_\gamma = 1 + \left(0.6(\tan\phi)^2 - 0.25\right)\left(\frac{B}{L}\right) \quad (for\ \phi \leq 30^0)$ $s_\gamma = 1 + \left(1.3(\tan\phi)^2 - 0.5\right)\left(\frac{L}{B}\right)^{1.5} e^{-\left(\frac{L}{B}\right)} \quad (for\ \phi > 30^0)$	Michalowski (1997)
	$s_c = 1 + C_1\left(\frac{B}{L}\right) + C_2\left(\frac{D_f}{B}\right)^{0.5} \quad (for\ \phi = 0)$ *B/L* *C1* *C2*	Salgado et al. (2004)

Factors	Equation	Investigator
	Circle 0.163 0.21 1.0 0.125 0.219 0.5 0.156 0.173 0.33 0.159 0.137 0.25 0.172 0.11 0.2 0.19 0.09	
Depth	For $\phi = 0^0$: $d_c = 1 + 0.2\left(\frac{D_f}{B}\right)$ $d_q = d_\gamma = 1$ For $\phi \geq 10^0$: $d_c = 1 + 0.2\left(\frac{D_f}{B}\right)\tan\left(45 + \frac{\phi}{2}\right)$ $d_q = d_\gamma = 1 + 0.1\left(\frac{D_f}{B}\right)\tan\left(45 + \frac{\phi}{2}\right)$	Meyerhof (1963)
	For $D_f/B \leq 1$: $d_c = 1 + 0.4\left(\frac{D_f}{B}\right)$ $(for\ \phi = 0)$ $d_c = d_q - \frac{1 - d_q}{N_q \tan\phi}$ (for $\phi > 0$) $d_q = 1 + 2\tan\phi(1 - \sin\phi)^2\left(\frac{D_f}{B}\right)$ $d_\gamma = 1$ For $D_f/B > 1$: $d_c = 1 + 0.4\tan^{-1}\left(\frac{D_f}{B}\right)$ $d_q = 1 + 2\tan\phi(1 - \sin\phi)^2\tan^{-1}\left(\frac{D_f}{B}\right)$ where, $\tan^{-1}(D_f/B)$ is in radians $d_\gamma = 1$	Hansen (1970), Vesic (1975)

Factors	Equation	Investigator
	$d_c = 1 + 0.27\left(\frac{D_f}{B}\right)^{0.5}$	Salgado et al. (2004)

2.2.2 Eccentric vertical condition

Meyerhof (1953) proposed an effective width method for foundations subjected to an eccentric load. The ultimate bearing capacity can be expressed as

$$q_u = cN_{cq} + 0.5\gamma B' N_{\gamma q} \quad (2.5)$$

B'= effective depth = B – 2e; γ = density of soil; c = unit cohesion; N_{cq}, $N_{\gamma q}$ = resultant bearing capacity factors for a central load and depend on ϕ and D/B'

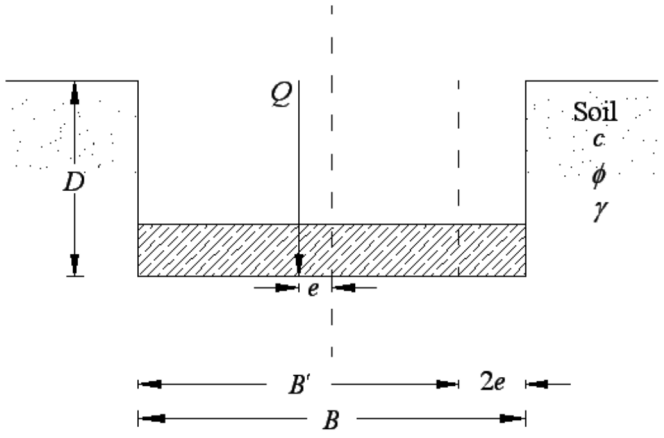

Figure 2.2: Eccentrically loaded strip footing

Prakash and Saran (1971) suggested a comprehensive mathematical formulation to estimate the ultimate bearing capacity of a c–ϕ soil of rough strip foundation under eccentric load is as follows

$$q = cN_{c(e)} + \gamma D_f N_{q(e)} + \frac{1}{2}\gamma B N_{\gamma(e)} \tag{2.6}$$

where $N_{c(e)}$, $N_{q(e)}$, $N_{\gamma(e)}$ are the bearing capacity factors, functions of e/B, ϕ and foundation contact factor x_1.

Purkayastha and Char (1977) performed stability analysis of an eccentrically loaded strip foundation on sand using the method of slices as proposed by Janbu (1957). Based on the analysis, they proposed that

$$R_k = 1 - \frac{q_{u(eccentric)}}{q_{u(centric)}} \tag{2.7}$$

$$\text{Reduction factor, } R_k = a\left(\frac{e}{B}\right)^k \tag{2.8}$$

The values of a and k depends on D_f/B.

Michalowski and You (1998) presented the bearing capacity of eccentrically loaded footings using the kinematic approach of limit analysis. To find the bearing capacity of strip footing, charts are provided between bearing pressure and e/B.

2.2.3 Central Inclined Condition

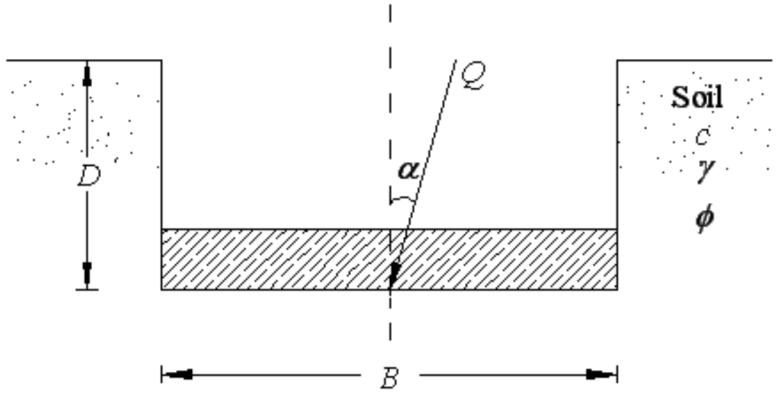

Figure 2.3: Ultimate load Q on a foundation for centric inclined load

Meyerhof (1953) extended his theory for ultimate bearing capacity under vertical loading to the case with inclined load. The ultimate bearing capacity q_u is expressed as vertical component of the ultimate bearing capacity, i.e.

$$q(v) = q\cos\alpha = cN_{cq} + \frac{1}{2}\gamma BN_{\gamma q} \tag{2.9}$$

N_{cq}, $N_{\gamma q}$ are functions of the soil friction angle (ϕ), depth of the foundation (D_f) and load inclination (α).

Meyerhof (1963) proposed that for rough foundations the vertical component of the bearing capacity (q) under a load inclined at an angle of α with the vertical can be expressed as

$$q = cN_c d_c i_c + \gamma DN_q d_q i_q + \frac{1}{2}\gamma BN_\gamma d_\gamma i_\gamma \tag{2.10}$$

where i_c, i_q, i_γ = inclination factors, d_c, d_q, d_γ = depth factors

Hansen (1970) proposed the relationships for inclination factors based on method of characteristics

$$\lambda_{qi} = \left(1 - \frac{0.5Q_u \sin\alpha}{Q_u \cos\alpha + BL\cot\phi}\right)^5 \tag{2.11}$$

$$\lambda_{ci} = \lambda_{qi} - \left(\frac{1-\lambda_{qi}}{N_q - 1}\right) \tag{2.12}$$

$$\lambda_{\gamma i} = \left(1 - \frac{0.7Q_u \sin\alpha}{Q_u \cos\alpha + BLc\cot\phi}\right)^5 \tag{2.13}$$

Dubrova (1973) proposed a equation for the ultimate bearing capacity of a continuous foundation with centric inclined load and is given by

$$q_u = c\left(N_q^* - 1\right)\cot\phi + 2qN_q^* + \gamma BN_\gamma^* \qquad (2.14)$$

The value of N_q^*, N_γ^* are presented in the form of graph with different values of tan α and ϕ.

Muhs and Weiss (1973) conducted field tests and given the ratio of the vertical component $Q_{u(v)}$ of the ultimate load with the inclination α with the vertical to the ultimate load Q_u, when the load is vertical (i.e. α = 0) and is given by

$$\frac{Q_{u(v)}}{Q_{u(v=o)}} = (1 - \tan\alpha)^2 \qquad (2.15)$$

Vesic (1975) proposed equation for inclination factors based on method of characteristics

$$i_c = 1 - \frac{mH}{AcN_c} \text{ for } \phi=0,\ i_c = i_q - \frac{1 - i_q}{Nq - 1} \text{ for } \phi>0 \qquad (2.16)$$

$$i_q = \left(1 - \frac{H}{V + cBL\cot\phi}\right)^m,\ i_\gamma = \left(1 - \frac{H}{V + cBL\cot\phi}\right)^{m+1} \qquad (2.17)$$

Sastry and Meyerhof (1987) carried out model tests to evaluate corresponding inclination factors for a surface strip footing on purely cohesive soil subjected to a central load at an inclination of α_L acting in the direction of the footing length

$$q_{uv} = i_c c_u N_c\ ; \qquad (2.18)$$

$$i_c = \left(1 - \frac{\alpha_L}{90}\right)^2 \qquad (2.19)$$

2.2.4 Eccentric Inclined Condition

Meyerhof (1963) extended the theory to incorporate load eccentricity and inclination for shallow foundations subjected to centric vertical load (Meyerhof 1951). According to his theory, the vertical component of the bearing capacity subjected to eccentric inclined loads is given by

$$q = cN_c s_c d_c i_c + \gamma D N_q s_q d_q i_q + \frac{1}{2}\gamma B' N_\gamma s_\gamma d_\gamma i_\gamma \tag{2.20}$$

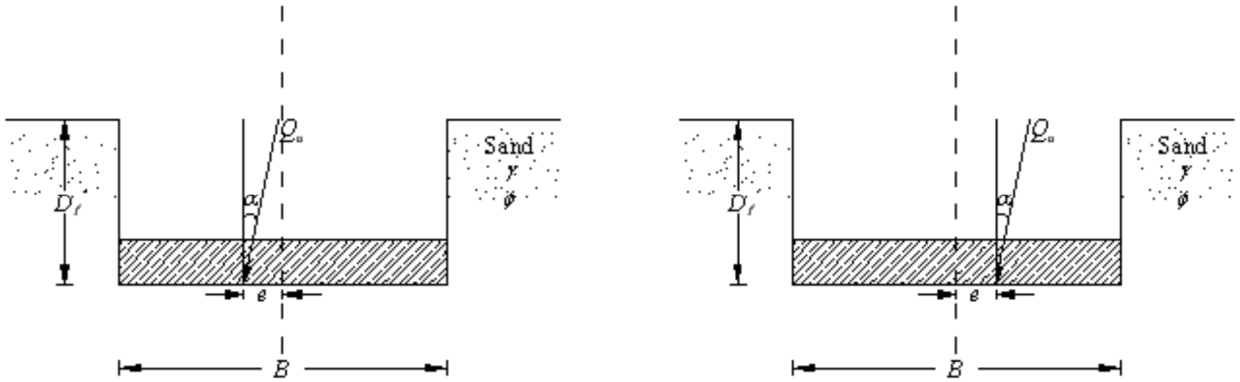

Figure 2.4: Eccentrically inclined load on a strip foundation: line of load application (a) towards the center line and (b) away from the center line of the footing

Saran and Agarwal (1991) used a similar technique to that of Prakash and Saran (1971) to theoretically evaluate the ultimate bearing capacity of a strip foundation subjected to eccentrically inclined load [Figure 2.10]. According to this analysis, the ultimate bearing capacity can be expressed as

$$q_u = cN_c + \gamma D_f N_q + \frac{1}{2}\gamma B N_\gamma \tag{2.21}$$

Bearing capacity factors expressed in terms of e and α.

Loukidis et al. (2008) performed finite element analysis to determine the ultimate bearing capacity of a rigid strip footing subjected to eccentric and inclined loading placed on a purely frictional soil is given by

$$q_{u(e/B,\alpha)} = \frac{1}{2}\gamma B N_{\gamma}\left(\frac{f_{ie}}{\cos\alpha}\right) \tag{2.22}$$

$$f_{ie} = \left[1 - \sqrt{3.7\left(e/B\right)^2 + 2.1(\tan\alpha)^2 + 1.5\frac{e}{B}\tan\alpha}\right]^2 \tag{2.23}$$

Patra et al. (2012a, 2012b) conducted laboratory tests to determine the reduction factor of a rigid strip footing placed on a purely frictional soil subjected to eccentric and inclined loading. The reduction factor for partially compensated case is given by

$$RF = \left[1 - 2\left(\frac{e}{B}\right)\right]\left(1 - \frac{\alpha}{\phi}\right)^{2-\frac{D_f}{B}} \tag{2.24}$$

The reduction factor for reinforced case is given by

$$RF = \left[1 - 2\left(\frac{e}{B}\right)\right]\left(1 - \frac{\alpha}{\phi}\right)^{1.5-0.7\left(\frac{D_f}{B}\right)} \tag{2.25}$$

Viladkar et al. (2013) has carried out a comprehensive parametric study to evaluate the behavior of footings on cohesionless soils and subjected to eccentric-inclined loads considering the non-linear elastic soil behavior and the soil-footing interface characteristics. Based on the data obtained from this parametric study, non-dimensional correlations have been developed for predicting the values of settlement, horizontal displacement, and tilt of eccentrically obliquely loaded footings.

Krabbenhoft et al. (2014) has presented the Lower-bound calculations based on the FEM are used to determine the bearing capacity of a strip foundation subjected to an inclined, eccentric

load on cohesionless soil. The results are reported as graphs showing the bearing capacity as a function of the friction angle, eccentricity, inclination, and surcharge.

2.3 Scope of the present study

The outlines of the analysis and results on the above aspects are discussed in subsequent chapters as mentioned below.

In Chapter 3, the methodology and modeling of test has been discussed.

In Chapter 4, the details of tests sequence are reported and the results of test results have been discussed when the line of load application is towards the center line of the footing. The results are compared with existing theories.

In Chapter 5, the details of tests sequence are reported and the results of test results have been discussed when the line of load application is away from the center line of the footing. The results are compared with existing theories. And comparison of results between partially compensated case with reinforced case have been discussed.

Chapter 6 brings all the conclusions drawn from the above chapters and suggests for future research work.

3. METHODOLOGY AND MODELLING

3.1 INTRODUCTION

Foundation engineering problems can be solved by two different approaches: experimentally, by conducting model and full-scale tests; or, analytically, by using methods such as finite elements. Full-scale tests are the ideal method for obtaining data, however, practical difficulties and economic considerations either eliminate or considerably restrict the possibility of full-scale testing. As an alternative model tests may be employed, but they have disadvantages. The results of these model tests are usually affected by the boundary conditions of the testing box, the size of the footing, the sample disturbance, the test setup and procedure. Due to the fortunate developments in numerical methods and computer programming, it is advantageous to use these techniques to simulate the conditions of model tests to verify the theoretical models. The theoretical study can then be extended to cover a wide range of field cases which engineers omitted using full-scale testing.

In the present study, Numerical analyses will be performed by using the program "Plaxis 3D". It is finite-element based software. The stresses, strains and failure aspects of a given problem can be evaluated by using this software.

3.2 METHODOLOGY

The finite element program Plaxis3D (2013), was used to model the tests of strip footing on granular sand previously described. Plaxis is intended for the analysis of deformation and stability in geotechnical engineering projects. The Mohr–Coulomb model was used for soil and Linear-Elastic model was used for the footing; undrained behavior is adopted for the analysis and

10-node tetrahedral elements were used for the analysis. The parameters used in the analysis are tabulated in Table 3.1 and Table 3.2.

Table 3.1: Soil properties

Sand type	**Unit weight, γ (kN/m³)**	**Relative density of sand (%)**	**Elasticity modulus, E (kN/m²)**	**Poisson's ratio ,ν**	**Friction angle, ϕ (°)**	**Dilatancy angle, ψ (°)**	**Cohesion, c (kN/m²)**
Dense	14.37	69	42000	0.33	40.8	10.8	0
Medium dense	13.97	51	32000	0.32	37.5	7.5	0

Table 3.2: Footing properties

Property	**units**	**Mild Steel plate**
Unit weight (γ)	kN/m^3	78
Young's modulus (E)	kN/m^2	$2*10^8$
Poisson's ratio (ν)		0.3

3.2.1 Modelling

First soil model of size 1m x 0.5m x 0.655m is created and a footing of size 0.1m x 0.5m x 0.03m is placed on the top surface of the soil model at the center. A very fine mesh is generated to the geometry. An incremental loading is applied at the center and top surface of the footing, a point i.e. at the center and top surface of the soil model is selected for the analysis and then analysis is done up to failure occur in the soil. After getting output from the analysis, a load-

settlement curve is drawn and ultimate bearing capacity of the strip footing is found out at that particular loading condition. Same procedure has been adopted for different loading conditions and changing the soil properties to get the ultimate bearing capacity of the strip footing at that particular loading condition.

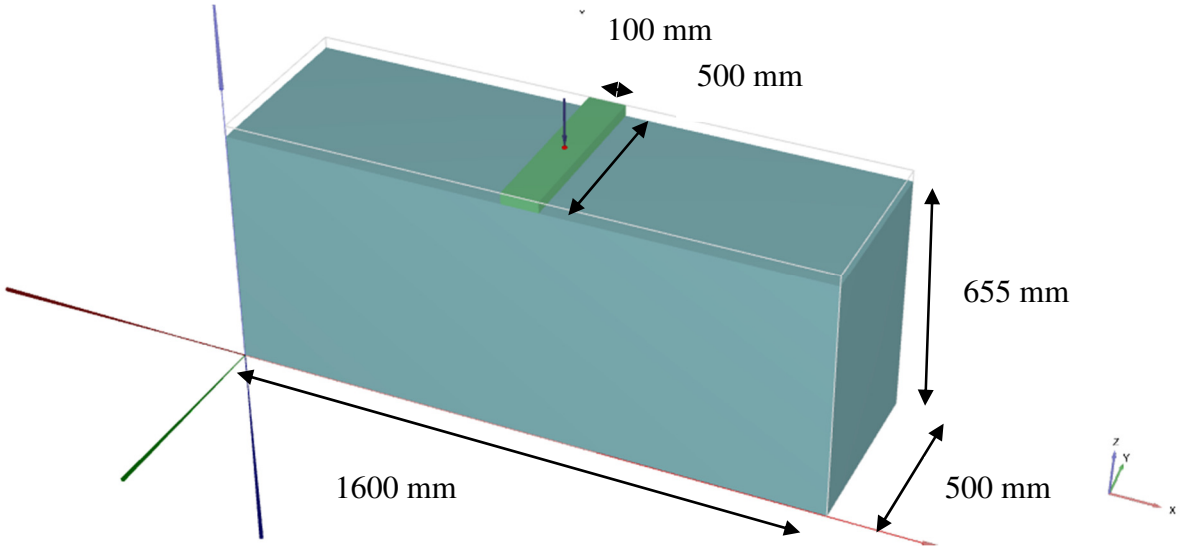

Figure 3.1: Geometric model for central vertical loading case

4. ULTIMATE BEARING CAPACITY OF ECCENTRICALLY INCLINED LOADED STRIP FOOTING WHEN THE LINE OF LOAD APPLICATION IS TOWARDS THE CENTER LINE OF THE FOOTING

4.1 Introduction

An eccentrically inclined load can be applied on the foundation in two ways. When the line of load application is acting inclined on the foundation towards the center line of the foundation [Figure 4.1] and then it can be referred to as *partially compensated* (Perloff and Baron, 1976) soil. To find the effect of load eccentricity and inclination with vertical line, large number of models have been developed on the strip footing supported by different density of sands (dense sand and medium dense sand). Based on the analysis of numerical models result, the numerical models results have been compared with developed non-dimensional reduction factor of Patra et al. (2012a), which will be used for estimating the ultimate bearing capacity. The developed reduction factor from the model tests results is also compared with the available theoretical and numerical approaches.

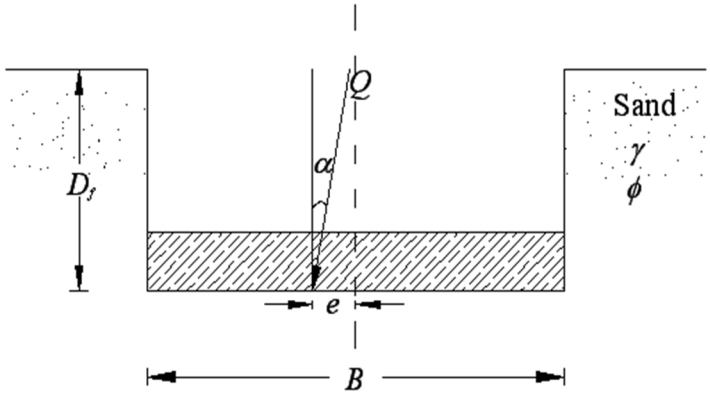

Figure 4.1: Eccentrically inclined load on strip foundation: line of load application towards the center line of the footing

4.2 Numerical Module

One hundred and twenty numbers of numeric models were developed under the condition when the line of load application is towards the center line of the footing. The detail sequence of numerical models in this condition are shown in Table 4.1 for dense sand and medium dense sand.

Table 4.1: Sequence of numerical models for Dense and Medium sand in *Partially Compensated* condition

D_f/B	e/B	α°	**Model No.**	
			Dense	**Medium**
0	0	0,5,10,15,20	1-5	61-65
0	0.05	0,5,10,15,20	6-10	66-70
0	0.1	0,5,10,15,20	11-15	71-75
0	0.15	0,5,10,15,20	16-20	76-80
0.5	0	0,5,10,15,20	21-25	81-85
0.5	0.05	0,5,10,15,20	26-30	86-90
0.5	0.1	0,5,10,15,20	31-35	91-95
0.5	0.15	0,5,10,15,20	36-40	96-100
1	0	0,5,10,15,20	41-45	101-105
1	0.05	0,5,10,15,20	46-50	106-110
1	0.1	0,5,10,15,20	51-55	111-115
1	0.15	0,5,10,15,20	56-60	116-120

4.3 Model Test Results

4.3.1 Central Vertical Loading Conditions

Nine number of numerical models were developed in central vertical condition (i.e. e/B =0, α = 0º). The details of the model parameters are shown in Table 4.2. Basically there are five different methods to interpret the ultimate bearing capacity from the load-settlement curve namely Log-Log method (DeBeer 1970), Tangent Intersection method (Trautmann and Kulhawy 1988), 0.1B method (Briaud and Jeanjean 1994), Hyperbolic method (Cerato 2005), and Break Point method

(Mosallanezhad et al. 2008)., the ultimate bearing capacity is determined by Break Point method [Figure 4.2] for the present test results, as after the point of "failure load" with small increase in load significant increase in settlement occurs.

Table 4.2: Numerical model parameters for Centric Vertical Loading condition

Sand type	**Unit weight, γ (kN/m³)**	**Relative density of sand (%)**	**Elasticity modulus, E (kN/m²)**	**Poisson's ratio , ν**	**Friction angle, ϕ (°)**	**Dilatancy angle, ψ (°)**	***Df/B***	***e/B***	***α*** **(°)**
Dense	14.37	69	42000	0.33	40.8	10.8	0	0	0
							0.5		
							1		
Medium dense	13.97	51	32000	0.32	37.5	7.5	0	0	0
							0.5		
							1		

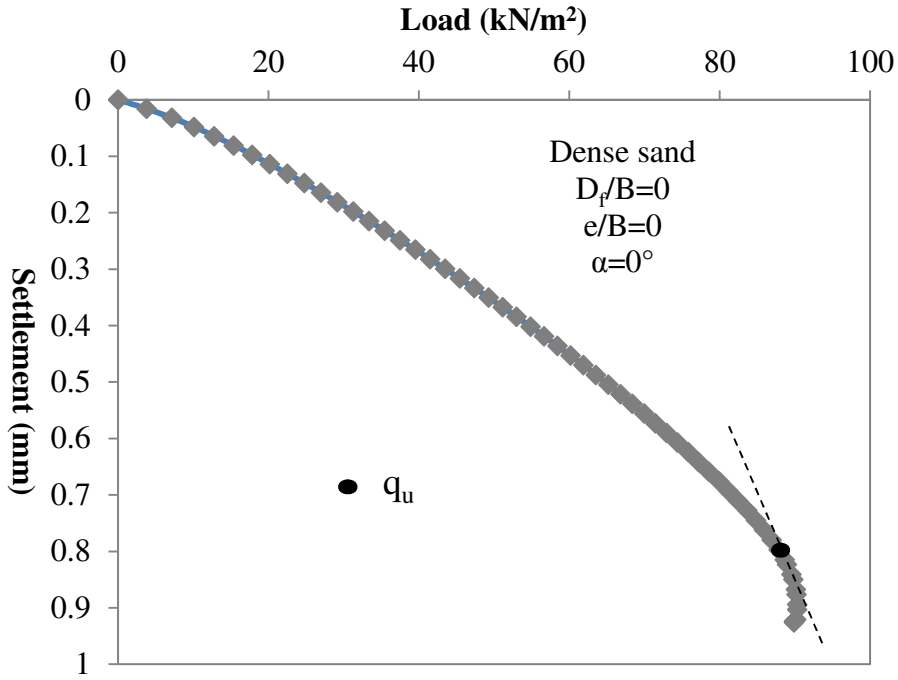

Figure 4.2: Interpretation of Ultimate bearing capacity q_u by Break Point method (Mosallanezhad et al. 2008).

The bearing capacity of footing increases with the increase in depth of embedment as well as relative density of sand has seen from Figures 4.3 and 4.4.

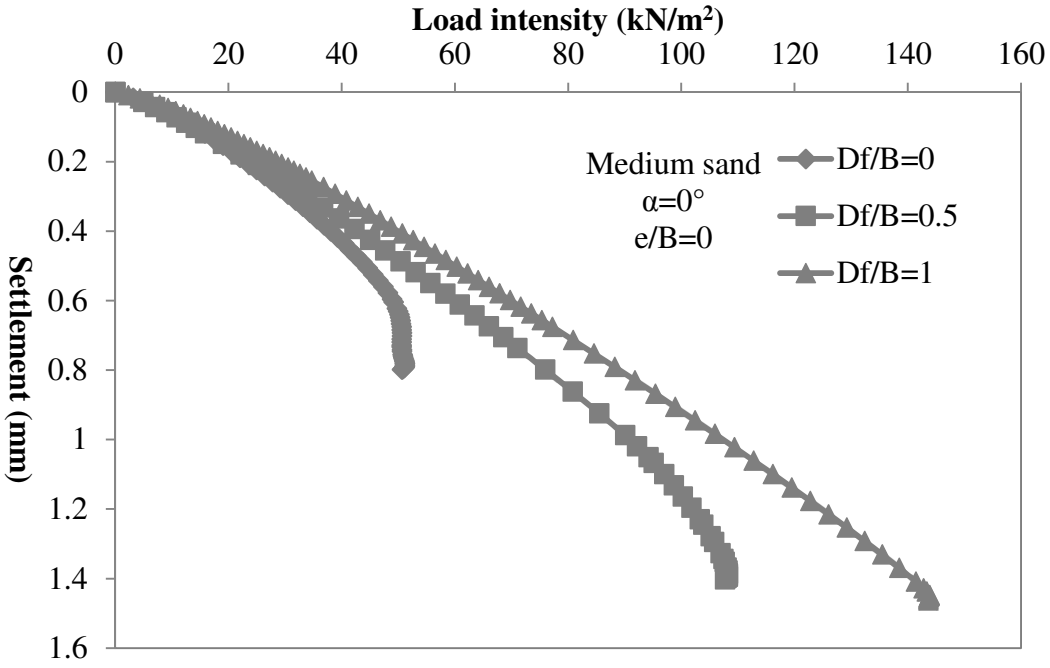

Figure 4.3: Variation of load-settlement curve with embedment ratio (D_f/B) at e/B=0 and α=0° in Medium dense sand

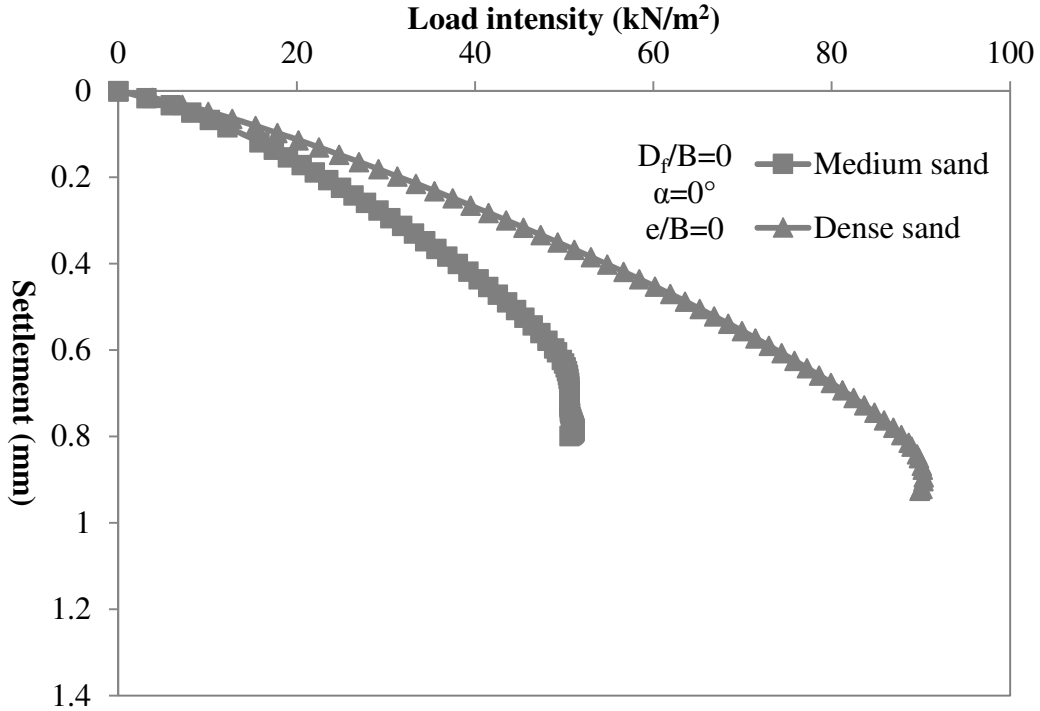

Figure 4.4: Variation of load-settlement curve with Relative Density (D_r) of sand at D_f/B=0, e/B=0 and α=0°

The ultimate bearing capacities for centric vertical loading (e/B = 0, α = 0°) at D_f/B = 0, 0.5 and 1.0 for dense and medium dense obtained using the expressions of existing theories. The values

are plotted in Figure 4.5 and also presented in Table 4.3 and 4.4. It can be seen that model tests bearing capacities for a given D_f/B are significantly in the range of existing theories values. Unlike experimental results, there is no scale effect associated with the model tests.

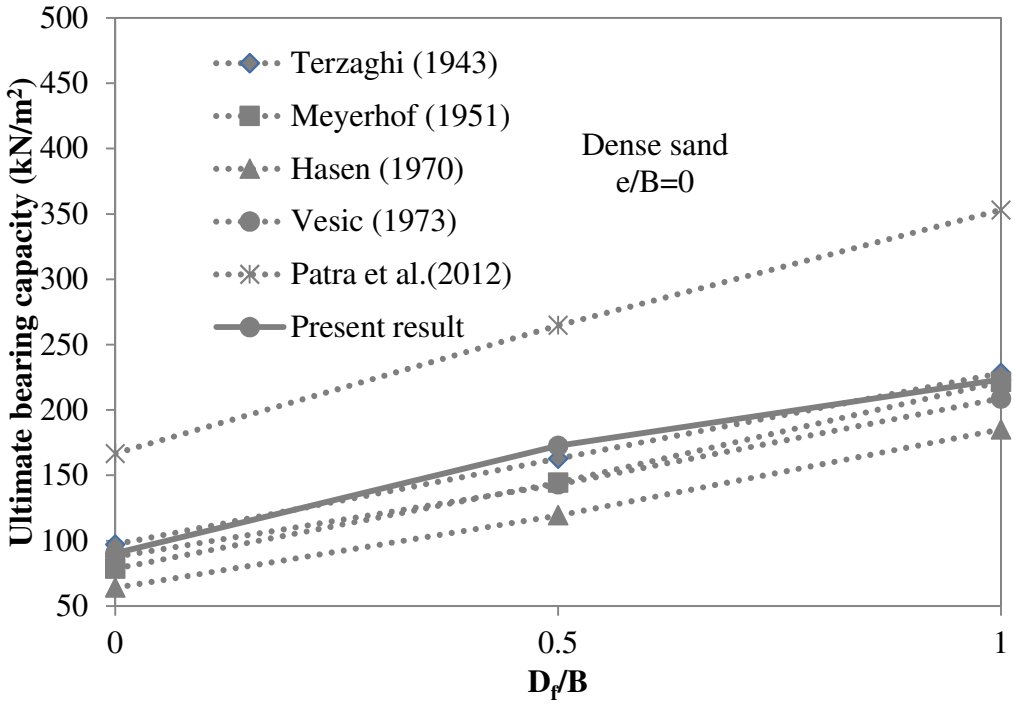

(a)

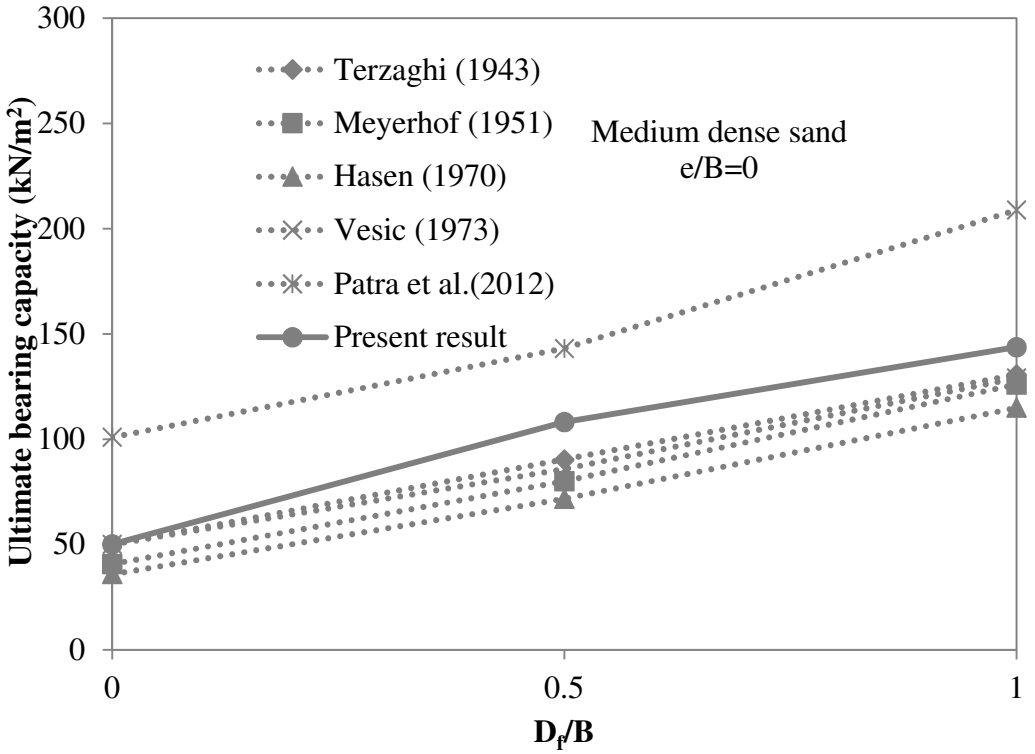

(b)

Figure 4.5: Variation of q_u with D_f/B for $\alpha = 0°$ and $e/B = 0$ using formulae of existing theories along with present model test values for (a) dense (b) medium dense sand

Table 4.3: Calculated values of ultimate bearing capacities q_u by Terzaghi (1943), Meyerhof (1951) and Hansen (1970) for centric vertical condition

e/B	D_f/B	Terzaghi (1943); q_u (kN/m²)		Meyerhof (1951); q_u (kN/m²)		Hansen (1970); q_u (kN/m²)	
		$\phi=37.5^o$	$\phi=40.8^o$	$\phi=37.5^o$	$\phi=40.8^o$	$\phi=37.5^o$	$\phi=40.8^o$
0	0	50.25	97.28	40.79	78.72	36.03	64.05
0	0.5	90.53	162.87	80.17	144.56	71.78	119.43
0	1	130.82	228.45	126.04	221.67	115.06	185.20

Table 4.4: Calculated values of ultimate bearing capacities q_u by Vesic (1973), Patra et al. (2012) for centric vertical condition along with Present results

e/B	D_f/B	Vesic (1973); q_u (kN/m²)		Patra et al. (2012); q_u (kN/m²)		Present result; q_u (kN/m²)	
		ϕ=33°	ϕ=37.5°	ϕ=37.5°	ϕ=40.8°	ϕ=33°	ϕ=37.5°
0	0	23.63	50.18	101.04	166.77	22.20	50.16
0	0.5	43.51	85.94	143.23	264.87	53.28	108.20
0	1	68.11	129.21	208.95	353.16	72.60	143.86

The observed failure surface for footing resting on dense sand in centric vertical condition (i.e. D_f/B=0, α=0°, e/B=0) is shown in Figure 4.6. Up to a depth of B the effect of applied load is prominent beyond that it gradually decreases and at a depth of 2B it almost diminishes.

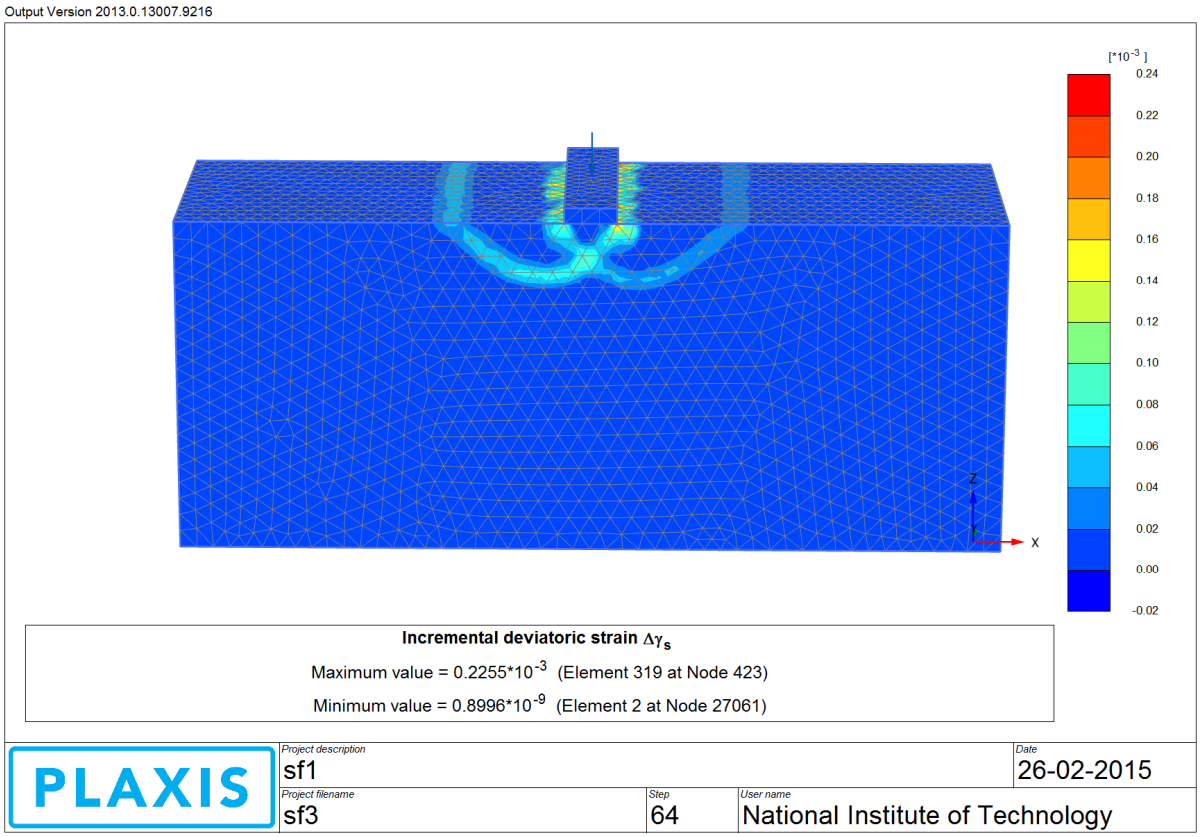

Figure 4.6: Failure surface observed in medium dense sand in surface condition at $D_f/B = 0$, $\alpha = 0°$ and $e/B = 0$

4.3.2 Eccentric Vertical Loading Conditions

Thirty two numbers of model tests are developed in eccentric vertical condition. The details of the numerical model parameters are shown in Table 4.5. The developed numerical model for one case of eccentric vertical loading condition is as shown in Figure 4.7. The load settlement curves of strip foundations (α=0° and *e/B*=0, 0.05, 0.1 and 0.15) on dense sand in surface condition are plotted in Figure 4.8. The load carrying capacity decreases with increase in *e/B* ratio. Similarly, Figures 4.9 and 4.10 show the variation of load-settlement curve with depth of embedment (D_f */B*) and relative density of sand respectively.

Table 4.5: Model test parameters for Eccentric Vertical Loading condition

Sand type	**Unit weight,γ (kN/m^3)**	**Relative density of sand (%)**	**Friction angle, ϕ (°)**	**D_f/B**	**e/B**	**α (°)**
Dense	14.37	69	40.8	0 0.5 1	0 0.05 0.1 0.15	0
Medium dense	13.97	51	37.5	0 0.5 1	0 0.05 0.1 0.15	0

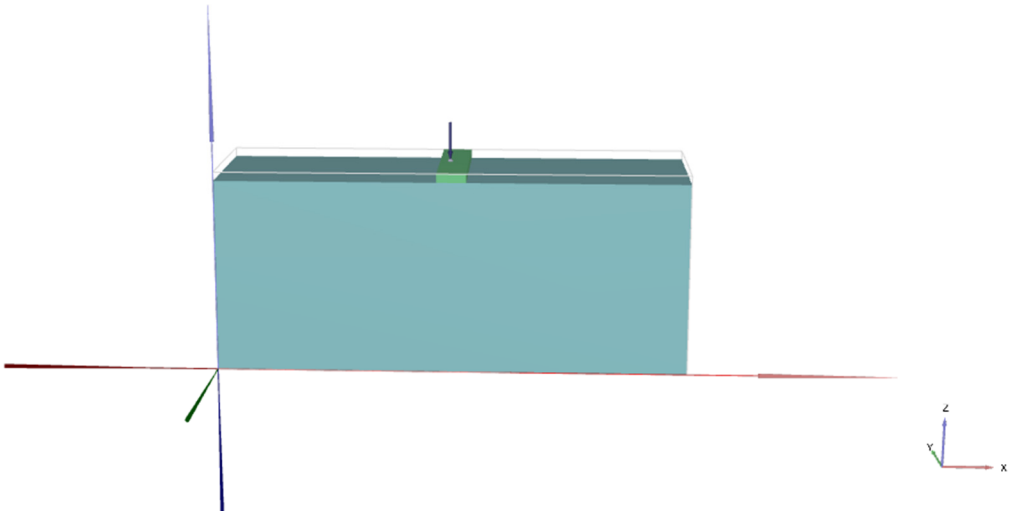

Figure 4.7: Developed numerical model for eccentric vertical loading condition

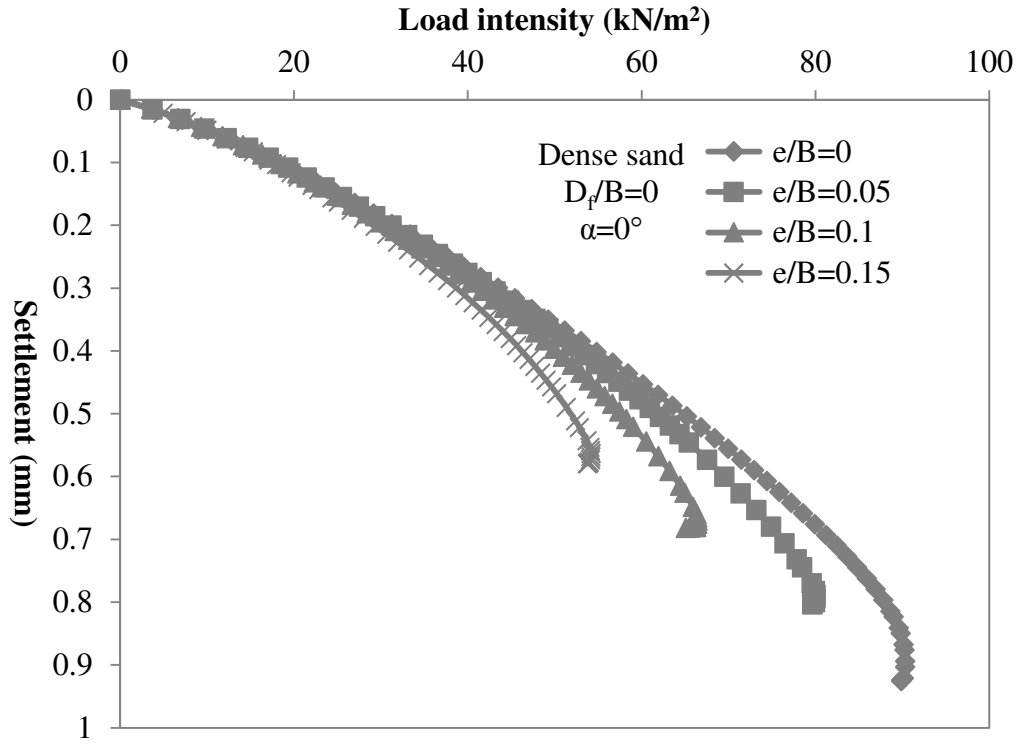

Figure 4.8: Variation of load-settlement curve with eccentricity in dense sand in surface condition for α=0°

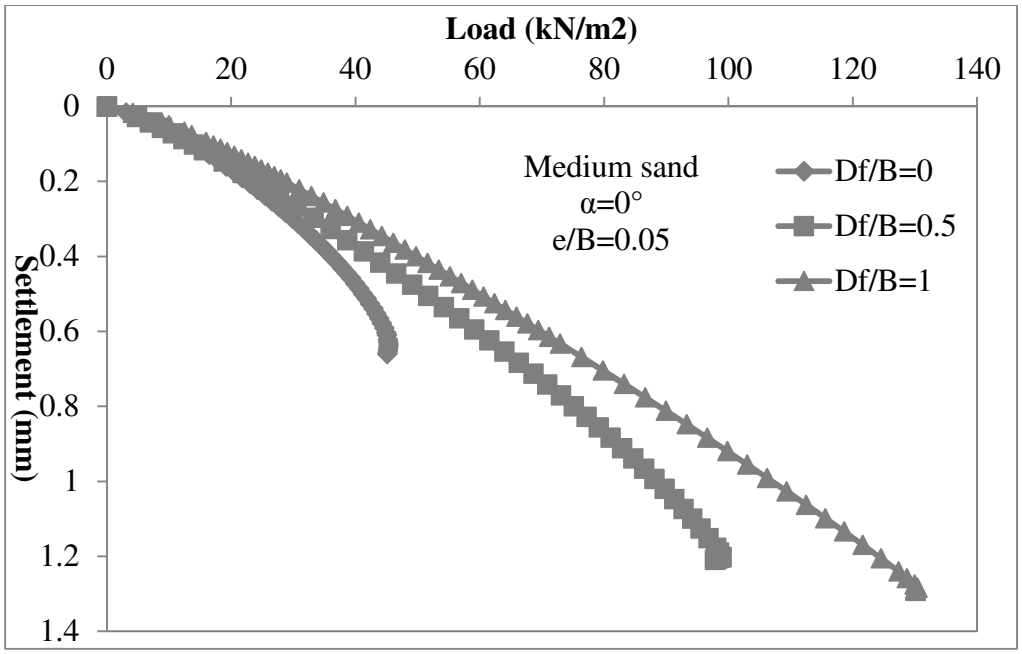

Figure 4.9: Effect of embedment on eccentricity in Medium sand for α=0°, *e/B*=0.05

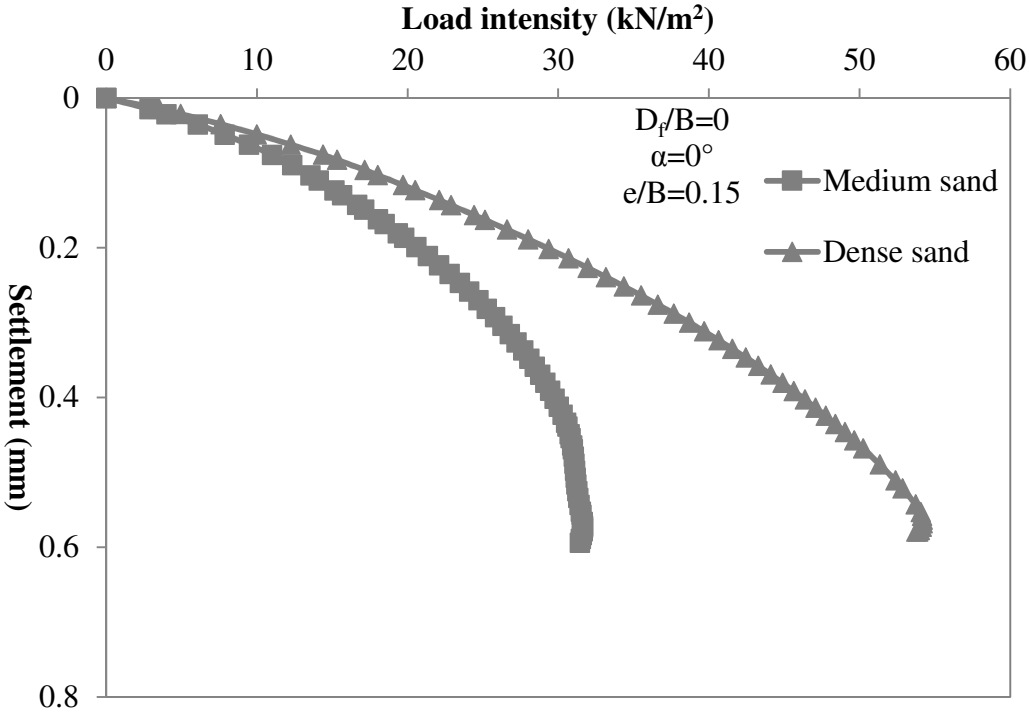

Figure 4.10: Variation of load settlement curve with relative density for α=0°, *e/B*=0.15 and D_f/B=1

The numerical models ultimate bearing capacities for eccentrically loaded foundations (*e/B*=0, 0.05, 0.1 and 0.15, D_f/B = 0, 0.5 and 1, and D_r = 69%, 51%) are plotted along with the bearing

capacities obtained by using existing theories. The results are shown Figure 4.11 and Table 4.6 and Table 4.7. The nature of decrease of bearing capacity with the increase in eccentricity as observed from numerical models results are in good agreement with those existing theories. The observed failure surface for footing resting on dense sand in eccentric vertical condition (i.e. D_f/B=0, α=0°, e/B=0.1) is shown in Figure 4.13.

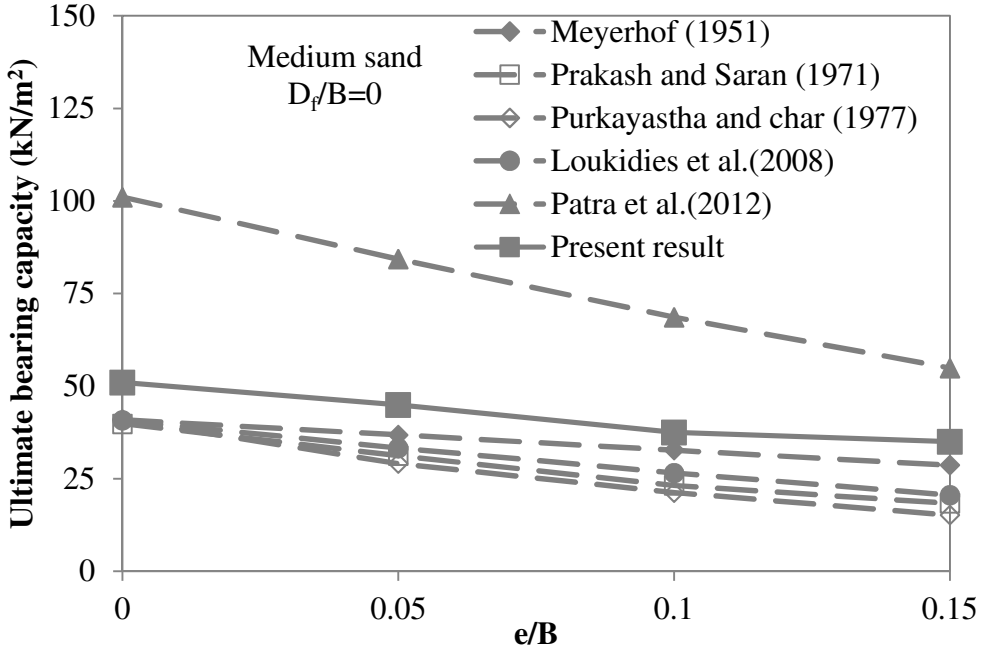

(a)

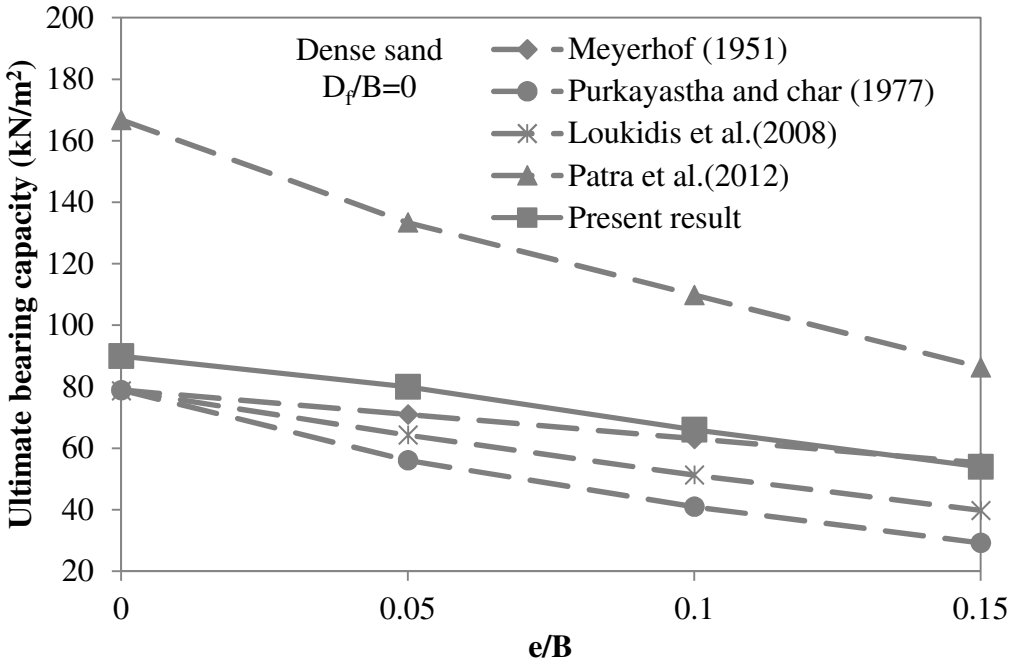

(b)

Figure 4.11: Comparison of ultimate bearing capacities of Present results with existing theories for (a) medium and (b) dense sand

Table 4.6: Calculated values of ultimate bearing capacities q_u by Meyerhof (1951), Prakash and Saran (1971) and Purkayastha and Char (1977) for centric vertical condition

e/B	***D_f/B***	**Meyerhof (1951); q_u (kN/m²)**		**Prakash and Saran (1971); q_u(kN/m²)**	**Purkayastha and Char (1977); q_u (kN/m²)**	
		ϕ=37.5º	**ϕ=40.8º**	**ϕ=37.5°**	**ϕ=37.5º**	**ϕ=40.8º**
0	0	40.98	78.94	39.88	40.98	78.94
0.05	0	36.88	71.05	31.29	29.14	56.13
0.1	0	32.78	63.15	23.26	21.31	41.05
0.15	0	28.69	55.26	18.44	15.21	29.29
0	0.5	80.45	144.86	76.69	80.45	144.86
0.05	0.5	75.94	136.1	63.63	63.79	114.32
0.1	0.5	71.43	127.35	52.32	51.43	91.69
0.15	0.5	66.91	118.59	43.44	41.48	73.53
0	1	126.42	222.04	113.5	126.42	222.04
0.05	1	121.5	212.43	95.97	105.71	184.81
0.1	1	116.57	202.81	81.37	88.59	154.14
0.15	1	111.64	193.2	68.45	73.68	127.51

Table 4.7: Calculated values of ultimate bearing capacities q_u by Loukidis et al. (2008), Patra et al. (2012) for centric vertical condition along with Present results

e/B	***D_f/B***	**Loukidis et al. (2008); q_u (kN/m²)**		**Patra et al. (2012); q_u (kN/m²)**		**Present result; q_u (kN/m²)**	
		ϕ=37.5º	**ϕ=40.8º**	**ϕ=37.5º**	**ϕ=40.8º**	**ϕ=37.5º**	**ϕ=40.8º**
0	0	40.79	78.72	101.04	166.77	51	90
0.05	0	33.32	64.31	84.37	133.42	45	80
0.1	0	26.61	51.35	68.67	109.87	37.5	66
0.15	0	20.65	39.85	54.94	86.33	35	54
0	0.5			143.23	264.87	108	172
0.05	0.5			123.61	226.61	99	164
0.1	0.5			103.99	195.22	90	150
0.15	0.5			87.31	164.81	81	140
0	1			208.95	353.16	144	223.3
0.05	1			193.26	313.92	130	196
0.1	1			175.60	278.60	120	159
0.15	1			156.96	245.25	110	144

The experimental reduction factor (*RF*) given by Purkayastha and Char (1977) are presented in Figure 4.11 and Table 4.8. The comparisons of reduction factor obtained from two approaches are reasonably good.

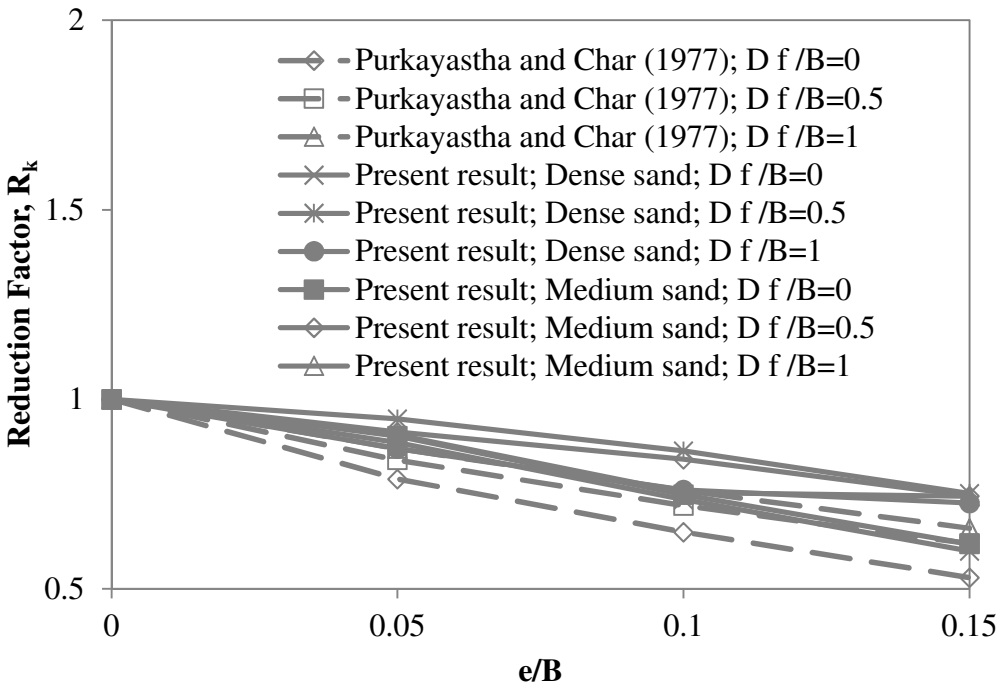

Figure 4.12: Comparison of Present model test results with Purkayastha and Char (1977)

Table 4.8: Calculated values of R_k by Purkayastha and Char (1977) for eccentric vertical condition along with Present results

e/B	D_f/B	**Present result**		**Purkayastha and Char (1977)**
		RF		R_k
		ϕ**=37.5º**	ϕ**=40.8º**	
0	0	1	1	1
0.05	0	0.903	0.886	0.79
0.1	0	0.748	0.736	0.65
0.15	0	0.618	0.600	0.53
0	0.5	1	1	1
0.05	0.5	0.914	0.948	0.84
0.1	0.5	0.843	0.864	0.72
0.15	0.5	0.745	0.752	0.62
0	1	1	1	1
0.05	1	0.906	0.870	0.87
0.1	1	0.754	0.761	0.76
0.15	1	0.744	0.727	0.66

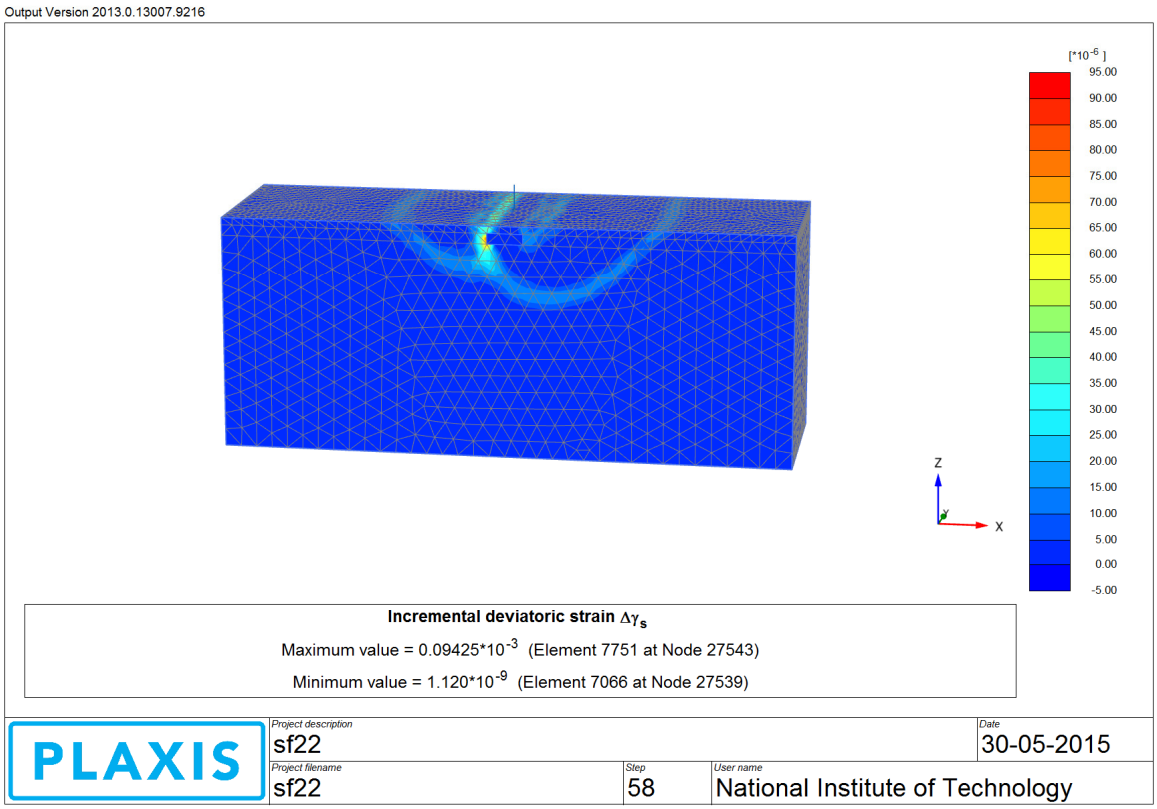

Figure 4.13: Failure surface observed in dense sand
at $D_f/B = 0.5$, $\alpha = 0°$ and $e/B = 0.15$

4.3.3 Centric Inclined Loading Condition

Thirty numbers of model tests are developed on central inclined loading condition. The detailed parameters are mentioned in Table 4.9. The developed numerical model for one case of centric inclined loading condition is as shown in Figure 4.14. Figures 4.15 and 4.16 show the variation of load intensity vs. settlement at various load inclination in surface condition for dense and medium dense respectively. It is seen from graphs for dense and medium dense that at any embedment ratio (D_f/B), the load carrying capacity decreases with increase in load inclination. Similarly, Figures 4.17 and 4.18 show the variation of ubc with embedment ratio (D_f/B) and relative density (D_r) of sand respectively. As the embedment ratio (D_f/B) and relative density of sand increases, the load carrying capacity increases.

Table 4.9: Model test parameters for Centric Inclined Loading condition

Sand type	**Unit weight,γ (kN/m³)**	**Relative density of sand (%)**	**Friction angle, ϕ (°)**	***D_f/B***	***e/B***	***α*** **(°)**
Dense	14.37	69	40.8	0 0.5 1	0	0 5 10 15 20
Medium dense	13.97	51	37.5	0 0.5 1	0	0 5 10 15 20

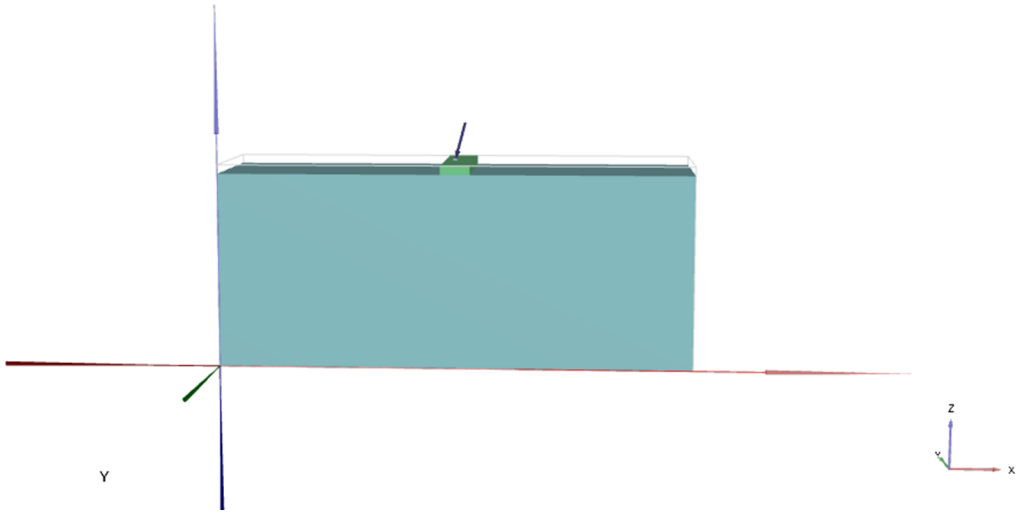

Figure 4.14: Developed numerical model for centric inclined loading condition

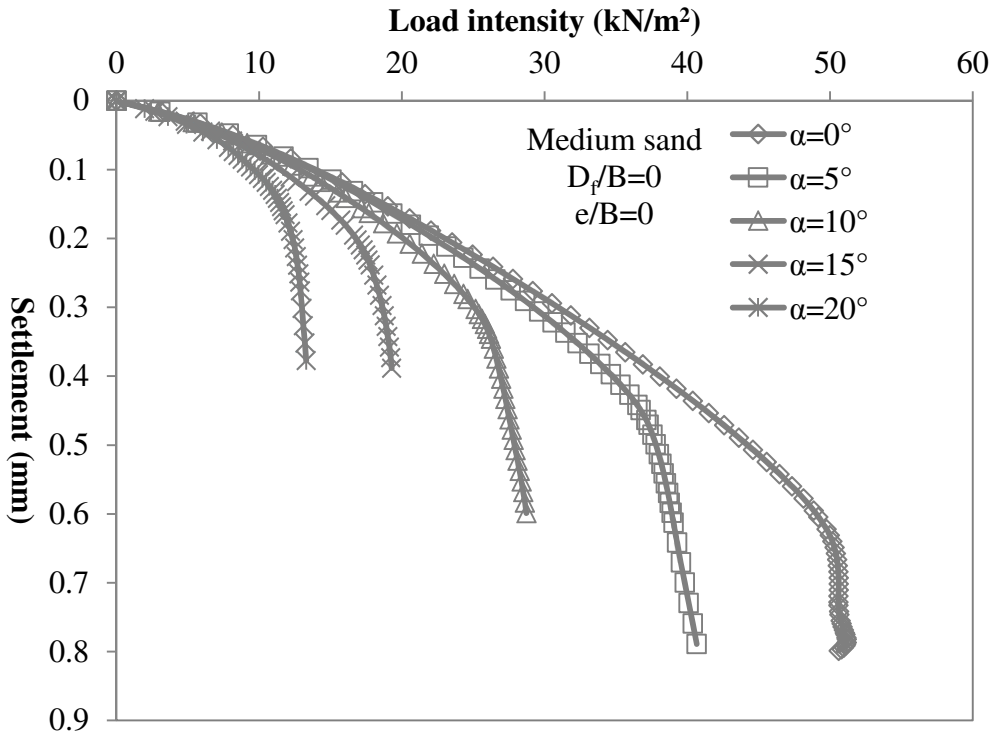

Figure 4.15: Variation of load settlement curve with load inclination (α) in medium sand for D_f/B=0 and e/B=0

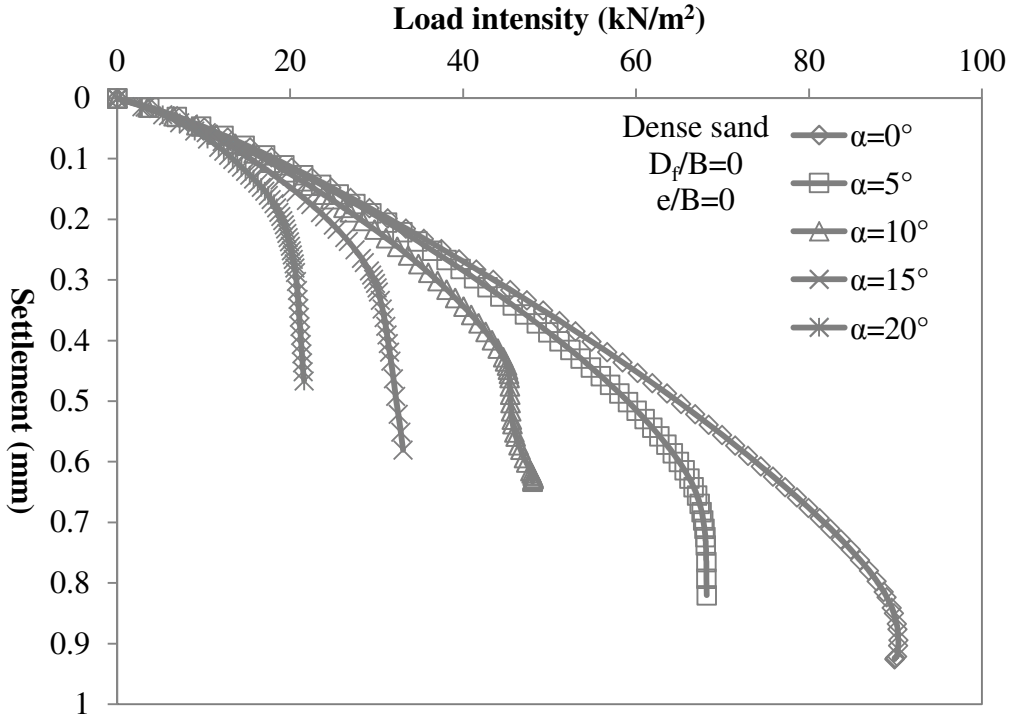

Figure 4.16: Variation of load-settlement curve with load inclination (α) in dense sand for D_f/B=0 and e/B=0

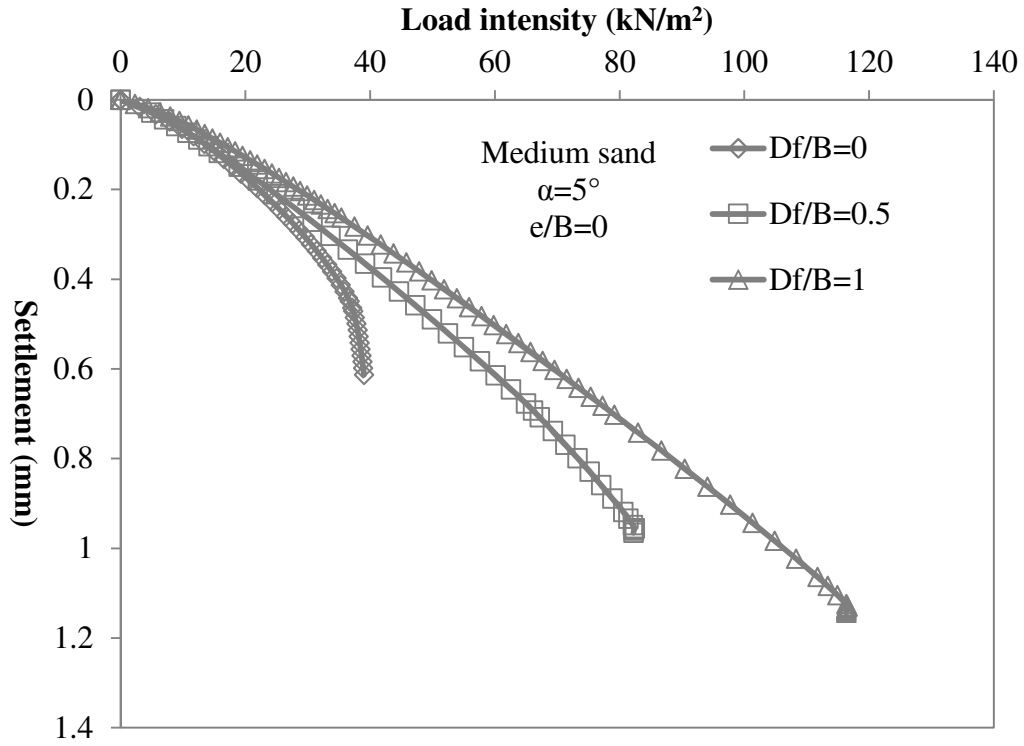

Figure 4.17: Variation of load-settlement curve with embedment ratio (D_f/B) in medium dense sand for $\alpha = 5°$, e/B=0

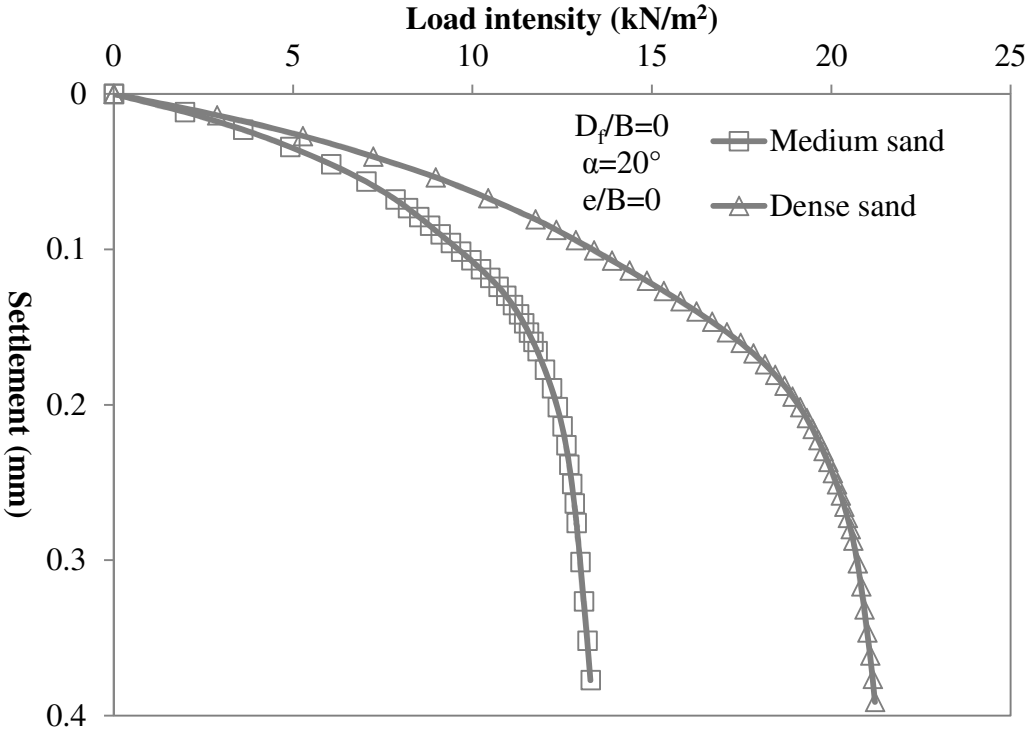

Figure 4.18: Variation of load-settlement curve with relative density of sand at α=20°, e/B = 0 and D_f/B=0

A comparison of the nature of variation of ultimate bearing capacities obtained from the model tests and those computed using various existing theories have been made and explained below. It is to be noted that in existing theories, q_u denotes the vertical component of the inclined load, whereas in the present model tests, q_u is considered as inclined load. So, in order to compare model test values with the values obtained using various theories, present numerical model value of q_u is multiplied with cosα (α is the load inclination with the vertical).

The calculated bearing capacity values as per Meyerhof (1963), Hansen (1970), Vesic (1975), Loukidis et al. (2008) and Patra et al. (2012) are shown in Figures 4.19 along with present values. The above comparison is also shown in Table 4.10 and Table 4.11. The numerical model values are significantly in the range of existing theories. The observed failure surface for footing resting on medium dense sand in centric inclined condition (i.e. D_f/B=0, α=10°, e/B=0) is shown in Figure 4.21.

Table 4.10: Calculated values of ultimate bearing capacities (q_u) by using formulae of existing theories for centric inclined condition along with Present numerical model values

α°	e/B	D_f/B	**Meyerhof (1963); q_u (kN/m^2)**		**Hansen (1970); q_u (kN/m^2)**		**Vesic (1975); q_u (kN/m^2)**	
			ϕ=37.5°	**ϕ=40.8°**	**ϕ=37.5°**	**ϕ=40.8°**	**ϕ=37.5°**	**ϕ=40.8°**
0	0	0	40.79	78.72	36.03	64.05	50.18	87.82
5	0	0	30.64	60.61	26.27	46.70	38.72	67.75
10	0	0	21.94	44.86	18.64	33.15	28.96	50.69
15	0	0	14.69	31.48	12.75	22.67	20.74	36.29
20	0	0	8.88	20.46	8.28	14.72	13.92	24.37
0	0	0.5	80.17	144.56	71.78	119.43	85.94	143.19
5	0	0.5	65.18	118.29	54.86	90.97	68.95	114.57
10	0	0.5	52.01	94.99	41.18	68.05	54.02	89.49
15	0	0.5	40.65	74.67	30.17	49.65	40.93	67.55
20	0	0.5	31.10	57.32	21.38	35.00	29.53	48.53
0	0	1	126.04	221.67	115.06	185.20	129.21	208.96
5	0	1	105.51	186.02	89.46	143.57	105.54	170.18

α°	e/B	D_f/B	Meyerhof (1963); q_u (kN/m^2)		Hansen (1970); q_u (kN/m^2)		Vesic (1975); q_u (kN/m^2)	
			ϕ=37.5°	ϕ=40.8°	ϕ=37.5°	ϕ=40.8°	ϕ=37.5°	ϕ=40.8°
10	0	1	87.21	154.02	68.46	109.52	84.35	135.59
15	0	1	71.12	125.68	51.25	81.69	65.36	104.69
20	0	1	57.25	101.00	37.23	59.10	48.41	77.22

Table 4.11: Calculated values of ultimate bearing capacities (q_u) by using formulae of existing theories for centric inclined condition along with Present numerical model values

α°	e/B	D_f/B	Loukidis et al. (2008); q_u (kN/m^2)		Patra et al. (2012); q_u (kN/m^2)		Present result; q_u (kN/m^2)	
			ϕ=37.5°	ϕ=40.8°	ϕ=37.5°	ϕ=40.8°	ϕ=37.5°	ϕ=40.8°
0	0	0	40.79	78.72	101.04	166.77	51.00	90.00
5	0	0	31.22	60.25	79.16	128.02	38.00	68.00
10	0	0	22.96	44.30	55.07	94.68	26.00	46.00
15	0	0	15.80	30.50	36.96	64.44	19.50	31.00
20	0	0	9.69	18.71	22.59	40.56	13.00	20.80
0	0	0.5			143.23	264.87	108.00	172.00
5	0	0.5			120.20	222.82	92.00	154.00
10	0	0.5			96.61	183.56	75.00	120.00
15	0	0.5			76.76	145.93	55.00	84.00
20	0	0.5			54.76	108.78	42.00	63.00
0	0	1			208.95	353.16	144.00	223.30
5	0	1			185.68	312.73	116.00	174.00
10	0	1			158.44	260.85	90.00	125.00
15	0	1			128.88	217.95	77.00	116.00
20	0	1			92.19	172.40	60.00	90.00

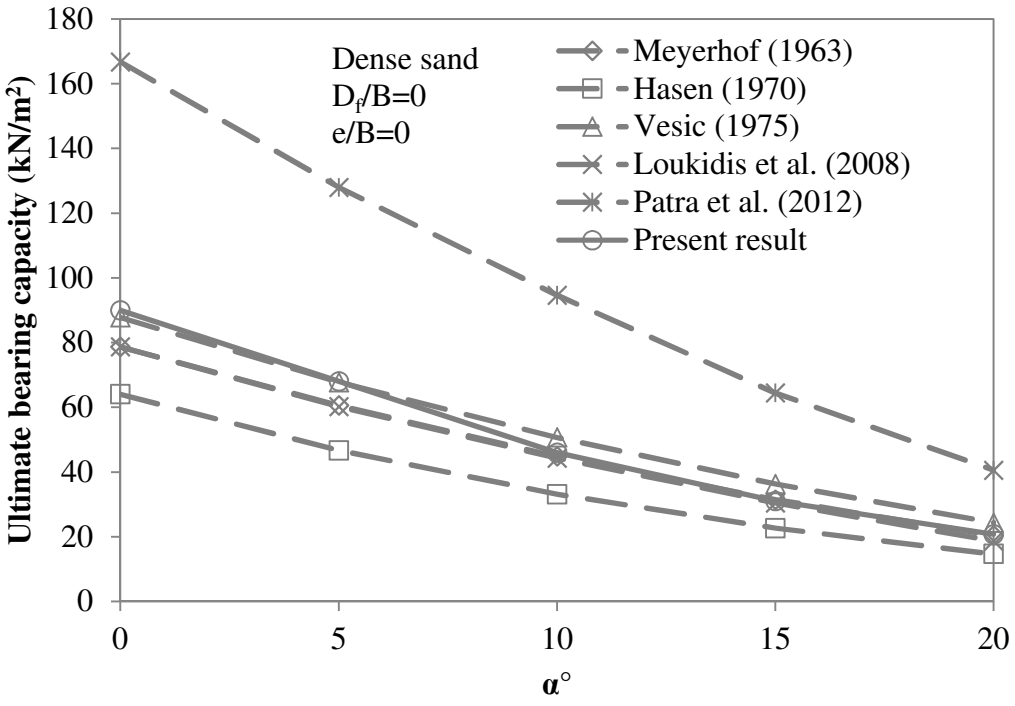

(a)

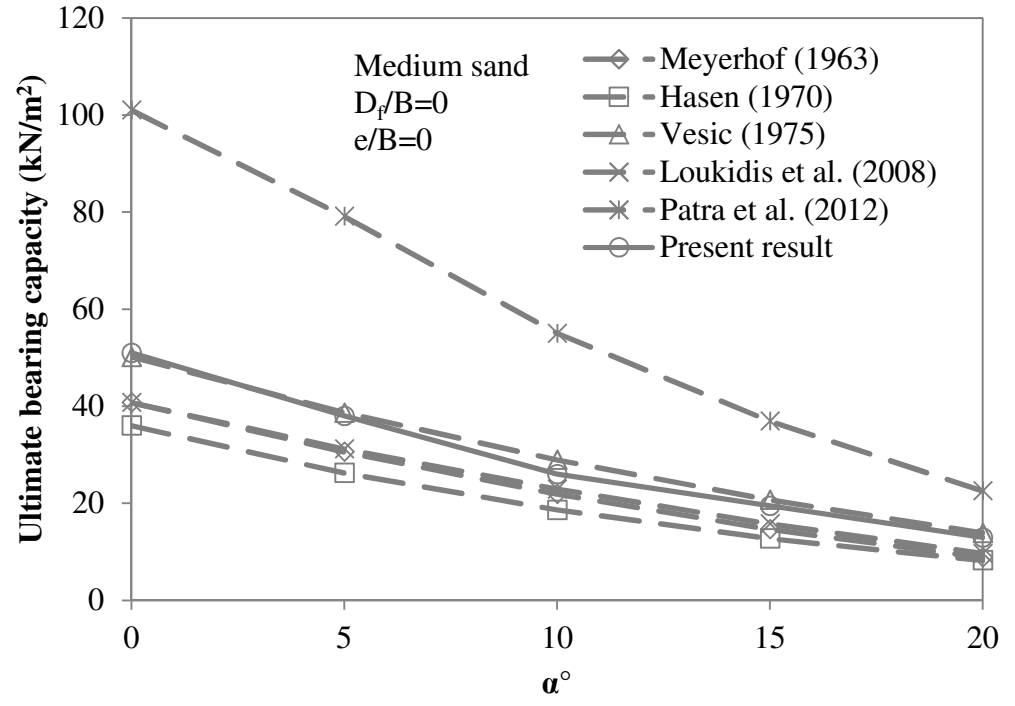

(b)

Figure 4.19: Comparison of ultimate bearing capacities of Present results with existing theories for (a) medium and (b) dense sand

Muhs and Weiss (1973) has given the ratio ($q_{u(v)}/q_{u(\alpha=0)}$) and plotted in Figure 4.20 along with present values for different load inclination (α=0-20°). The values are shown in Table 4.12. The computed values as per Muhs and Weiss (1973) are in good agreement with present numerical model values for dense and medium sand.

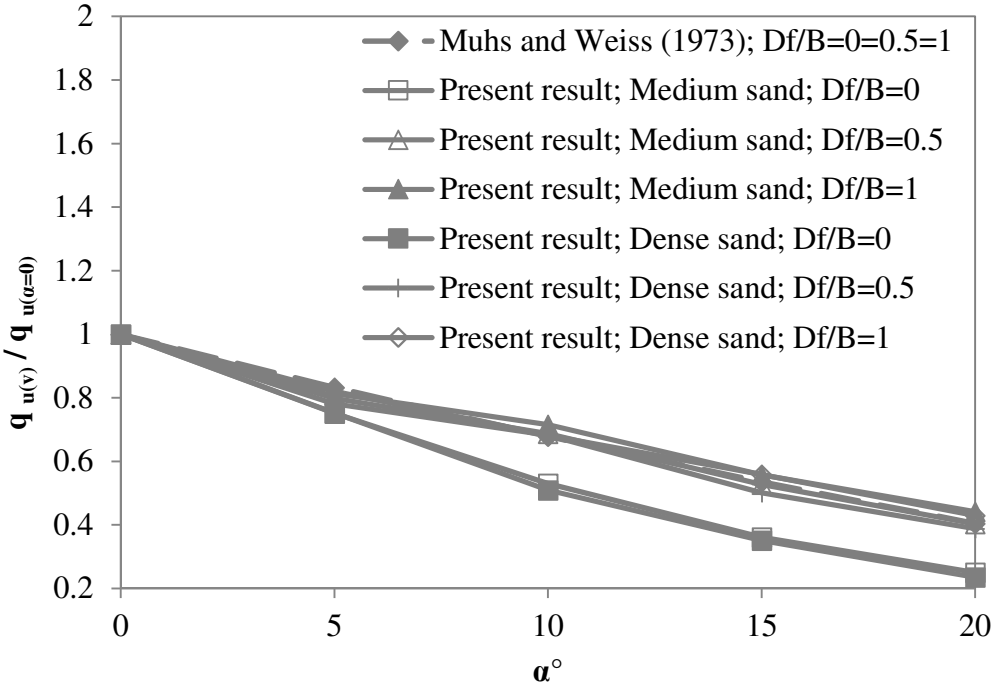

Figure 4.20: Comparison of Present numerical models results with Muhs and Weiss (1973)

Table 4.12: Calculated values of Muhs and Weiss (1973) ratio for centric inclined condition along with Present numerical models values

Inclination (α)	***e/B***	***D_f/B***	**Muhs and Weiss (1973)**	**Present result**	
				RF	
			$q_{u(v)}/q_{u(\alpha=0)} = (1-\tan\alpha)^2$	**ϕ=37.5°**	**ϕ=40.8°**
0	0	0	1	1	1
5	0	0	0.833	0.750	0.752
10	0	0	0.678	0.530	0.509
15	0	0	0.536	0.361	0.351
20	0	0	0.405	0.250	0.236
0	0	0.5	1	1	1

Inclination (α)	e/B	D_f/B	Muhs and Weiss (1973)	Present result	
				RF	
			$q_{u(v)}/q_{u(\alpha=0)} = (1-\tan\alpha)^2$	ϕ=37.5°	ϕ=40.8°
5	0	0.5	0.833	0.798	0.820
10	0	0.5	0.678	0.687	0.682
15	0	0.5	0.536	0.527	0.501
20	0	0.5	0.405	0.403	0.388
0	0	1	1	1	1
5	0	1	0.833	0.813	0.781
10	0	1	0.678	0.716	0.682
15	0	1	0.536	0.558	0.559
20	0	1	0.405	0.441	0.430

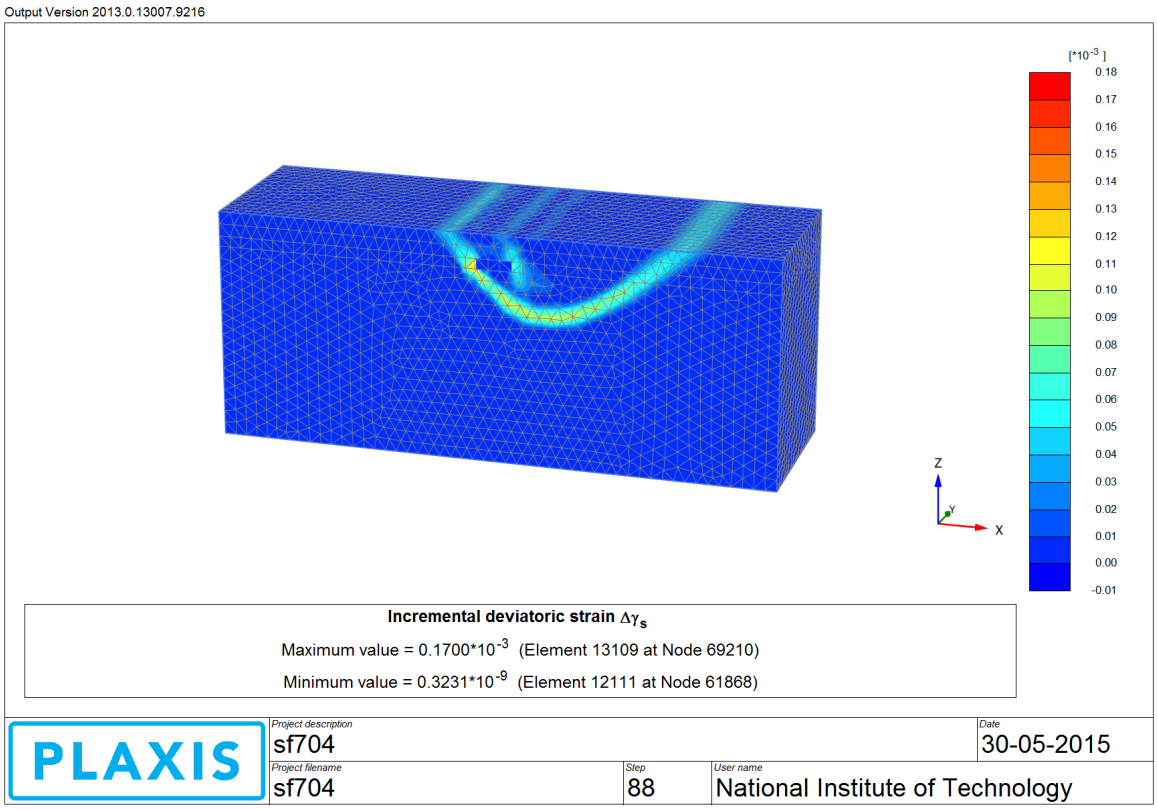

Figure 4.21: Failure surface observed in dense sand
at $D_f/B = 1$, $\alpha = 15°$ and $e/B = 0$

4.3.4 Eccentric Inclined Loading Conditions

Seventy two numerical models have been developed for eccentric and inclined loading condition. The combination of parameters chosen for these numerical models is listed in Table 4.13. The developed numerical model for one case of eccentric inclined loading condition when the line of load application is towards the center line is as shown in Figure 4.22.

Table 4.13: Numerical model parameters for Eccentric Inclined Loading condition

Sand type	**Unit weight,γ (kN/m^3)**	**Relative density of sand (%)**	**Friction angle, ϕ (°)**	***D_f/B***	***e/B***	***α°***
Dense	14.37	69	40.8	0 0.5 1	0 0.05 0.1 0.15	0 5 10 15 20
Medium dense	13.97	51	37.5	0 0.5 1	0	0 5 10 15 20

The variation of ubc with load inclination at all embedment ratios and eccentricity ratios for dense sand and medium dense sand have been observed. Figure 4.23 shows one such plot of the nature of load-settlement curve with load inclination at a particular embedment ratio D_f/B = 0.5 and e/B = 0.05 in dense sand. It is seen from the graph that the ultimate bearing capacity decreases with increase in load inclination. This is true for all eccentricities and all depth of embedment. Similarly, the variation of ubc with load eccentricity at all embedment ratios and load inclinations for dense sand and medium dense sand have been observed. One combination of such plot is shown in Figure 4.24 where the variation of ubc with e/B at a particular embedment ratio D_f/B =0 and α = 10° in medium dense sand is presented. It is observed that

the ultimate bearing capacity decreases with increase in *e/B* ratio. The ubc increases with increase in embedment ratio (D_f/B) for all eccentricities and all load inclinations. One such variation of ubc with embedment ratio (D_f/B) at $e/B = 0.15$ and $\alpha = 20°$ in dense sand is shown in Figure 4.25. It is also observed that the bearing capacity increases with increase in relative density for all combinations of D_f/B=0.5, e/B=0.1 and α=10°. One such plot is shown in Figure 4.26. The values of eccentric inclined loading condition results represented in Table 4.14. The observed failure surface for footing resting on medium dense sand in eccentric inclined condition (i.e. D_f/B=0, α=15°, e/B=0.05) is shown in Figure 4.27.

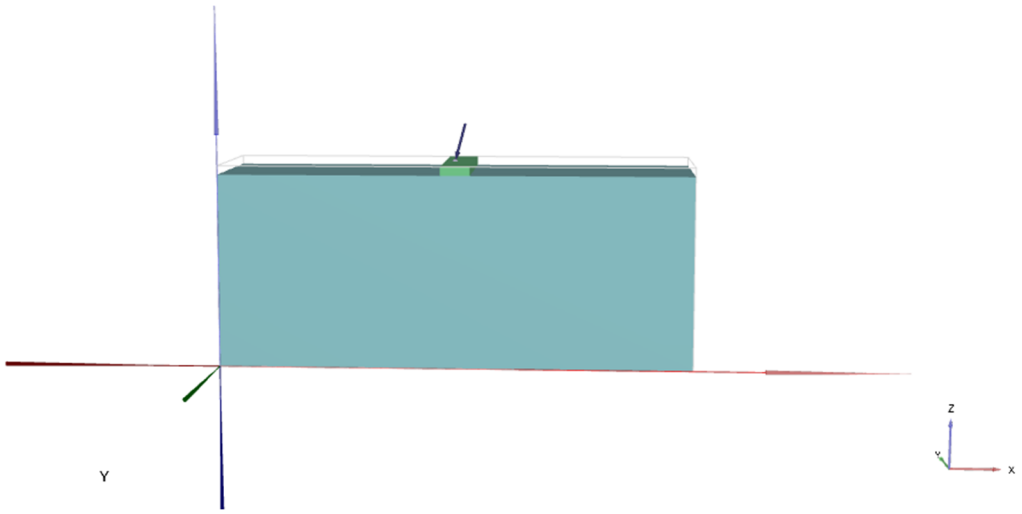

Figure 4.22: Developed numerical model for eccentric inclined loading condition when the line of load application is towards the center line

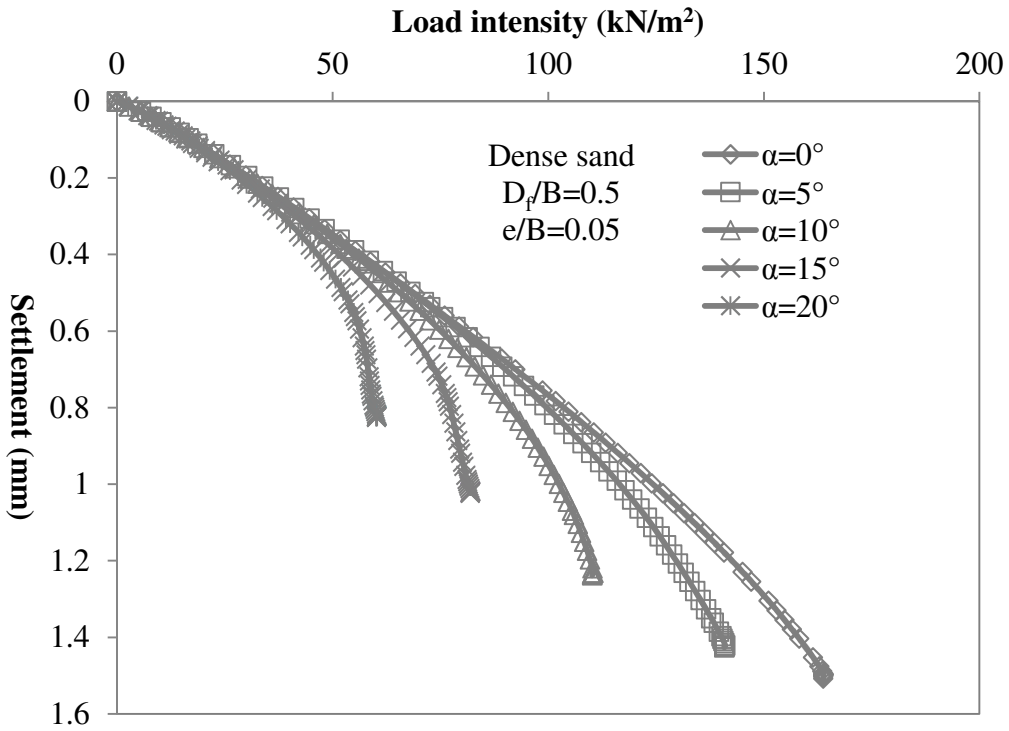

Figure 4.23: Variation of load-settlement curve with load inclination (α) at D_f/B=0.5 and e/B=0.05 in dense sand

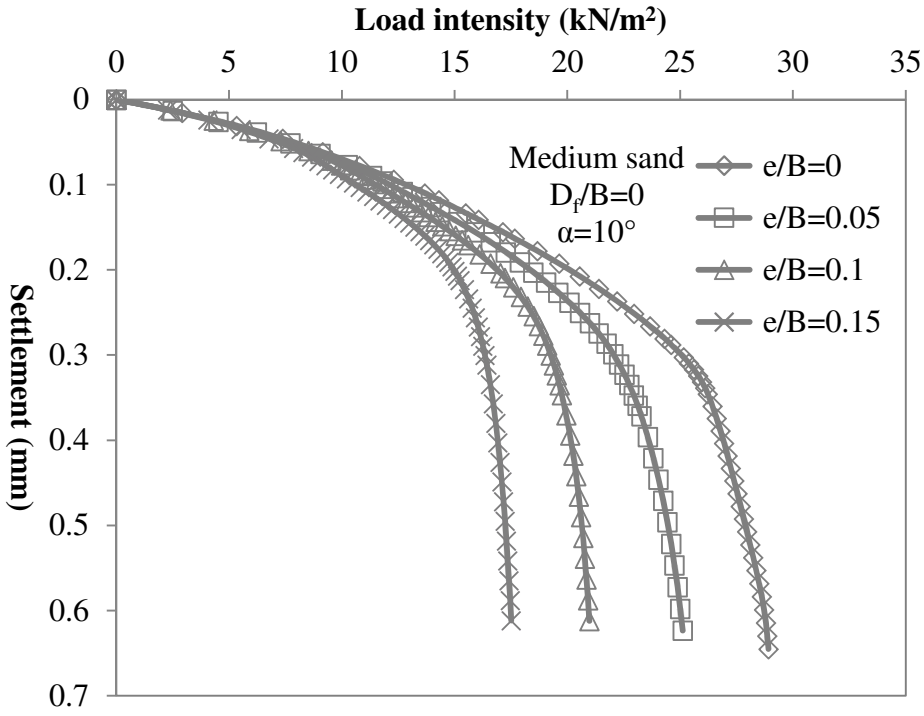

Figure 4.24: Variation of load-settlement curve with e/B at D_f/B=0 and α=10° in medium dense sand

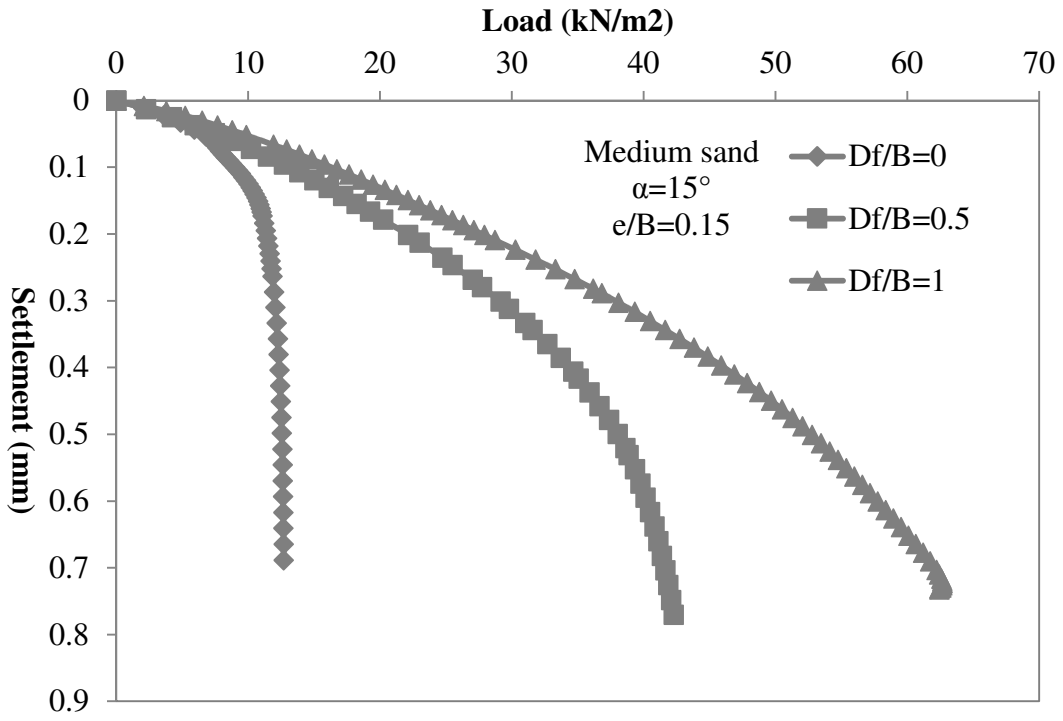

Figure 4.25: Variation of load-settlement curve with embedment ratio (D_f/B) at e/B =0.15 and α=20° in medium dense sand

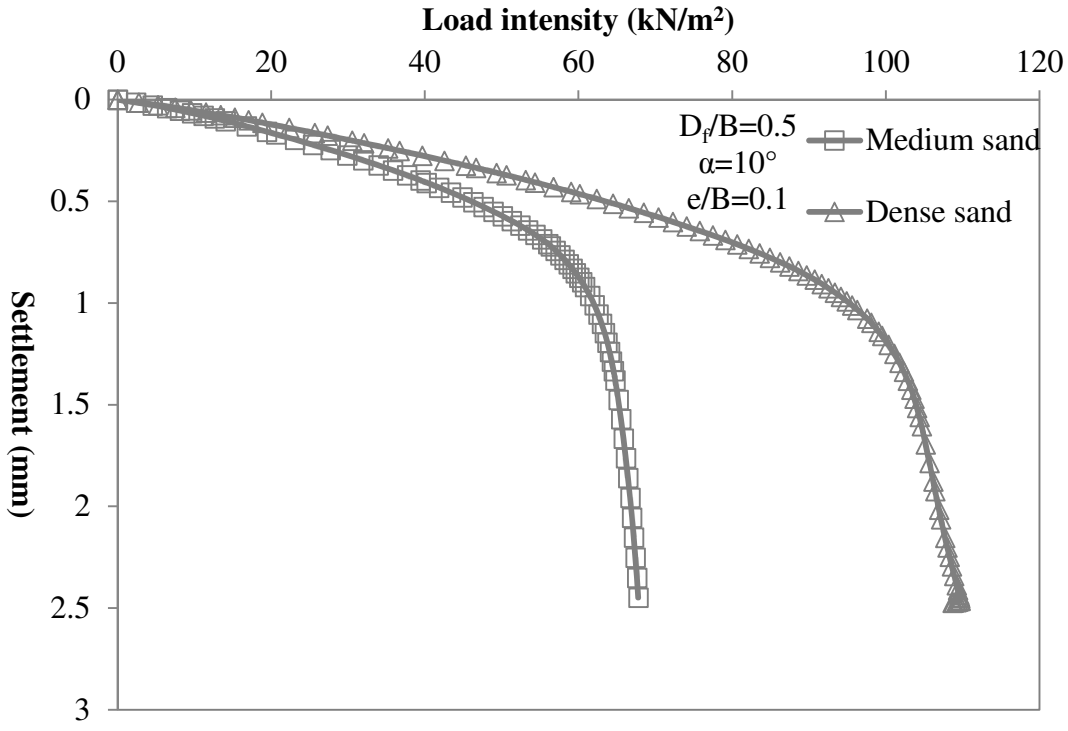

Figure 4.26: Variation of load-settlement curve with Relative Density (D_r) at e/B =0.1, α=10°and D_f/B=0.5

Table 4.14: Numerical models results for eccentric inclined condition

D_f/B	e/B	α	Present result			
			ϕ=37.5°		ϕ=40.8°	
			$q_{u(pc)}$ (kN/m^2)	RF	$q_{u(pc)}$ (kN/m^2)	RF
0	0	0	51.0	1	90.0	1
0	5	0	38.0	0.745	68.0	0.756
0	10	0	26.0	0.510	46.0	0.511
0	15	0	19.5	0.382	31.0	0.344
0	20	0	13.0	0.255	20.8	0.231
0	0	0.05	45.0	0.882	80.0	0.889
0	5	0.05	37.0	0.725	61.0	0.678
0	10	0.05	25.5	0.500	42.0	0.467
0	15	0.05	18.6	0.365	28.0	0.311
0	20	0.05	12.4	0.243	19.3	0.214
0	0	0.1	37.5	0.735	66.0	0.733
0	5	0.1	29.5	0.578	51.0	0.567
0	10	0.1	21.5	0.422	34.0	0.378
0	15	0.1	14.4	0.282	23.0	0.256
0	20	0.1	10.6	0.208	14.8	0.164
0	0	0.15	35.0	0.686	54.0	0.600
0	5	0.15	24.5	0.480	42.0	0.467
0	10	0.15	17.6	0.345	30.7	0.341
0	15	0.15	12.5	0.245	20.0	0.222
0	20	0.15	8.8	0.173	12.8	0.142
0.5	0	0	108.0	1	172.0	1
0.5	5	0	92.0	0.852	154.0	0.895
0.5	10	0	75.0	0.694	120.0	0.698
0.5	15	0	55.0	0.509	84.0	0.488
0.5	20	0	42.0	0.389	63.0	0.366
0.5	0	0.05	99.0	0.917	164.0	0.953
0.5	5	0.05	83.0	0.769	135.0	0.785
0.5	10	0.05	65.0	0.602	108.0	0.628
0.5	15	0.05	53.5	0.495	77.0	0.448
0.5	20	0.05	41.0	0.380	56.0	0.326
0.5	0	0.1	90.0	0.833	150.0	0.872
0.5	5	0.1	78.0	0.722	130.0	0.756
0.5	10	0.1	62.0	0.574	101.0	0.587

D_f/B	e/B	α	Present result			
			ϕ=37.5°		ϕ=40.8°	
			$q_{u(pc)}$ (kN/m^2)	RF	$q_{u(pc)}$ (kN/m^2)	RF
0.5	15	0.1	47.0	0.435	69.5	0.404
0.5	20	0.1	35.5	0.329	54.0	0.314
0.5	0	0.15	81.0	0.750	140.0	0.814
0.5	5	0.15	67.0	0.620	114.0	0.663
0.5	10	0.15	56.5	0.523	89.0	0.517
0.5	15	0.15	40.0	0.370	69.0	0.401
0.5	20	0.15	33.0	0.306	51.0	0.297
1	0	0	144.0	1	223.3	1
1	5	0	116.0	0.806	174.0	0.779
1	10	0	90.0	0.625	135.0	0.605
1	15	0	77.0	0.535	116.0	0.519
1	20	0	60.0	0.417	90.0	0.403
1	0	0.05	130.0	0.903	196.0	0.878
1	5	0.05	112.0	0.778	162.0	0.725
1	10	0.05	89.0	0.618	130.0	0.582
1	15	0.05	69.0	0.479	106.0	0.475
1	20	0.05	56.5	0.392	86.0	0.385
1	0	0.1	120.0	0.833	159.0	0.712
1	5	0.1	102.0	0.708	138.0	0.618
1	10	0.1	81.0	0.563	122.0	0.546
1	15	0.1	63.5	0.441	95.0	0.425
1	20	0.1	48.5	0.337	77.0	0.345
1	0	0.15	110.0	0.764	144.0	0.645
1	5	0.15	89.0	0.618	127.0	0.569
1	10	0.15	75.0	0.521	120.0	0.537
1	15	0.15	56.0	0.389	88.0	0.394
1	20	0.15	43.0	0.299	71.0	0.318

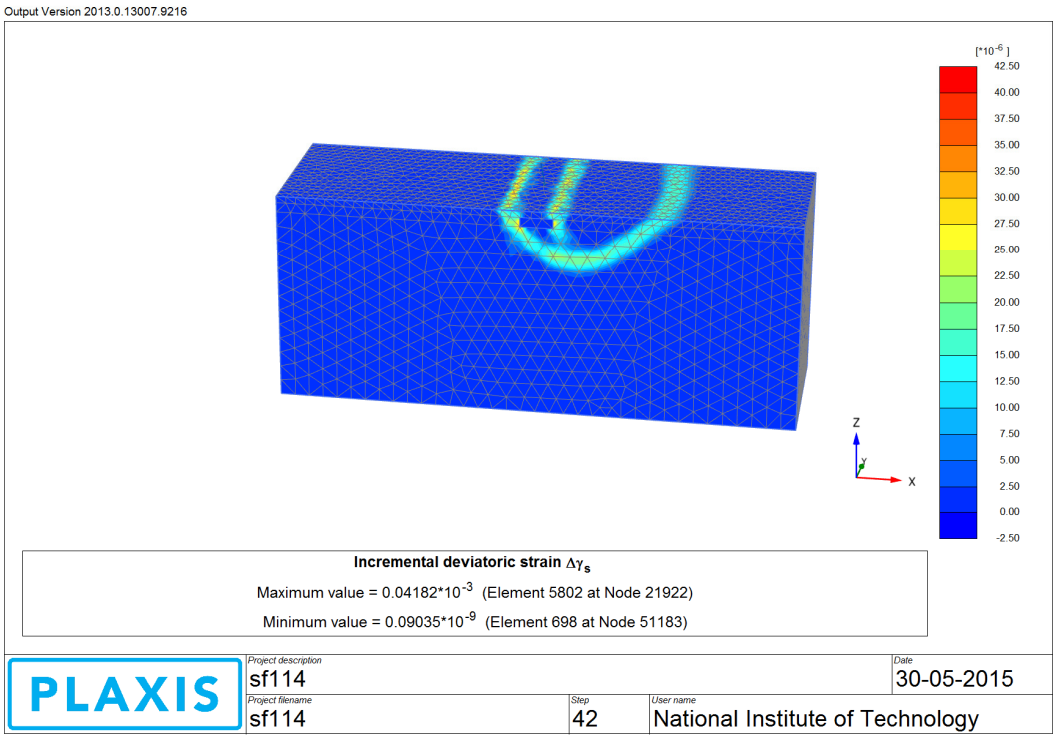

Figure 4.27: Failure surface observed in dense sand
at $D_f/B = 0.5$, $\alpha = 10°$ and $e/B = 0.1$

The reduction factor for the eccentric inclined load is calculated for the present study as the ratio of ultimate bearing capacity of strip footing subjected to eccentric inclined load at any embedment ratio to the ultimate bearing capacity of strip footing subjected to centric vertical load at that corresponding embedment ratio. The equation is as follows

$$RF = \frac{q_{u(D_f/B,e/B,\alpha/\phi)}}{q_{u(D_f/B,e/B=0,\alpha/\phi=0)}}$$

Patra et al. (2012a) conducted laboratory tests to determine the reduction factor of a rigid strip footing placed on a purely frictional soil subjected to eccentric and inclined loading. The reduction factor for partially compensated case is given by

$$RF = \left[1-2\left(\frac{e}{B}\right)\right]\left(1-\frac{\alpha}{\phi}\right)^{2-\frac{D_f}{B}}$$

4.4 Comparison

4.4.1 Comparison with Patra et al. [2012a]

The comparison of the values of *RF* using Patra et al. (2012a) as discussed above has been made with that using present reduction factor (*RF)* values shown in Figure 4.28. The same has been presented in the Table 4.15.The comparison seems to be good.

Table 4.15: Comparison of Reduction Factors corresponding to Patra et al. (2012a) with present results

D_f/B	α	e/B	ϕ=40.8°			ϕ=37.5°		
			Present result *RF*	**Patra et al. (2012) *RF***	**Deviation (%) Col.5-Col.4 / Col.5**	**Present result *RF***	**Patra et al. (2012) *RF***	**Deviation (%) Col.9-Col.8 / Col.9**
0	0	0	1	1	0.00	1	1	0.00
0	0	0.05	0.889	0.900	1.23	0.882	0.900	1.96
0	0	0.1	0.733	0.800	8.33	0.735	0.800	8.09
0	0	0.15	0.600	0.700	14.29	0.686	0.700	1.96
0	5	0	0.756	0.770	1.87	0.745	0.751	0.80
0	5	0.05	0.678	0.693	2.19	0.725	0.676	-7.32
0	5	0.1	0.567	0.616	8.00	0.578	0.601	3.74
0	5	0.15	0.467	0.539	13.41	0.480	0.526	8.63
0	10	0	0.511	0.570	10.31	0.510	0.538	5.20
0	10	0.05	0.467	0.513	9.01	0.500	0.484	-3.31
0	10	0.1	0.378	0.456	17.14	0.422	0.430	2.01
0	10	0.15	0.341	0.399	14.49	0.345	0.376	8.33
0	15	0	0.344	0.400	13.86	0.382	0.360	-6.21
0	15	0.05	0.311	0.360	13.55	0.365	0.324	-12.56
0	15	0.1	0.256	0.320	20.11	0.282	0.288	1.96
0	15	0.15	0.222	0.280	20.61	0.245	0.252	2.74
0	20	0	0.231	0.260	11.08	0.255	0.218	-17.05
0	20	0.05	0.214	0.234	8.32	0.243	0.196	-24.05
0	20	0.1	0.164	0.208	20.91	0.208	0.174	-19.30
0	20	0.15	0.142	0.182	21.83	0.173	0.152	-13.19
0.5	0	0	1	1	0.00	1	1	0.00
0.5	0	0.05	0.953	0.900	-5.94	0.917	0.900	-1.85
0.5	0	0.1	0.872	0.800	-9.01	0.833	0.800	-4.17
0.5	0	0.15	0.814	0.700	-16.28	0.750	0.700	-7.14

D_f/B	α	e/B	ϕ=40.8°			ϕ=37.5°		
			Present result *RF*	**Patra et al. (2012) *RF***	**Deviation (%) Col.5-Col.4 / Col.5**	**Present result *RF***	**Patra et al. (2012) *RF***	**Deviation (%) Col.9-Col.8 / Col.9**
0.5	5	0	0.895	0.822	-8.93	0.852	0.807	-5.58
0.5	5	0.05	0.785	0.740	-6.10	0.769	0.726	-5.84
0.5	5	0.1	0.756	0.658	-14.95	0.722	0.645	-11.89
0.5	5	0.15	0.663	0.575	-15.20	0.620	0.565	-9.84
0.5	10	0	0.698	0.656	-6.37	0.694	0.628	-10.58
0.5	10	0.05	0.628	0.590	-6.37	0.602	0.565	-6.49
0.5	10	0.1	0.587	0.525	-11.91	0.574	0.502	-14.27
0.5	10	0.15	0.517	0.459	-12.70	0.523	0.440	-19.01
0.5	15	0	0.488	0.503	2.88	0.509	0.465	-9.58
0.5	15	0.05	0.448	0.453	1.08	0.495	0.418	-18.43
0.5	15	0.1	0.404	0.402	-0.44	0.435	0.372	-17.05
0.5	15	0.15	0.401	0.352	-13.97	0.370	0.325	-13.84
0.5	20	0	0.366	0.364	-0.63	0.389	0.319	-21.99
0.5	20	0.05	0.326	0.328	0.62	0.380	0.287	-32.31
0.5	20	0.1	0.314	0.291	-7.81	0.329	0.255	-28.89
0.5	20	0.15	0.297	0.255	-16.37	0.306	0.223	-36.92
1	0	0	1	1	0.00	1	1	0.00
1	0	0.05	0.878	0.900	2.47	0.903	0.900	-0.31
1	0	0.1	0.712	0.800	10.99	0.833	0.800	-4.17
1	0	0.15	0.645	0.700	7.88	0.764	0.700	-9.13
1	5	0	0.779	0.877	11.19	0.806	0.867	7.05
1	5	0.05	0.725	0.790	8.13	0.778	0.780	0.28
1	5	0.1	0.618	0.702	11.96	0.708	0.693	-2.16
1	5	0.15	0.569	0.614	7.40	0.618	0.607	-1.88
1	10	0	0.605	0.755	19.91	0.625	0.733	14.77
1	10	0.05	0.582	0.679	14.31	0.618	0.660	6.36
1	10	0.1	0.546	0.604	9.53	0.563	0.587	4.12
1	10	0.15	0.537	0.528	-1.70	0.521	0.513	-1.46
1	15	0	0.519	0.632	17.85	0.535	0.600	10.88
1	15	0.05	0.475	0.569	16.59	0.479	0.540	11.27
1	15	0.1	0.425	0.506	15.90	0.441	0.480	8.13
1	15	0.15	0.394	0.443	10.97	0.389	0.420	7.41
1	20	0	0.403	0.510	20.94	0.417	0.467	10.71
1	20	0.05	0.385	0.459	16.06	0.392	0.420	6.58

D_f/B	α	e/B	ϕ=40.8°			ϕ=37.5°		
			Present result *RF*	**Patra et al. (2012) *RF***	**Deviation (%) Col.5-Col.4 / Col.5**	**Present result *RF***	**Patra et al. (2012) *RF***	**Deviation (%) Col.9-Col.8 / Col.9**
1	20	0.1	0.345	0.408	15.45	0.337	0.373	9.78
1	20	0.15	0.318	0.357	10.90	0.299	0.327	8.59

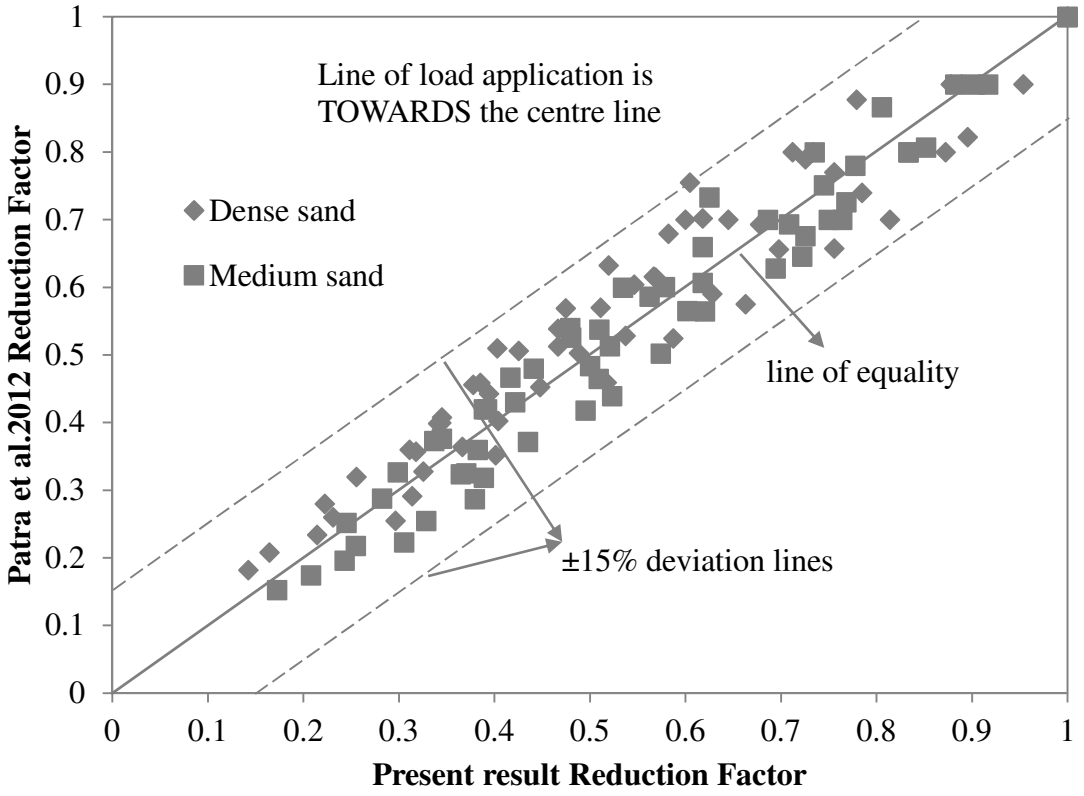

Figure 4.28: Comparison of Present results with Patra et al. (2012a) for dense and medium dense sand

From the Figure 4.28 the comparison between the reduction factor of Patra et al. (2012a) and reduction factor of present results for dense sand and medium dense sand are in good agreement and not exceeding the ±15% deviation line.

4.4.2 Comparison with Meyerhof [1963]

The comparison of the values of *RF* using Meyerhof's method as discussed above has been made with that using present reduction factor (*RF)* values shown in Figure 4.29. The same has been presented in the Table 4.16.

Table 4.16: Reduction Factor Comparison of Meyerhof (1963) with Present results

D_f/B	$\alpha°$	e/B	Present result *RF*	Meyerhof (1963) *RF*	Present result *RF*	Meyerhof (1963) *RF*
			ϕ=37.5°		ϕ=40.8°	
0	0	0	1	1	1	1
0	0	0.05	0.882	0.810	0.898	0.810
0	0	0.1	0.735	0.640	0.756	0.640
0	0	0.15	0.686	0.490	0.631	0.490
0	5	0	0.745	0.754	0.822	0.723
0	5	0.05	0.725	0.611	0.747	0.585
0	5	0.1	0.578	0.483	0.622	0.463
0	5	0.15	0.480	0.369	0.524	0.354
0	10	0	0.510	0.546	0.604	0.493
0	10	0.05	0.500	0.442	0.551	0.400
0	10	0.1	0.422	0.349	0.462	0.316
0	10	0.15	0.345	0.268	0.387	0.242
0	15	0	0.382	0.373	0.444	0.308
0	15	0.05	0.365	0.302	0.391	0.249
0	15	0.1	0.282	0.239	0.338	0.197
0	15	0.15	0.245	0.183	0.289	0.151
0	20	0	0.255	0.232	0.329	0.165
0	20	0.05	0.243	0.188	0.280	0.134
0	20	0.1	0.208	0.148	0.244	0.106
0	20	0.15	0.173	0.114	0.222	0.081
0.5	0	0	1	1	1	1
0.5	0	0.05	0.917	0.850	0.960	0.855
0.5	0	0.1	0.833	0.710	0.880	0.720
0.5	0	0.15	0.750	0.582	0.780	0.595
0.5	5	0	0.852	0.816	0.884	0.809
0.5	5	0.05	0.769	0.696	0.820	0.695
0.5	5	0.1	0.722	0.585	0.800	0.589

D_f/B	α°	e/B	Present result RF	Meyerhof (1963) RF	Present result RF	Meyerhof (1963) RF
			ϕ=37.5°		ϕ=40.8°	
0.5	5	0.15	0.620	0.483	0.730	0.490
0.5	10	0	0.694	0.659	0.720	0.648
0.5	10	0.05	0.602	0.565	0.680	0.561
0.5	10	0.1	0.574	0.478	0.650	0.479
0.5	10	0.15	0.523	0.397	0.610	0.401
0.5	15	0	0.509	0.525	0.580	0.513
0.5	15	0.05	0.495	0.454	0.560	0.448
0.5	15	0.1	0.435	0.387	0.520	0.386
0.5	15	0.15	0.370	0.324	0.470	0.327
0.5	20	0	0.389	0.413	0.466	0.404
0.5	20	0.05	0.380	0.360	0.430	0.356
0.5	20	0.1	0.329	0.310	0.410	0.310
0.5	20	0.15	0.306	0.262	0.370	0.266
1	0	0	1	1	1	1
1	0	0.05	0.903	0.865	0.959	0.870
1	0	0.1	0.833	0.738	0.863	0.747
1	0	0.15	0.764	0.618	0.788	0.630
1	5	0	0.806	0.840	0.836	0.838
1	5	0.05	0.778	0.730	0.795	0.732
1	5	0.1	0.708	0.625	0.764	0.632
1	5	0.15	0.618	0.527	0.660	0.536
1	10	0	0.625	0.703	0.685	0.699
1	10	0.05	0.618	0.613	0.658	0.614
1	10	0.1	0.563	0.528	0.614	0.533
1	10	0.15	0.521	0.447	0.575	0.455
1	15	0	0.535	0.584	0.562	0.582
1	15	0.05	0.479	0.513	0.548	0.514
1	15	0.1	0.441	0.444	0.507	0.449
1	15	0.15	0.389	0.378	0.468	0.386
1	20	0	0.417	0.483	0.460	0.484
1	20	0.05	0.392	0.427	0.438	0.431
1	20	0.1	0.337	0.372	0.405	0.378
1	20	0.15	0.299	0.319	0.384	0.327

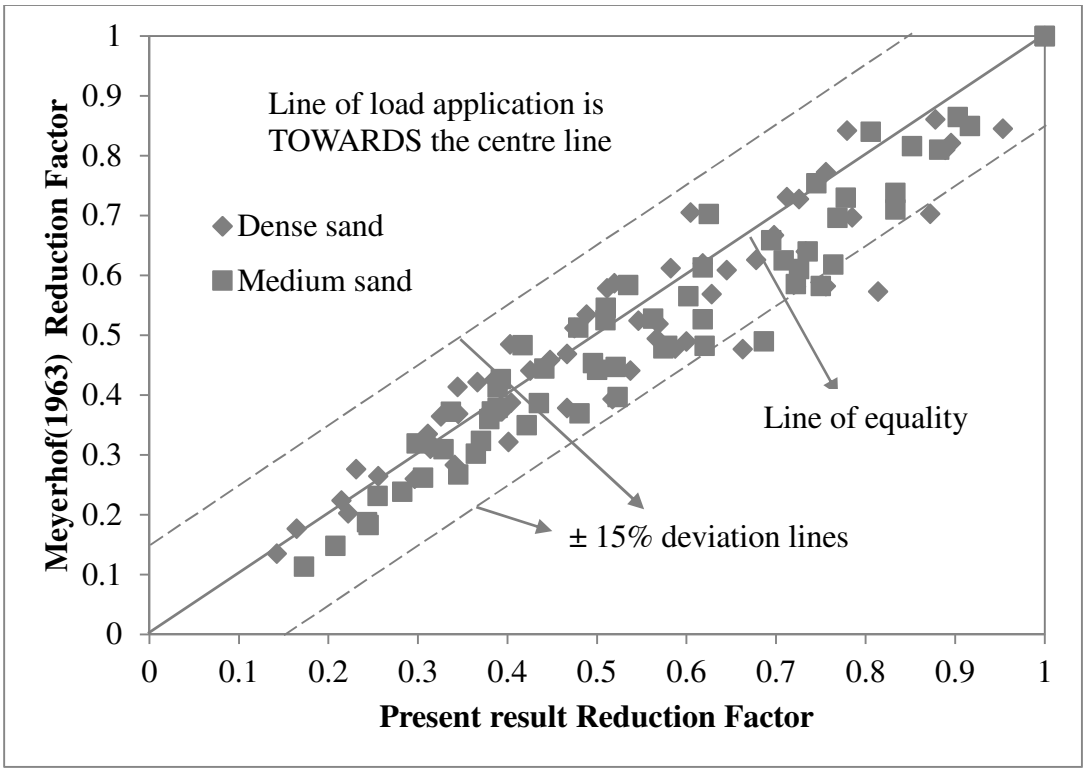

Figure 4.29: Comparison of Present results with Meyerhof (1963)

Table 4.16 and Figure 4.29 show the comparison, and the agreement is reasonably good.

4.4.3 Comparison with Saran and Agarwal [1991]

Values of *RF* for bearing capacity corresponding to Saran and Agarwal (1991) is calculated and compared with present *RF* values as shown in Figure 4.30. This is shown in Table 4.17.

Table 4.17: Comparison of Reduction Factors corresponding to Saran and Agarwal (1991) along with Present results

D_f/B	α	e/B	**Present result *RF***	**Saran & Agarwal (1991) *RF***
0	0	0	1	1
0	0	0.1	0.735	0.54
0	10	0	0.510	0.44
0	10	0.1	0.422	0.33
0	20	0	0.255	0.36

D_f/B	α	e/B	Present result *RF*	Saran & Agarwal (1991) *RF*
0	20	0.1	0.208	0.18
0.5	0	0	1	1
0.5	0	0.1	0.833	0.60
0.5	10	0	0.694	0.52
0.5	10	0.1	0.574	0.38
0.5	20	0	0.389	0.38
0.5	20	0.1	0.329	0.22
1	0	0	1	1
1	0	0.1	0.833	0.63
1	10	0	0.625	0.56
1	10	0.1	0.563	0.41
1	20	0	0.417	0.39
1	20	0.1	0.337	0.24

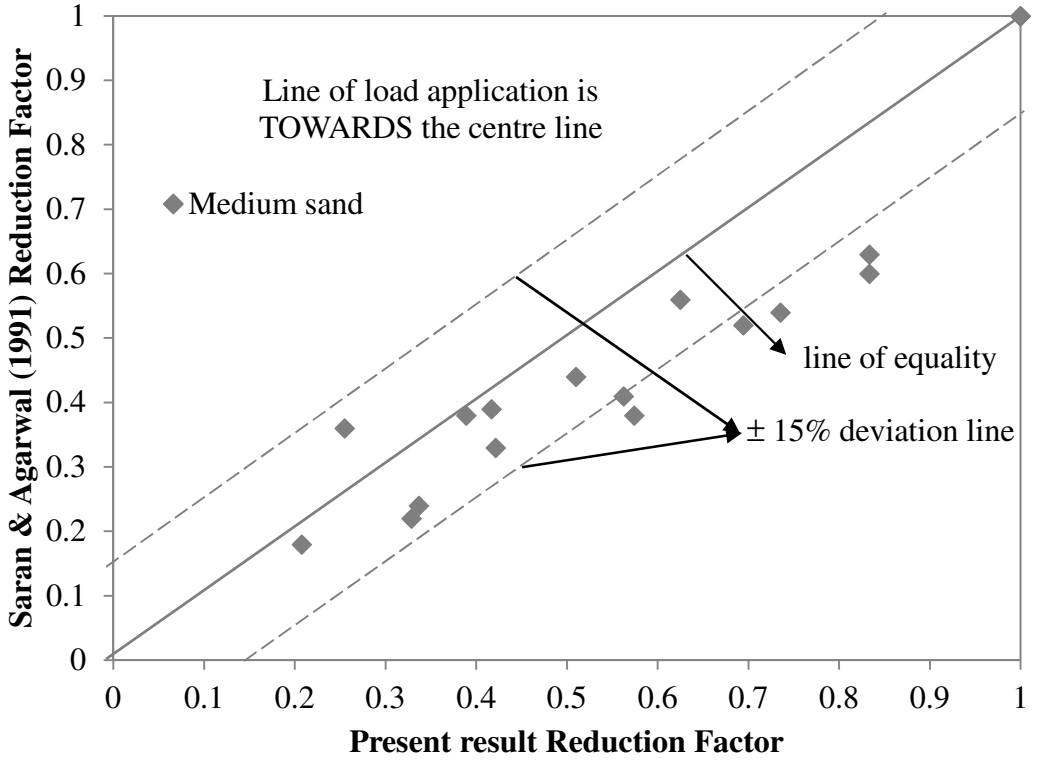

Figure 4.30: Comparison: Present results with Saran and Agarwal (1991)

4.4.4 Comparison with Loukidis et al. [2008]

The comparison of the values of *RF* using Loukidis et al. (2008) as discussed above has been made with that using present reduction factor (*RF)* values shown in Figure 4.31. The same has been presented in the Table 4.18.The comparison seems to be good.

Table 4.18: Comparison of Reduction Factors corresponding to Loukidis et al. (2008) for $D_f/B = 0$ with present results

D_f/B	α°	e/B	**Present result *RF***	**Loukidis et al. 2008 *RF***	**Present result *RF***	**Loukidis et al. 2008 *RF***
			ϕ=37.5°		**ϕ=40.8°**	
0	0	0	1	1	1	1
0	0	0.05	0.882	0.817	0.898	0.817
0	0	0.1	0.735	0.652	0.756	0.652
0	0	0.15	0.686	0.506	0.631	0.506
0	5	0	0.745	0.765	0.822	0.765
0	5	0.05	0.725	0.677	0.747	0.677
0	5	0.1	0.578	0.554	0.622	0.554
0	5	0.15	0.480	0.431	0.524	0.431
0	10	0	0.510	0.563	0.604	0.563
0	10	0.05	0.500	0.503	0.551	0.503
0	10	0.1	0.422	0.417	0.462	0.417
0	10	0.15	0.345	0.325	0.387	0.325
0	15	0	0.382	0.387	0.444	0.387
0	15	0.05	0.365	0.343	0.391	0.343
0	15	0.1	0.282	0.283	0.338	0.283
0	15	0.15	0.245	0.217	0.289	0.217
0	20	0	0.255	0.238	0.329	0.238
0	20	0.05	0.243	0.205	0.280	0.205
0	20	0.1	0.208	0.163	0.244	0.163
0	20	0.15	0.173	0.119	0.222	0.119

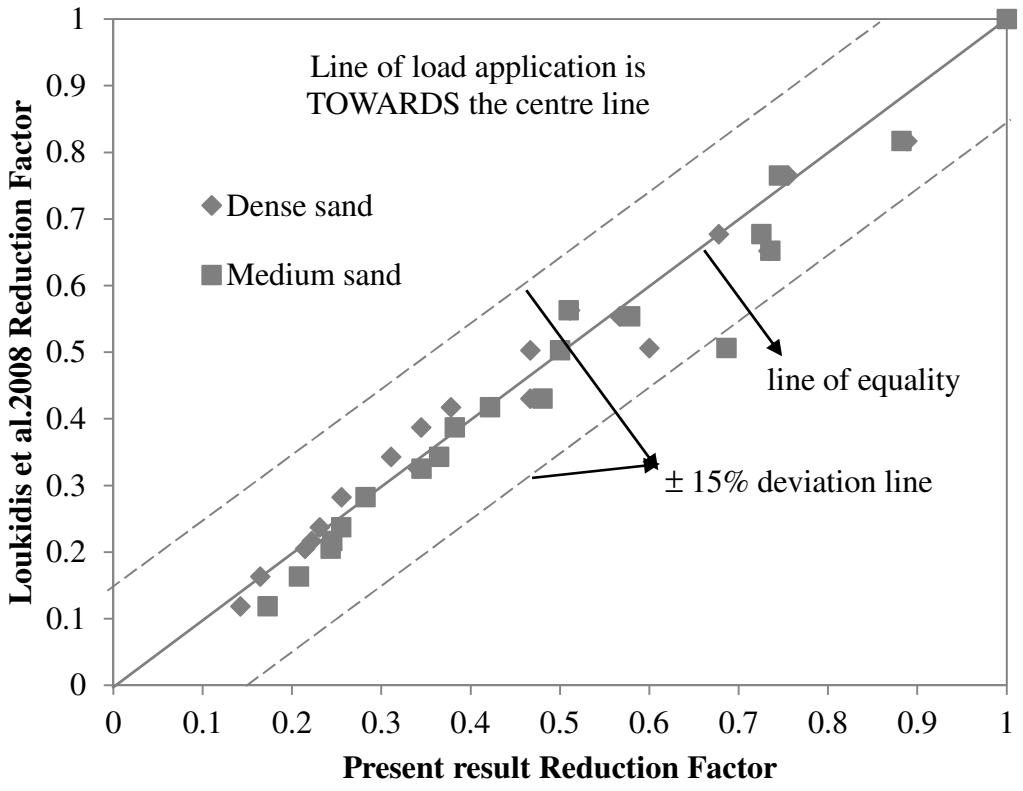

Figure 4.31: Comparison of Present results with Loukidis et al. (2008)

4.4.5 Comparison with Viladkar et al. [2013]

The comparison of the values of *RF* using Viladkar et al. (2013) as discussed above has been made with that using Patra et al(2012a) reduction factor (*RF)* values shown in Figure 4.32. The same has been presented in the Table 4.19. The comparison seems to be good.

Table 4.19: Comparison of Reduction Factors corresponding to Viladkar et al. (2013) with Patra et al. (2012a)

D_f/B	e/B	$\alpha°$	Viladkar et al. (2013)		Patra et al. (2012a)
			q_u (kN/m^2)	*RF*	*RF*
0	0	0	321.3	1	1
0	0	5	267.3	0.832	0.771
0	0	10	188.4	0.586	0.572
0	0	15	131.1	0.408	0.402
0	0	20	87.5	0.272	0.262

D_f/B	e/B	α°	Viladkar et al. (2013)		Patra et al. (2012a)
			q_u (kN/m^2)	RF	RF
0	0.1	0	224.3	0.698	0.8
0	0.1	5	180	0.560	0.617
0	0.1	10	128.6	0.400	0.457
0	0.1	15	89.6	0.279	0.322
0	0.1	20	59	0.184	0.210
0	0.2	0	120.2	0.374	0.6
0	0.2	5	96.8	0.301	0.463
0	0.2	10	72.9	0.227	0.343
0	0.2	15	48.2	0.150	0.241
0	0.2	20	33.7	0.105	0.157
0	0.3	0	54.1	0.168	0.4
0	0.3	5	42.3	0.132	0.308
0	0.3	10	31.4	0.098	0.229
0	0.3	15	23.1	0.072	0.161
0	0.3	20	14.5	0.045	0.105
0.5	0	0	518.3	1	1
0.5	0	5	422.5	0.815	0.823
0.5	0	10	310.7	0.599	0.657
0.5	0	15	240.3	0.464	0.505
0.5	0	20	186.4	0.360	0.367
0.5	0.1	0	336.3	0.649	0.8
0.5	0.1	5	283.1	0.546	0.658
0.5	0.1	10	225	0.434	0.526
0.5	0.1	15	175.6	0.339	0.404
0.5	0.1	20	139.7	0.270	0.293
0.5	0.2	0	231	0.446	0.6
0.5	0.2	5	187.8	0.362	0.494
0.5	0.2	10	166.4	0.321	0.394
0.5	0.2	15	134.3	0.259	0.303
0.5	0.2	20	106	0.205	0.220
0.5	0.3	0	130.1	0.251	0.4
0.5	0.3	5	107.2	0.207	0.329
0.5	0.3	10	95	0.183	0.263
0.5	0.3	15	72.7	0.140	0.202
0.5	0.3	20	56.3	0.109	0.147

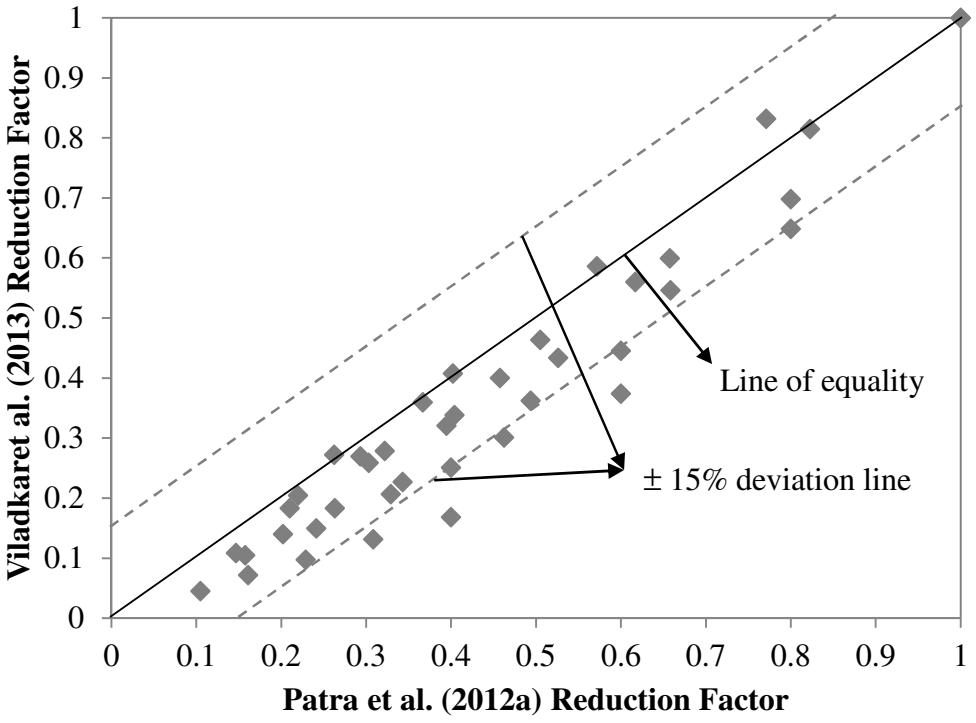

Figure 4.32: Comparison of Reduction factor corresponding to Viladkar et al. (2013) with Patra et al. (2012a)

5. ULTIMATE BEARING CAPACITY OF ECCENTRICALLY INCLINED LOADED STRIP FOOTING ON GRANULAR SOIL WHEN THE LINE OF LOAD APPLICATION IS AWAY FROM THE CENTER LINE OF THE FOOTING

5.1 Introduction

Shallow strip foundations are at times subjected to eccentrically inclined loads. Figure 5.1 shows two possible modes of load application. In this figure B is the width of the foundation, e is the load eccentricity, α is the load inclination, and Q_u is the ultimate load per unit length of the foundation. In Figure 5.1(a) the line of load application of the foundation is inclined towards the center line of the foundation and is referred to as *partially compensated* by Perloff and Baron (1976). It is also possible for the line of load application on the foundation to be inclined away from the center line of the foundation as shown in Figure 5.1(b). Perloff and Baron (1976) called this type of loading as *reinforced* case.

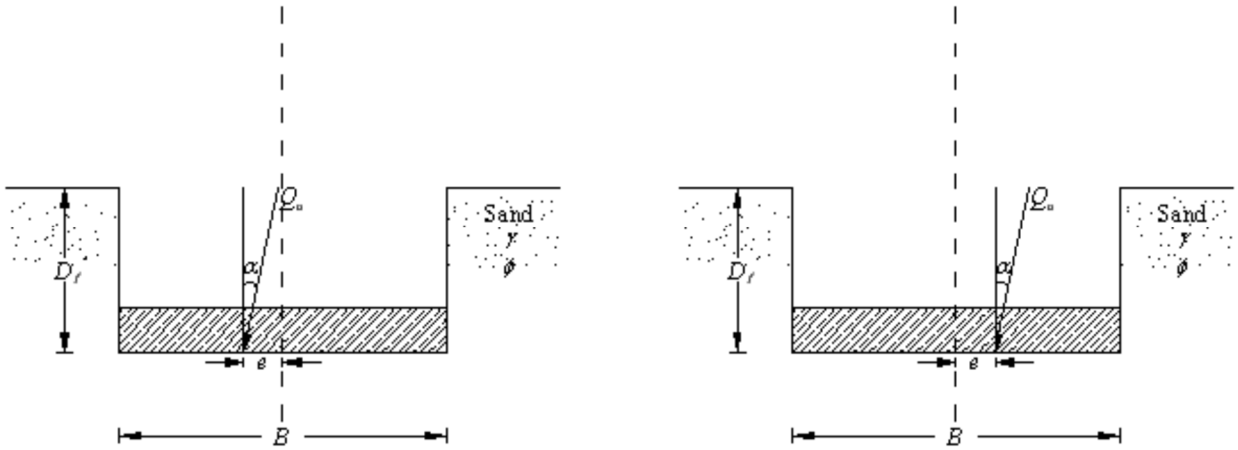

Figure 5.1: Eccentrically inclined load on a strip foundation: (a) *Partially compensated* case, (b) *Reinforced* case

5.2 Numerical Module

Seventy two numbers of numerical models were developed in this reinforced case. The details of the numerical models are mentioned in Table 5.1.

Table 5.1: Sequence of numerical models for Dense and Medium sand in *Reinforced* condition

D_f/B	e/B	α°	Model No.	
			Dense	**Medium**
0	0.05	5,10,15,20	1-4	37-40
0	0.1	5,10,15,20	5-8	41-44
0	0.15	5,10,15,20	9-12	45-48
0.5	0.05	5,10,15,20	13-16	49-52
0.5	0.1	5,10,15,20	17-20	53-56
0.5	0.15	5,10,15,20	21-24	57-60
1	0.05	5,10,15,20	25-28	61-64
1	0.1	5,10,15,20	29-32	65-68
1	0.15	5,10,15,20	33-36	69-72

5.3 Numerical Models Result

The ultimate bearing capacities q_u obtained from the present numerical models are given in Table 5.2. Other ultimate bearing capacity test results for vertical loading conditions ($\alpha = 0^\circ$ with e/B varying from 0.05 to 0.15) relevant to the present study as mentioned in case of *partially compensated* type (Chapter 4) are summarized in Table 5.2. The developed numerical model for one case of eccentric inclined loading condition when the line of load application is away from the center line is as shown in Figure 5.2.

As observed in the case of *partially compensated* type of loading, the ultimate bearing capacity (ubc) decreases with increase in the values of e/B and α for the case of *reinforced* type of loading. Similarly increase in ubc occurs with increase in D_f/B and relative density of sand as seen with partially compensated type of loading. These are shown in Figures 5.3 through 5.7.

The observed failure surface for footing resting on medium dense sand in eccentric inclined condition (i.e. D_f/B=0, α=10°, e/B=0.1) is shown in Figure 5.8.

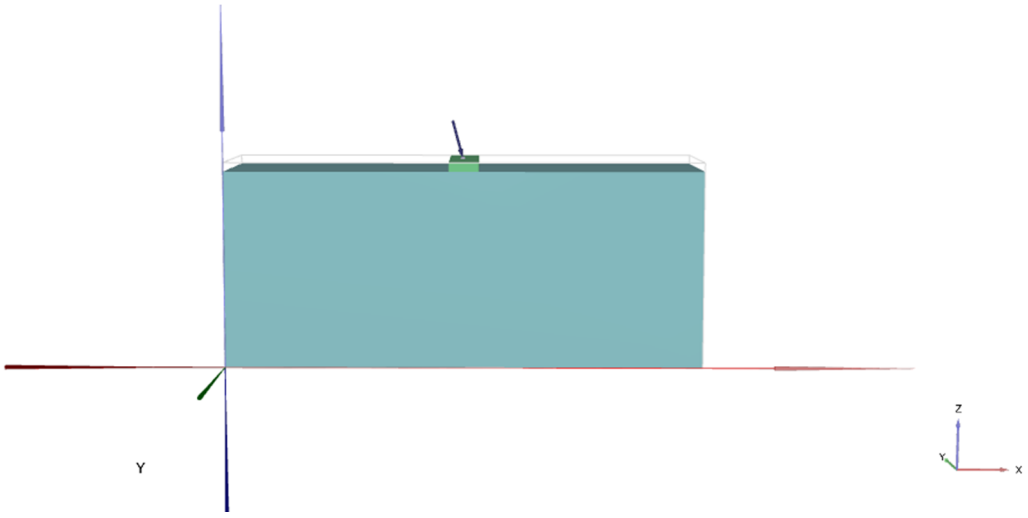

Figure 5.2: Developed numerical model for eccentric inclined loading condition when the line of load application is away from the center line

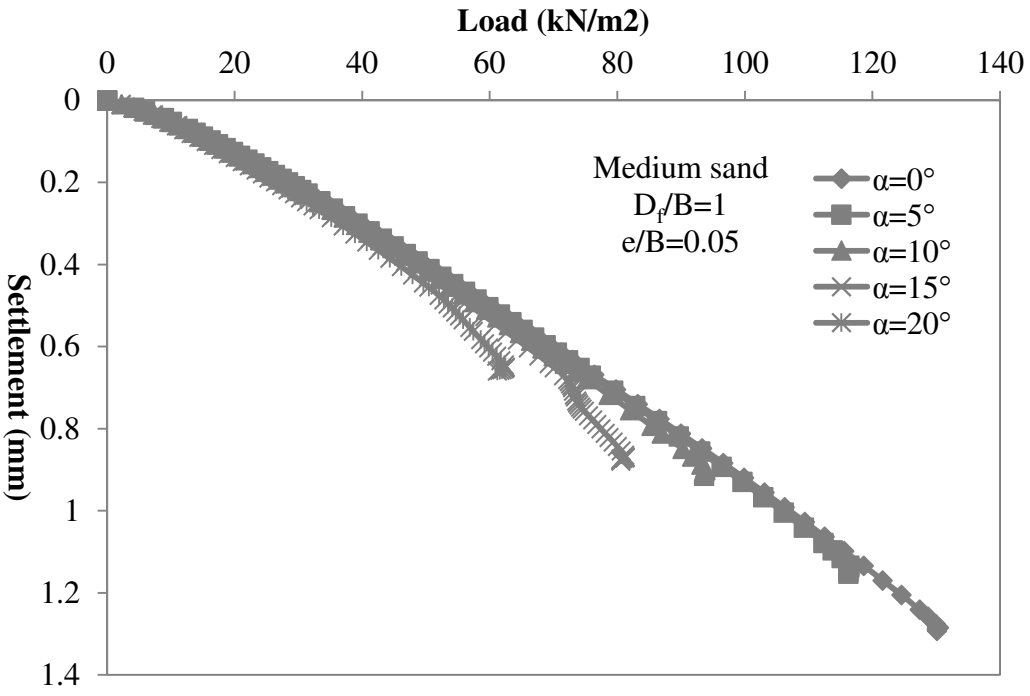

Figure 5.3: Variation of load-settlement curve with α at D_f/B=1, e/B =0.05 in medium dense sand

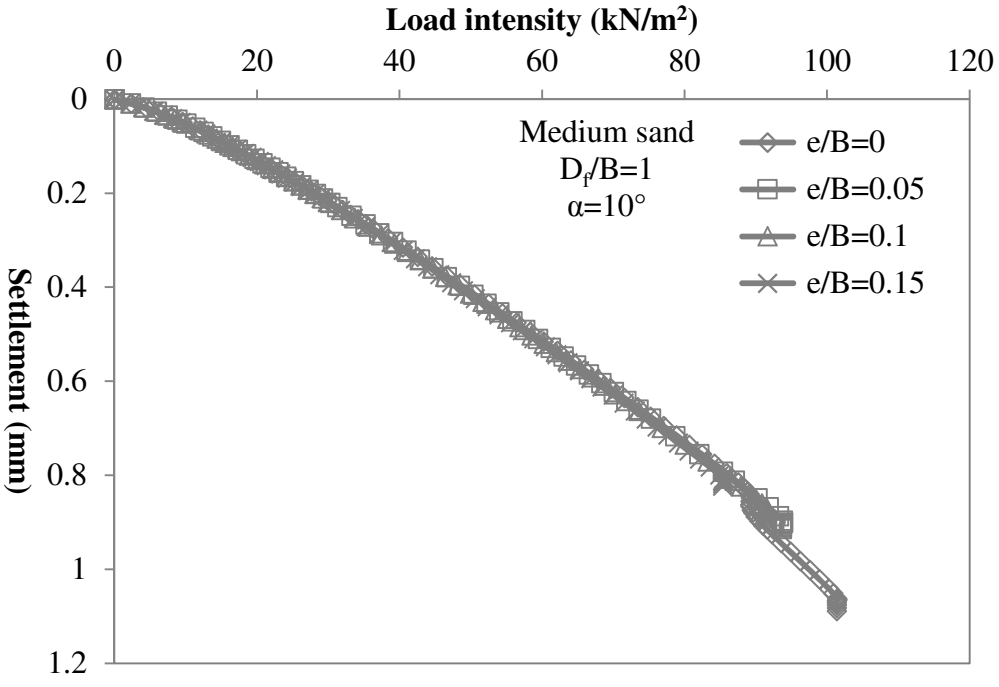

Figure 5.4: Variation of load-settlement curve with *e/B* at D_f/B=1, α=10° in medium dense sand

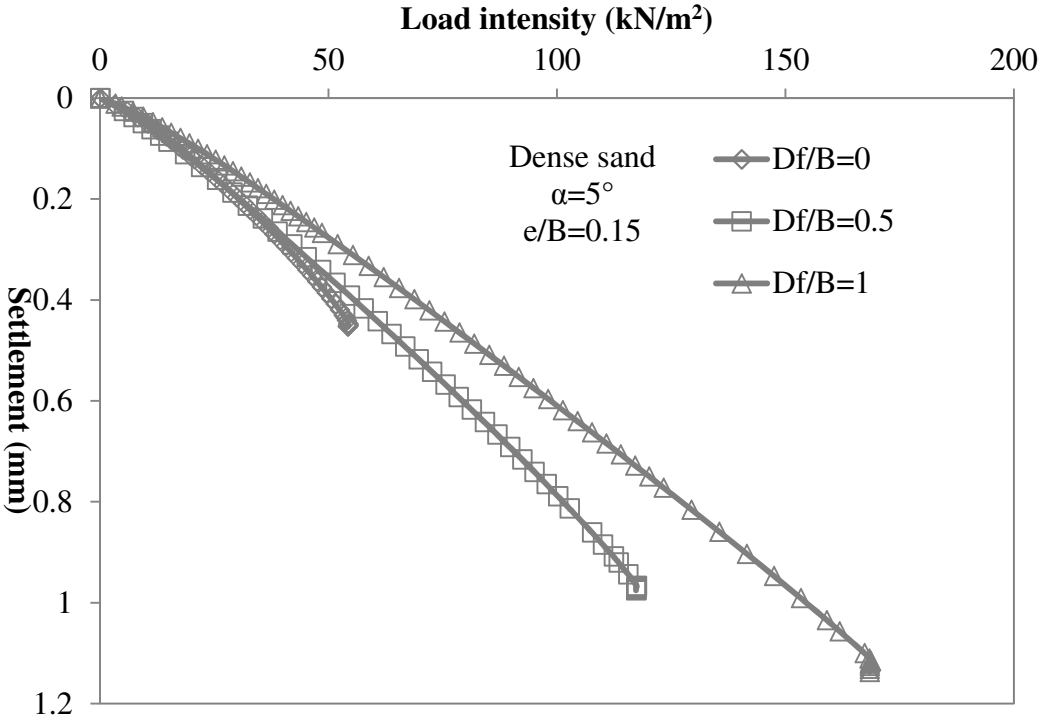

Figure 5.5: Variation of load-settlement curve with D_f/B *at* α=5 °, *e/B* =0.15 in dense sand

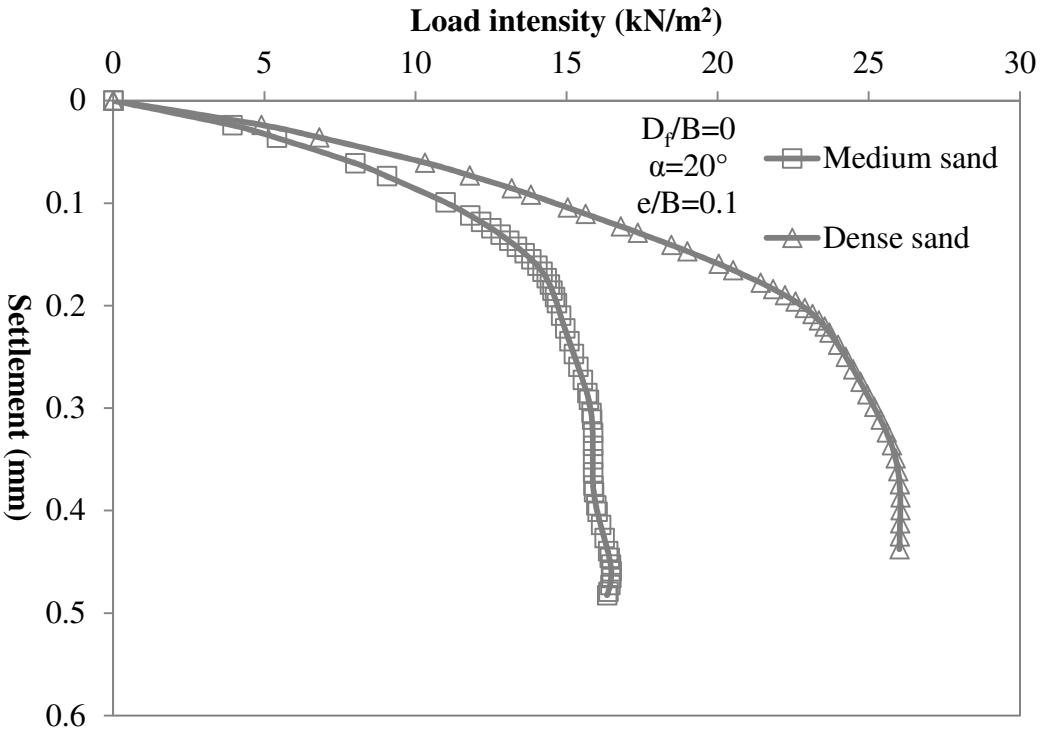

Figure 5.6: Variation of load-settlement curve with relative density (D_r) *at* D_f/B=1, α=20°, *e/B* =0.15

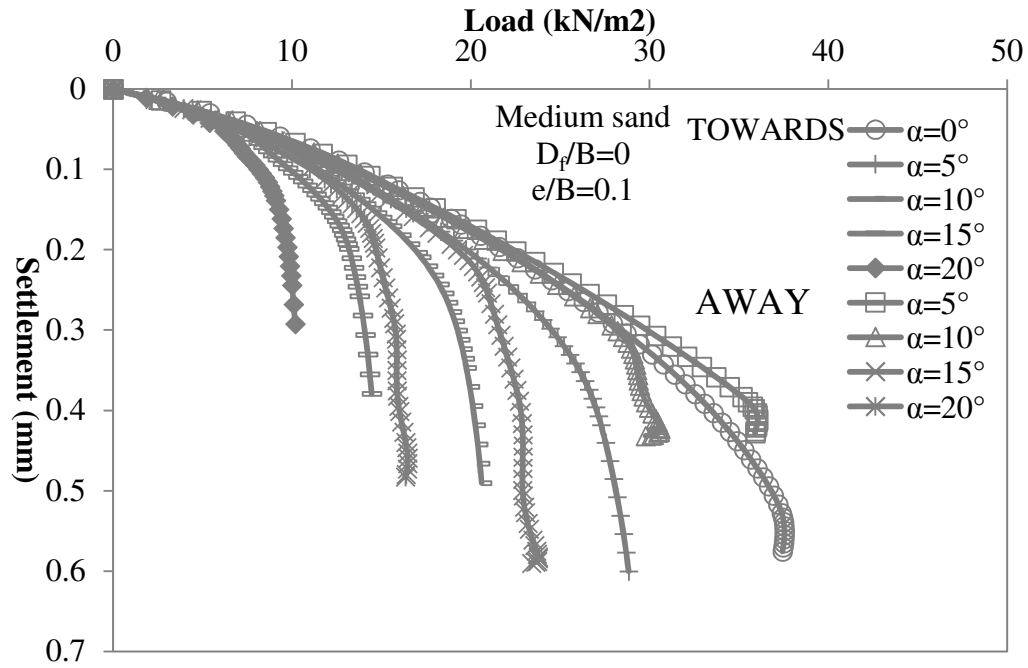

Figure 5.7: Variation of load-settlement curve with load inclination (α) for towards and away cases *at* D_f/B=0.5, α=20°, *e/B* =0.05 for medium dense sand

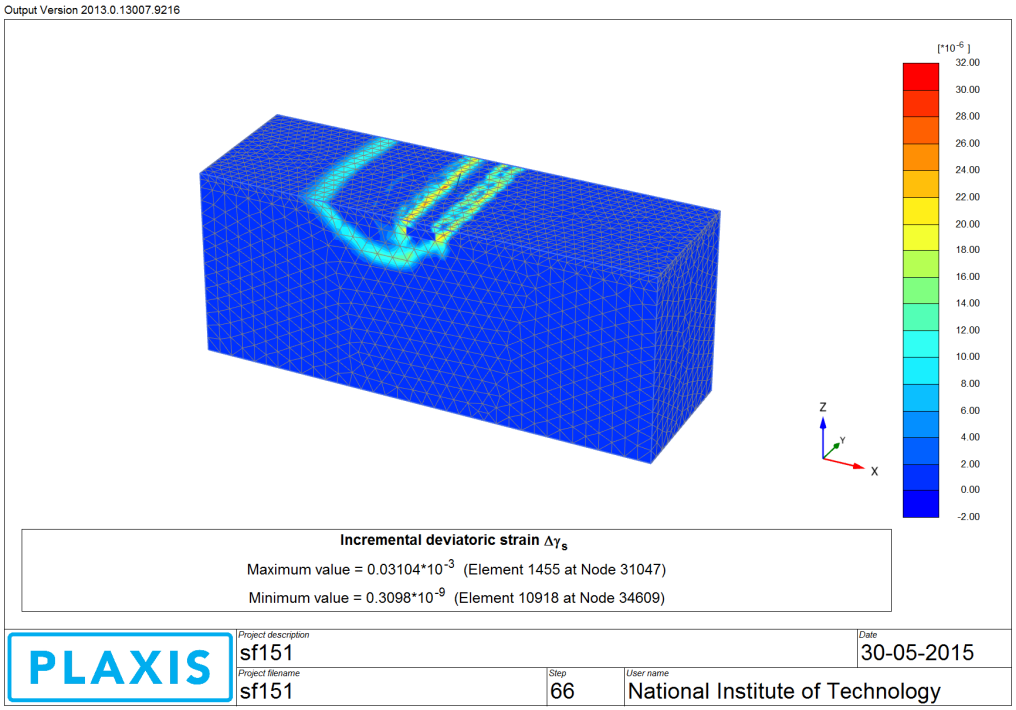

Figure 5.8: Failure surface observed in dense sand
at $D_f/B = 0.5$, $\alpha = 15°$ and $e/B = 0.1$

A comparison has been made with the ultimate bearing capacities of partially compensated and reinforced type of footings as discussed. Figure 5.9 shows the plot of the ratio of the ultimate bearing capacities of q_u– reinforced determined from the present numerical models (Table 5.2) to q_u– partially compensated provided in for similar values of D_f/B, e/B (>0) and α (>0). These figures show that:

a. For given values of D_f/B and e/B, the magnitude of (q_u –reinforced)/(q_u –partially compensated) increases with the load inclination α.

b. Generally speaking, for similar values of α and e/B, the ratio shows a tendency to decrease with the increase in embedment ratio.

c. For a given value of D_f/B and α, the ratio increases with the increase in e/B.

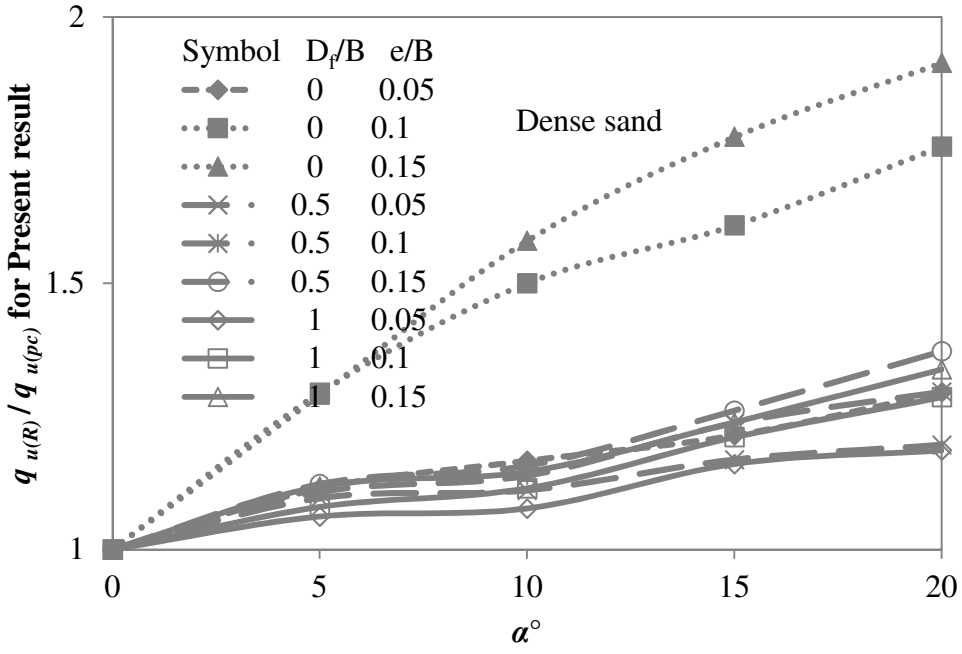

(a)

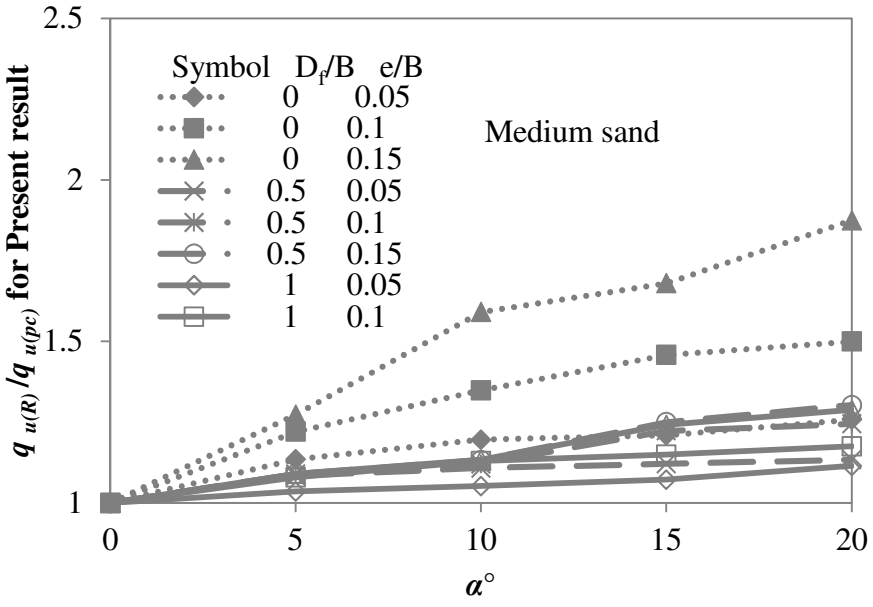

(b)

Figure 5.9: Plot of (q_u– reinforced)/(q_u– partially compensated) for cases of eccentrically inclined loading in (a) dense and (b) medium sand

Table 5.2: Ratio of ultimate bearing capacity q_u in both conditions i.e. partially compensated and reinforced case with ultimate bearing capacity q_u in central vertical condition and ratio of q_u- reinforced to q_u- partially compensated

Type of sand	D_f/B	α°	e/B	Present result				
				$q_{u(pc)}$ (kN/m^2)	$RF_{(pc)}$	$q_{u(R)}$ (kN/m^2)	$RF_{(R)}$	$q_{u\,(R)}/q_{u\,(pc)}$
Dense	0	5	0.05	61.0	0.678	68.0	0.756	1.11
	0	10	0.05	42.0	0.467	49.0	0.544	1.17
	0	15	0.05	28.0	0.311	34.0	0.378	1.21
	0	20	0.05	19.3	0.214	25.0	0.278	1.30
	0	5	0.1	51.0	0.567	66.0	0.733	1.29
	0	10	0.1	34.0	0.378	51.0	0.567	1.50
	0	15	0.1	23.0	0.256	37.0	0.411	1.61
	0	20	0.1	14.8	0.164	26.0	0.289	1.76
	0	5	0.15	42.0	0.467	54.2	0.602	1.29
	0	10	0.15	30.7	0.341	48.5	0.539	1.58
	0	15	0.15	20.0	0.222	35.5	0.394	1.78
	0	20	0.15	12.8	0.142	24.5	0.272	1.91
	0.5	5	0.05	135.0	0.785	148.0	0.860	1.10
	0.5	10	0.05	108.0	0.628	120.0	0.698	1.11
	0.5	15	0.05	77.0	0.448	90.0	0.523	1.17
	0.5	20	0.05	56.0	0.326	67.0	0.390	1.20
	0.5	5	0.1	130.0	0.756	144.0	0.837	1.11
	0.5	10	0.1	101.0	0.587	115.0	0.669	1.14
	0.5	15	0.1	69.5	0.404	86.0	0.500	1.24
	0.5	20	0.1	54.0	0.314	70.0	0.407	1.30
	0.5	5	0.15	114.0	0.663	128.0	0.744	1.12
	0.5	10	0.15	89.0	0.517	103.0	0.599	1.16
	0.5	15	0.15	69.0	0.401	87.0	0.506	1.26
	0.5	20	0.15	51.0	0.297	70.0	0.407	1.37
	1	5	0.05	162.0	0.725	172.0	0.770	1.06
	1	10	0.05	130.0	0.582	140.0	0.627	1.08
	1	15	0.05	106.0	0.475	123.0	0.551	1.16
	1	20	0.05	86.0	0.385	102.0	0.457	1.19
	1	5	0.1	138.0	0.618	149.0	0.667	1.08
	1	10	0.1	122.0	0.546	136.0	0.609	1.11
	1	15	0.1	95.0	0.425	115.0	0.515	1.21

Type of sand	D_f/B	α°	e/B	Present result				
				$q_{u(pc)}$ (kN/m^2)	$RF_{(pc)}$	$q_{u(R)}$ (kN/m^2)	$RF_{(R)}$	$q_{u\,(R)}/q_{u\,(pc)}$
	1	20	0.1	77.0	0.345	99.0	0.443	1.29
	1	5	0.15	127.0	0.569	142.0	0.636	1.12
	1	10	0.15	120.0	0.537	137.5	0.616	1.15
	1	15	0.15	88.0	0.394	109.0	0.488	1.24
	1	20	0.15	71.0	0.318	95.0	0.425	1.34
Medium	0	5	0.05	37.0	0.725	42.0	0.824	1.14
	0	10	0.05	25.5	0.500	30.5	0.598	1.20
	0	15	0.05	18.6	0.365	22.5	0.441	1.21
	0	20	0.05	12.4	0.243	15.6	0.306	1.26
	0	5	0.1	29.5	0.578	36.0	0.706	1.22
	0	10	0.1	21.5	0.422	29.0	0.569	1.35
	0	15	0.1	14.4	0.282	21.0	0.412	1.46
	0	20	0.1	10.6	0.208	15.9	0.312	1.50
	0	5	0.15	24.5	0.480	31.2	0.612	1.27
	0	10	0.15	17.6	0.345	28.0	0.549	1.59
	0	15	0.15	12.5	0.245	21.0	0.412	1.68
	0	20	0.15	8.8	0.173	16.5	0.324	1.88
	0.5	5	0.05	83.0	0.769	90.0	0.833	1.08
	0.5	10	0.05	65.0	0.602	72.0	0.667	1.11
	0.5	15	0.05	53.5	0.495	60.0	0.556	1.12
	0.5	20	0.05	41.0	0.380	46.5	0.431	1.13
	0.5	5	0.1	78.0	0.722	85.0	0.787	1.09
	0.5	10	0.1	62.0	0.574	69.5	0.644	1.12
	0.5	15	0.1	47.0	0.435	57.5	0.532	1.22
	0.5	20	0.1	35.5	0.329	44.2	0.409	1.25
	0.5	5	0.15	67.0	0.620	73.0	0.676	1.09
	0.5	10	0.15	56.5	0.523	64.0	0.593	1.13
	0.5	15	0.15	40.0	0.370	50.0	0.463	1.25
	0.5	20	0.15	33.0	0.306	43.0	0.398	1.30
	1	5	0.05	112.0	0.778	116.0	0.806	1.04
	1	10	0.05	89.0	0.618	93.6	0.650	1.05
	1	15	0.05	69.0	0.479	74.0	0.514	1.07
	1	20	0.05	56.5	0.392	63.0	0.438	1.12
	1	5	0.1	102.0	0.708	110.0	0.764	1.08
	1	10	0.1	81.0	0.563	91.5	0.635	1.13

Type of sand	D_f/B	α°	e/B	Present result				
				$q_{u(pc)}$ (kN/m^2)	$RF_{(pc)}$	$q_{u(R)}$ (kN/m^2)	$RF_{(R)}$	$q_{u\,(R)}/q_{u\,(pc)}$
	1	15	0.1	63.5	0.441	73.0	0.507	1.15
	1	20	0.1	48.5	0.337	57.0	0.396	1.18
	1	5	0.15	89.0	0.618	97.0	0.674	1.09
	1	10	0.15	75.0	0.521	85.0	0.590	1.13
	1	15	0.15	56.0	0.389	69.5	0.483	1.24
	1	20	0.15	43.0	0.299	55.4	0.385	1.29

The reduction factor for the eccentric inclined load is calculated as the ratio of ultimate bearing capacity of strip footing subjected to eccentric inclined load at any embedment ratio to the ultimate bearing capacity of strip footing subjected to centric vertical load at that corresponding embedment ratio. The equation is as follows

$$RF = \frac{q_{u(D_f/B,e/B,\alpha/\phi)}}{q_{u(D_f/B,e/B=0,\alpha/\phi=0)}}$$

Patra et al. (2012) conducted laboratory tests to determine the reduction factor of a rigid strip footing placed on a purely frictional soil subjected to eccentric and inclined loading. The reduction factor for reinforced case is given by

$$RF = \left[1-2\left(\frac{e}{B}\right)\right]\left(1-\frac{\alpha}{\phi}\right)^{1.5-0.7\left(\frac{D_f}{B}\right)}$$

5.4 Comparison

5.4.1 Comparison with Patra et al. [2012b]

The comparisons with Patra et al. (2012b) and present results have been shown in Figures 5.10. Also the comparisons are presented in Table 5.3. It appears that the results from analysis are in good agreement.

Table 5.3: Comparison of Reduction Factors corresponding to Patra et al. (2012b) with present results

Type of Sand	D_f/B	α°	e/B	Present result			Patra et al.2012			Deviation (%) for *Reinforced* case
				$RF_{(pc)}$	$RF_{(R)}$	$q_{u(R)}/q_{u(pc)}$	$RF_{(pc)}$	$RF_{(R)}$	$q_{u(R)}/q_{u(pc)}$	
Dense	0	5	0.05	0.678	0.756	1.115	0.693	0.740	1.068	-2.1
	0	10	0.05	0.467	0.544	1.167	0.513	0.590	1.151	7.8
	0	15	0.05	0.311	0.378	1.214	0.360	0.453	1.258	16.5
	0	20	0.05	0.214	0.278	1.295	0.234	0.328	1.401	15.2
	0	5	0.1	0.567	0.733	1.294	0.616	0.658	1.068	-11.5
	0	10	0.1	0.378	0.567	1.500	0.456	0.525	1.151	-8.0
	0	15	0.1	0.256	0.411	1.609	0.320	0.402	1.258	-2.2
	0	20	0.1	0.164	0.289	1.757	0.208	0.291	1.401	0.8
	0	5	0.15	0.467	0.602	1.290	0.539	0.575	1.068	-4.7
	0	10	0.15	0.341	0.539	1.580	0.399	0.459	1.151	-17.4
	0	15	0.15	0.222	0.394	1.775	0.280	0.352	1.258	-12.1
	0	20	0.15	0.142	0.272	1.914	0.182	0.255	1.401	-6.8
	0.5	5	0.05	0.785	0.860	1.096	0.740	0.774	1.047	-11.1
	0.5	10	0.05	0.628	0.698	1.111	0.590	0.651	1.103	-7.1
	0.5	15	0.05	0.448	0.523	1.169	0.453	0.531	1.174	1.5
	0.5	20	0.05	0.326	0.390	1.196	0.328	0.415	1.266	6.1
	0.5	5	0.1	0.756	0.837	1.108	0.658	0.688	1.047	-21.6
	0.5	10	0.1	0.587	0.669	1.139	0.525	0.579	1.103	-15.5
	0.5	15	0.1	0.404	0.500	1.237	0.402	0.472	1.174	-5.9
	0.5	20	0.1	0.314	0.407	1.296	0.291	0.369	1.266	-10.4
	0.5	5	0.15	0.663	0.744	1.123	0.575	0.602	1.047	-23.6
	0.5	10	0.15	0.517	0.599	1.157	0.459	0.507	1.103	-18.2
	0.5	15	0.15	0.401	0.506	1.261	0.352	0.413	1.174	-22.4
	0.5	20	0.15	0.297	0.407	1.373	0.255	0.323	1.266	-26.2
	1	5	0.05	0.725	0.770	1.062	0.790	0.811	1.026	5.0
	1	10	0.05	0.582	0.627	1.077	0.679	0.719	1.058	12.8
	1	15	0.05	0.475	0.551	1.160	0.569	0.624	1.096	11.7
	1	20	0.05	0.385	0.457	1.186	0.459	0.525	1.144	13.0
	1	5	0.1	0.618	0.667	1.080	0.702	0.721	1.026	7.4
	1	10	0.1	0.546	0.609	1.115	0.604	0.639	1.058	4.7
	1	15	0.1	0.425	0.515	1.211	0.506	0.554	1.096	7.1
	1	20	0.1	0.345	0.443	1.286	0.408	0.467	1.144	5.0

Type of Sand	D_f/B	α°	e/B	Present result			Patra et al.2012			Deviation (%) for
	1	5	0.15	0.569	0.636	1.118	0.614	0.630	1.026	-0.9
	1	10	0.15	0.537	0.616	1.146	0.528	0.559	1.058	-10.2
	1	15	0.15	0.394	0.488	1.239	0.443	0.485	1.096	-0.6
	1	20	0.15	0.318	0.425	1.338	0.357	0.408	1.144	-4.2
Medium	0	5	0.05	0.725	0.824	1.135	0.676	0.726	1.074	-13.4
	0	10	0.05	0.500	0.598	1.196	0.484	0.565	1.168	-5.8
	0	15	0.05	0.365	0.441	1.210	0.324	0.418	1.291	-5.5
	0	20	0.05	0.243	0.306	1.258	0.196	0.287	1.464	-6.6
	0	5	0.1	0.578	0.706	1.220	0.601	0.645	1.074	-9.4
	0	10	0.1	0.422	0.569	1.349	0.430	0.502	1.168	-13.2
	0	15	0.1	0.282	0.412	1.458	0.288	0.372	1.291	-10.7
	0	20	0.1	0.208	0.312	1.500	0.174	0.255	1.464	-22.2
	0	5	0.15	0.480	0.612	1.273	0.526	0.565	1.074	-8.3
	0	10	0.15	0.345	0.549	1.591	0.376	0.440	1.168	-24.9
	0	15	0.15	0.245	0.412	1.680	0.252	0.325	1.291	-26.6
	0	20	0.15	0.173	0.324	1.875	0.152	0.223	1.464	-45.0
	0.5	5	0.05	0.769	0.833	1.084	0.726	0.763	1.051	-9.2
	0.5	10	0.05	0.602	0.667	1.108	0.565	0.630	1.115	-5.8
	0.5	15	0.05	0.495	0.556	1.121	0.418	0.500	1.196	-11.1
	0.5	20	0.05	0.380	0.431	1.134	0.287	0.375	1.306	-14.9
	0.5	5	0.1	0.722	0.787	1.090	0.645	0.679	1.051	-16.0
	0.5	10	0.1	0.574	0.644	1.121	0.502	0.560	1.115	-14.9
	0.5	15	0.1	0.435	0.532	1.223	0.372	0.445	1.196	-19.8
	0.5	20	0.1	0.329	0.409	1.245	0.255	0.333	1.306	-22.9
	0.5	5	0.15	0.620	0.676	1.090	0.565	0.594	1.051	-13.8
	0.5	10	0.15	0.523	0.593	1.133	0.440	0.490	1.115	-20.9
	0.5	15	0.15	0.370	0.463	1.250	0.325	0.389	1.196	-19.0
	0.5	20	0.15	0.306	0.398	1.303	0.223	0.291	1.306	-36.6
	1	5	0.05	0.778	0.806	1.036	0.780	0.803	1.029	-0.4
	1	10	0.05	0.618	0.650	1.052	0.660	0.702	1.064	7.4
	1	15	0.05	0.479	0.514	1.072	0.540	0.598	1.108	14.1
	1	20	0.05	0.392	0.438	1.115	0.420	0.489	1.165	10.6
	1	5	0.1	0.708	0.764	1.078	0.693	0.713	1.029	-7.1
	1	10	0.1	0.563	0.635	1.130	0.587	0.624	1.064	-1.8
	1	15	0.1	0.441	0.507	1.150	0.480	0.532	1.108	4.6
	1	20	0.1	0.337	0.396	1.175	0.373	0.435	1.165	9.0
	1	5	0.15	0.618	0.674	1.090	0.607	0.624	1.029	-7.9

Type of Sand	D_f/B	α°	e/B	Present result			Patra et al.2012			Deviation (%) for
	1	10	0.15	0.521	0.590	1.133	0.513	0.546	1.064	-8.1
	1	15	0.15	0.389	0.483	1.241	0.420	0.465	1.108	-3.8
	1	20	0.15	0.299	0.385	1.288	0.327	0.380	1.165	-1.1

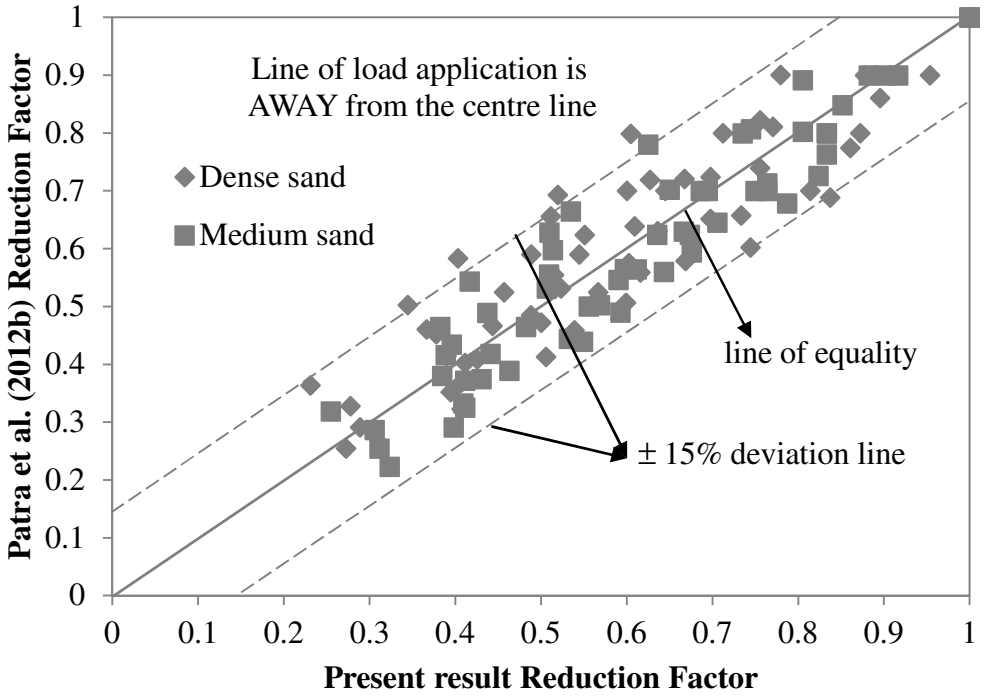

Figure 5.10: Comparison of reduction factor corresponding to Patra et al. (2012b) with present results for medium dense and dense sand

From the Figure 5.10 the comparison between the reduction factor of Patra et al. (2012b) and reduction factor of present results for dense sand and medium dense sand are in good agreement and not exceeding the ±15% deviation line.

5.4.2 Comparison with Loukidis et al. [2008]

The comparisons with Loukidis et al. (2008) and present results have been shown in Figures 5.11 and 5.12. Also the comparisons are presented in Table 5.4. It appears that the results from analysis are in good agreement.

Table 5.4: Comparison of Reduction Factors corresponding to Loukidis et al. (2008) with present result for $D_f/B = 0$

Type of Sand	D_f/B	α°	e/B	Present result			Loukidis et al. (2008)		
				$RF_{(pc)}$	$RF_{(R)}$	$q_{u(R)}/q_{u(pc)}$	$RF_{(pc)}$	$RF_{(R)}$	$q_{u(R)}/q_{u(pc)}$
Dense	0	5	0.05	0.678	0.756	1.115	0.677	0.748	1.104
	0	10	0.05	0.467	0.544	1.167	0.503	0.575	1.143
	0	15	0.05	0.311	0.378	1.214	0.343	0.406	1.183
	0	20	0.05	0.214	0.278	1.295	0.205	0.255	1.246
	0	5	0.1	0.567	0.733	1.294	0.554	0.643	1.161
	0	10	0.1	0.378	0.567	1.500	0.417	0.533	1.277
	0	15	0.1	0.256	0.411	1.609	0.283	0.393	1.389
	0	20	0.1	0.164	0.289	1.757	0.163	0.255	1.560
	0	5	0.15	0.467	0.602	1.290	0.431	0.517	1.201
	0	10	0.15	0.341	0.539	1.580	0.325	0.456	1.401
	0	15	0.15	0.222	0.394	1.775	0.217	0.352	1.625
	0	20	0.15	0.142	0.272	1.914	0.119	0.236	1.989
Medium	0	5	0.05	0.725	0.824	1.135	0.677	0.748	1.104
	0	10	0.05	0.500	0.598	1.196	0.503	0.575	1.143
	0	15	0.05	0.365	0.441	1.210	0.343	0.406	1.183
	0	20	0.05	0.243	0.306	1.258	0.205	0.255	1.246
	0	5	0.1	0.578	0.706	1.220	0.554	0.643	1.161
	0	10	0.1	0.422	0.569	1.349	0.417	0.533	1.277
	0	15	0.1	0.282	0.412	1.458	0.283	0.393	1.389
	0	20	0.1	0.208	0.312	1.500	0.163	0.255	1.560
	0	5	0.15	0.480	0.612	1.273	0.431	0.517	1.201
	0	10	0.15	0.345	0.549	1.591	0.325	0.456	1.401
	0	15	0.15	0.245	0.412	1.680	0.217	0.352	1.625
	0	20	0.15	0.173	0.324	1.875	0.119	0.236	1.989

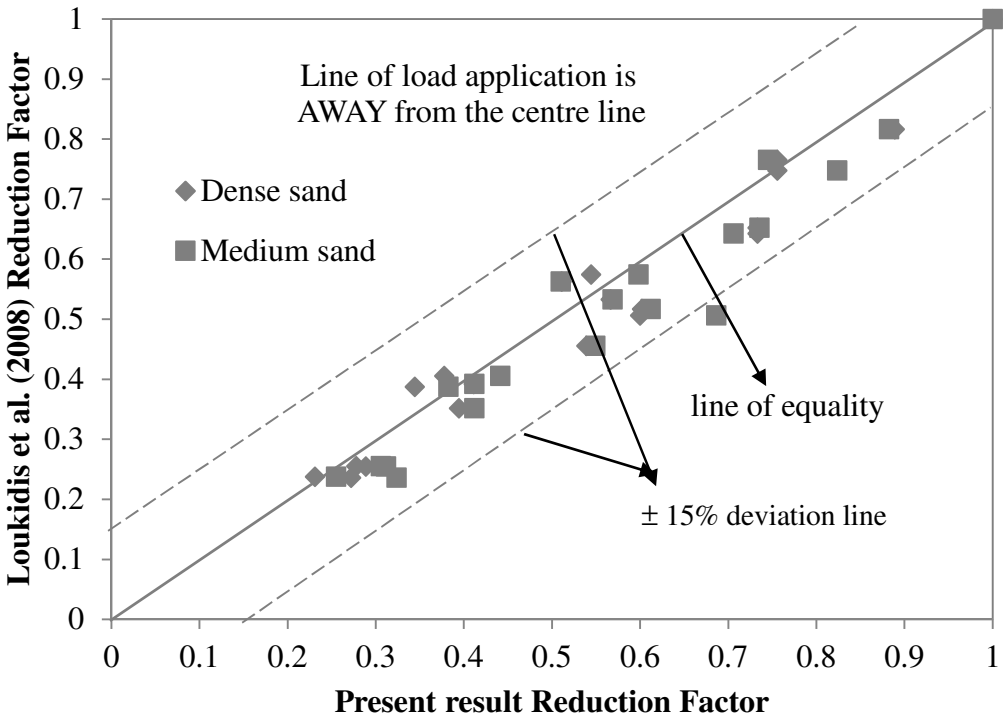

Figure 5.11: Comparison of RF corresponding to Loukidis et al. (2008) with present results

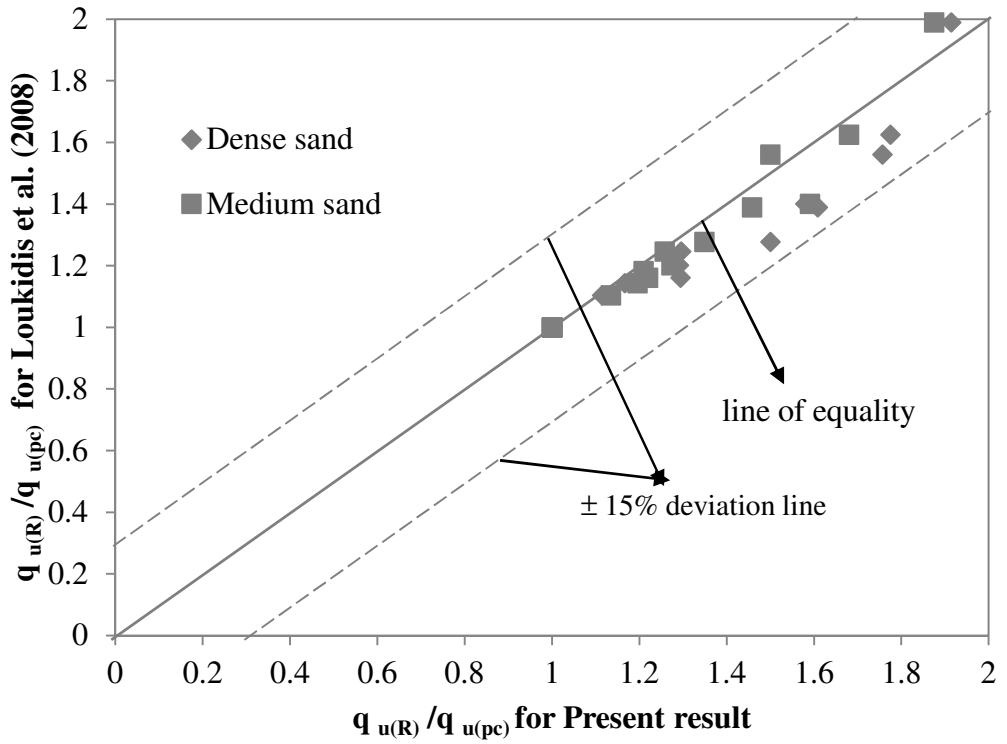

Figure 5.12: Comparison of (q_u– reinforced)/(q_u– partially compensated) for Present results with Loukidis et al. (2008)

6. Conclusions and Scope for Future Research Work

6.1 Conclusions

One hundred ninety two numbers of numerical models are developed using PLAXIS 3D to determine the ultimate bearing capacity of a strip foundation supported by sand and subjected to an eccentrically inclined load. The embedment ratio (D_f/B) is varied from zero to one. Models are developed on dense and medium dense sand bed. The load eccentricity ratio (e/B) is varied from 0 to 0.15, and the load inclination (α) is varied from 0° to 20° with an increment of 5°. Based on the analysis of numerical model results and within the range of parameters studied, the following conclusions are drawn:

- For given values of D_f/B and e/B, the magnitude of (q_u– reinforced)/(q_u– partially compensated) increases with the load inclination α.
- For similar values of α and e/B, the above ratio shows a tendency to decrease with the increase in embedment ratio (D_f/B).
- For a given value of D_f/B and α, the ratio (q_u– reinforced)/(q_u– partially compensated) increases with the increase in e/B.
- For both *partially compensated* case and *reinforced* case, the comparison of present results with Loukidis et al. (2008) and Patra et al. (2012a, 2012b) are in good agreement.
- A comparison between the reduction factors obtained from the numerical model results and those obtained from experimental results of Patra et al. (2012a, 2012b) show, in general, a variation of ±15% or less. In some cases, the deviation is about 20 to 25%.
- The developed reduction factors are also in well agreement with existing theories.

6.2 Scope of the research work

The present thesis pertains to the study on the bearing capacity of eccentrically inclined loaded strip footing. The future research work may address the below mentioned points:

- Settlement, failure pattern and stress distribution of eccentrically inclined loaded footing can be studied.
- The present work can be extended loose sand.
- The present work can be extended to foundations on cohesive soil.
- The present work can be extended to reinforced soil condition.
- The present work can be extended to seismic analysis.

REFERENCES

DeBeer, E.E. (1965). "Bearing capacity and settlement of shallow foundations on sand." *Proceedings*, Symposium on Bearing Capacity and Settlement of Foundations, Duke University, 15-33.

DeBeer, E.E. (1970). "Experimental determination of the shape factors and the bearing capacity factors of sand." *Geotechnique*. 20(4), 387-411.

Dubrova, G.A. (1973). "Interaction of Soils and Structures.*" Rechnoy Transport*, Moscow.

Hansen, J.B. (1970). "A revised and extended formula for bearing capacity." *Bull. No. 28*, Danish Geotechnical Institute, Copenhagen.

Hjiaj, M., Lyamin, A.V., Sloan, S.W. (2004). "Bearing capacity of a cohesive-frictional soil under non-eccentric inclined loading." *Comp. and Geotech.*, 31, 491–516.

Hjiaj, M., Lyamin, A.V. and Sloan, S.W. (2005). "Numerical limit analysis solutions for the bearing capacity factor $N\gamma$." *Int. J. of Soils and Struc.* 43, 1681.

Janbu, N. (1957). "Earth pressures and bearing capacity calculations by generalized procedure of slices." *Proc. of 4th Int. Conf. on Soil Mech, and Found. Eng*., London, 2, 207-211.

Krabbenhoft Sven; Damkilde Lars; and Krabbenhoft Kristian (2014), "Bearing Capacity of Strip Footings in Cohesionless Soil Subject to Eccentric and Inclined Loads", *Int. J. Geomech. 2014.14.*, ASCE, 04014003-1-18.

Loukidis, D., Chakraborty, T. and Salgado, R. (2008). "Bearing capacity of strip footings on purely frictional soil under eccentric and inclined loads." *Can. Geotech. J.*, 45(6), 768-787.

Meyerhof, G.G. (1951). "The ultimate bearing capacity of foundations." *Geotechnique*, 2, 301.

Meyerhof, G.G. (1953). "The bearing capacity of foundations under eccentric and inclined loads." *Proc.*, *3rd Int. Conf. on Soil Mech. and Found. Eng.*, 1, 440-445.

Meyerhof, G.G. (1963). “Some recent research on the bearing capacity of foundations.” *Canadian Geotechnical Journal*, 1(1): 16-26.

Meyerhof, G.G. (1965). “Shallow foundations.” *J. Soil Mech. Found. Div.,* ASCE, 91(SM2), 21-31.

Meyerhof, G.G., and Koumoto, T. (1987). “Inclination factors for bearing capacity of shallow footings.” *J. of Geotech. Eng.,* ASCE*,* 113(9), 1013-1018.

Michalowski, R.L. (1997). “An estimate of the influence of soil weight on bearing capacity using limit analysis.” *Soils and Foundations.* 37(4), 57-64.

Michalowski, R.L., and You, L. (1998). “Effective width rule in calculations of bearing capacity of shallow footings.” *Comp. and Geotech.*, 23, 237-253.

Mosallanezhad, M., Hataf, N., and Ghahramani, A. (2008). “Bearing capacity of square footings on reinforced layered soil.” *J. of Geotech. and Geolog. Eng.,* 26, 299- 312.

Muhs, H., and Weiss, K. (1973). “Inclined load tests on shallow strip footing.” *Proc., 8th Int. Conf. on Soil Mech. and Found. Eng.*, Moscow, 1.3. Nova, R. and Montrasio, L. (1991). Settlement of shallow foundations on sand.” *Geotechnique*, 41(2), 243-256.

Patra C.R., Behera R.N., Shivakugan N. and Das B.M. (2012a), “Ultimate bearing capacity of shallow strip foundation on eccentrically inclined load, Part I.” *International Journal of Geotechnical Engineering (2012),* 6(3), 343-352.

Patra C.R., Behera R.N., Shivakugan N. and Das B.M. (2012b), “Ultimate bearing capacity of shallow strip foundation on eccentrically inclined load, Part II.” *International Journal of Geotechnical Engineering (2012),* 6(4), 507-514.

Perloff, W.H., and Barron, W. (1976). *Soil Mechanics: Principles and Applications.* Ronald Press, New York.

Poulos, H.G., Carter, J.P. and Small, J. C. (2001). "Foundations and retaining structures—research and practice." in *Proc. of 15th Intl. Conf. Soil Mech. Found. Eng.*, Istanbul, Turkey, 4, A. A. Balkema, Rotterdam, 2527.

Prakash, S. and Saran, S. (1971). "Bearing capacity of eccentrically loaded footings." *J. Soil Mech. and Found. Div.*, ASCE, 97(1), 95-117.

Prandtl, L. (1921). "Uber die eindringungs-festigkeit plastisher baustoffe und die festigkeit von schneiden." *Z. Ang. Math. Mech.*, 1(1), 15.

Purkayastha, R.D., Char, R.A.N., (1977). "Stability analysis for eccentrically loaded footings." *J. Geotech. Eng. Div.,* ASCE, 103(6), 647–651.

Reissner, H. (1924). "Zum erddruckproblem." *Proc. of 1st Int. Cong. of Appl. Mech*., 295-311.

Saran, S. and Agarwal, R.K. (1991). "Bearing capacity of eccentrically obliquely loaded foundation." *J. Geotech. Eng.*, ASCE, 117(11), 1669-1690.

Salgado, R., Lyamin, A.V., Sloan, S.W. and Yu, H.S. (2004). Two- and three dimensional bearing capacity of foundations in clay. *Geotechnique.* 54(5), 297-306.

Salgado, R. (2008). *The engineering of foundations,* New York, McGraw-Hill.

Sastry, V.V.R.N., Meyerhof, G.G. (1987). "Inclination factors for strip footings." *Journal of Geotechnical Engineering*, ASCE, 113(5), 524-527.

Schmertmann, J.H. (1970). "Static cone to compute static settlement over sand." *J. Soil Mech. Found. Div.,* ASCE, 96(3), 1011-1043.

Terzaghi, K. (1943). *Theoretical Soil Mechanics*, Wiley, New York.

Terzaghi, K., and Peck, R.B. (1948). *Soil mechanics in engineering practice,* 1st Edition, John Wiley & Sons, New York.

Vesic, A.S. (1973). "Analysis of ultimate loads of shallow foundations." *J. of Soil Mech. and Found. Div.*, ASCE, 99(1), 45-73.

Vesic, A.S. (1975). Bearing capacity of Shallow foundations. *In* Geotechnical Engineering and book. Edited by Braja M. Das, Chapter 3, J. Ross Publishing, Inc., U.S.A.

Viladkar M. N., Adnan Jayed Zedan and Swami Saran (2013), "Non-dimensional correlations for design of eccentrically obliquely loaded footings on cohesionless soils", *International Journal of Geotechnical Engineering*, 7 (4), 333-345.

Viladkar M. N., Adnan Jayed Zedan and Swami Saran (2015), "Nonlinear elastic analysis of shallow footings subjected to eccentric inclined loads", *Geomechanics and Geoengineering: An International Journal,* 10 (1), 45–56.